Université Mohamed Khider Biskra
Faculté des Sciences et de la Technologie
Département : Génie Electrique
Ref :…….

جامعة محمد خيضر بسكرة
كلية العلوم و التكنولوجيا
قسم: الهندسة الكهربائية
المرجع:……..

Thèse présentée en vue de l'obtention
du diplôme de

Doctorat LMD en Génie Electrique

Filière : Électrotechnique Option : Energie renouvelable

Power system performance improvement in the presence of renewable sources

---

Présentée par :

NECIRA Abdelouahab

Devant le jury composé de :

MECHGOUG Raihane	M. C. A	President	Biskra University
NAIMI Djemai	Professeur	Rapporteur	Biskra University
SALHI Ahmed	M. C. A	Examinateur	Biskra University
ZELLOUMA laid	Professeur	Examinateur	Eloued university

2021/2022

With all respect and love I dedicate this work to my dear parents, my family and all my friends

Abdelouahab

Acknowledgement

First of all, I would like to express my thanks to my thesis director

Pr. NAIMI Djemai, Professor at Mohamed KHIDER Biskra University, for supporting and trusting me during these years with great patience. With his experience in research and teaching, with his advice, I was able to discover the world of scientific research in the field of power system stability and analysis. It is indeed a great pleasure for me to work under his supervision.

I would like to warmly thank Dr. SALHI Ahmed, research professor at Mohamed KHIDER Biskra University, for his contribution, his help and his encouragement that he lavished on me during the period of the thesis.

I would like to sincerely thank the members of the jury:

1. Dr. MECHGOUG Raihane, Professor at Mohamed KHIDER Biskra University, finds here the expression of my most sincere thanks for agreeing to chair this thesis.

2. Pr. ZELLOUMA laid, Professor at Eloued University, for the interest shown in our work and his participation in the jury as an examiner.

Publications & Communications associated with the thesis

The contributions presented in this thesis manuscript have been published in the following articles.

I. International Publications

A. Necira, D. Naimi, A. Salhi, S. Salhi, and S. Menani, "Dynamic crow search algorithm based on adaptive parameters for large-scale global optimization," *Evolutionary Intelligence,* pp. 1-17, 2021.

S Souheil, N Djemai, S Ahmed, A Saleh**, N Abdelouahab**, "A novel hybrid approach based artificial bee colony and salp swarm algorithms for solving ORPD problem," Indonesian Journal of Electrical Engineering and Computer Science 23, 1825_1837.

II. International communications

A. Necira, D. Naimi, " PSS-PID Controller Parameters Optimal Tuning for enhancing Power System Stability," at the 1st International Conference on Electrical Engineering and Modern Technologies CIETM'22, 18-19 February 2022, Souk Ahras, Algeria.

S Souheil, S Ahmed, N Djemai, **N Abdelouahab**, " a novel optimization algorithm for optimal reactive power dispatch: salp swarm algorithm ," at the second internatinal conference on electrical engineering ICEEB "18 ," december 2018, Biskra, Algeria.

ملخص
الاهتزازت الكهروميكانيكية هي ظاهرة يهتز فيها المولد مقابل المولدات الأخرى في نظام الطاقة ، وبالتالي أصبح تخميد هذه الاهتزازت هدفًا ذا أولوية ، والهدف من عملنا هو ضمان أقصى قدر من التخميد لتذبذبات التردد المنخفض ولضمان الاستقرار العام للنظام لنقاط تشغيل مختلفة باستخدام مثبتات الطاقة (PSS). لتحقيق هذا الهدف، قمنا بتطوير خوارزمية محسنة بناءً على خوارزمية بحث الغربان (CSA) المطبقة على وظيفة موضوعية مستخرجة من تحليل القيمة الذاتية لنظام الطاقة. تم إجراء دراسة مقارنة باستخدام مثبت كلاسيكي ، PSS القائم على الخوارزمية الجينية (GA-PSS)، PSS القائم على سرب الجسيمات (PSO-PSS) ومثبتات أخرى تعتمد على الخوارزميات الحديثة. تم تقييم أداء طرق التحسين هذه على جهاز واحد متصل بسبار لانهائي (SMIB) عبر محاكاة المجال الزمني للنموذج الخطي. من ناحية أخرى ، يتم عرض تأثير دمج المولد الكهروضوئي على استقرار نظام الطاقة ، بالإضافة إلى حلول لزيادة كمية تكامل المولد الكهروضوئي دون فقدان استقرار النظام.

Abstract

Electromechanical oscillations is a phenomenon in which a generator oscillates against other generators in the power system, the damping of these oscillations has therefore become a priority objective, The objective of our work is to ensure maximum damping of low frequency oscillations and to guarantee the overall stability of the system for different operating points by the use of power stabilizers (PSSs). To achieve this goal, we developed an improved metaheuristic optimization method based on the crows search algorithm (CSA) applied on an objective function extracted from the eigenvalue analysis of the power system. A comparative study was made, with a classic stabilizer, genetic algorithm-based PSS (GA-PSS), a particle-swarm-based PSS (PSO-PSS) and other stabilizers based on recent algorithms. The performances of these optimization methods were evaluated on a single machine connected to an infinite bus (SMIB) via a linear model time domain simulation. On the other hand, the effect of integrating a photovoltaic PV generator on the stability of the power system is presented, as well as solutions to increase the amount of integration of the PV generator without losing the stability of the system.

KEY WORDS: Low frequency oscillations, Power stabilizer, Dynamic crow search algorithm, PV generator integration.

Résumé

Les oscillations électromécaniques est un phénomène dans lequel un générateur oscille contre d'autres générateurs du réseau, l'amortissement de ces oscillations est donc devenu un objectif prioritaire, L'objectif de notre travail est d'assurer un amortissement maximal des oscillations à faible fréquence et de garantir la stabilité globale du système pour différents points de fonctionnement par l'utilisation des stabilisateurs de puissance (PSSs). Pour atteindre cet objectif, nous avons développé une méthode d'optimisation métaheuristique améliorée basée sur l'algorithme de recherche des corbeaux (CSA) appliquée sur une fonction objectif extrait à partir de l'analyse des valeurs propres du système de puissance. Une étude comparative a été faite, avec un stabilisateur classique, stabilisateur à base d'algorithme génétique (GA-PSS), un stabilisateur à base essaime particule (PSO-PSS) et d'autres stabilisateurs basés sur des algorithmes récents. Les performances de ces méthodes d'optimisation ont été évalué sur un réseau mono machine relié à un jeu de barres infini (SMIB) via une simulation de domaine temporel de modèle linéaire. D'autre part, l'effet d'intégration d'un générateur PV photovoltaïque sur la stabilité du système électrique est présenté, ainsi que des solutions pour augmenter la quantité d'intégration du générateur PV sans perdre la stabilité du système.

MOTS CLES: Oscillations à faible fréquence, Stabilisateur de puissance, Methode dynamique de recherche de corbeau, Intégration de générateur PV.

Table of contents

Figure list

General introduction

The role of a power system is to generate and transport electrical power to the load, a balance between the energy generated and the energy consumed must be maintained at all times in a fast and flexible manner in the deregulated environment, which led to phenomena of instability.

A power system is a highly non-linear system that operates in a continuously changing environment: loads, generation power, network topology, etc. The system may also be subject to disturbances, the disturbance can be small or large. Small disturbances, in the form of load variations, occur continuously. The system must be able to "respond" satisfactorily to the needs of the load. The system must also be able to withstand many disturbances of a severe nature such as lightning, the loss of a generation unit, a short circuit on a transmission line, etc.

Following a transient disturbance, if the system is stable, it will reach a new state of equilibrium. If the system is unstable, this will result, for example, in a gradual increase in the gap between the rotor angles of the generators or in a gradual decrease in the voltages of the power system buses. An unstable state of the system may lead to cascading failures and disconnection of a large part of the power system.

The problems of instabilities related to electromechanical oscillations at low frequencies due to power systems with weakly interconnected lines or with a radial structure have become significant problems. These oscillations limit the power transmission capacity in the power system, and they lead to a loss of synchronism or even a blackout in the entire system.

The use of voltage regulators characterized by fast responses and high gains improves transient stability but increases the potential for negative damping. To overcome this problem and improve the damping of the system, additional stabilizing signals are introduced into the excitation system via its voltage regulator. These stabilizing signals will produce torques in phase with the generator speed variation to compensate the phase delay introduced by the excitation system.

The use of additional excitation signals for improving the dynamic stability of electrical systems has received much attention. Extensive research has been done on the effect of power system stabilizer (PSS) on system stability, PSS input signals, best PSS locations, and PSS optimization techniques.

Power System Stabilizers, thanks to their advantages in terms of economic cost and efficiency, are the best means, not only to eliminate the negative effects of voltage regulators, but also to dampen electromechanical oscillations and ensuring the overall stability of the system.

In the last decades, PSS have been introduced in power systems because they have proven their profitability in terms of controlling the damping of electrodynamics oscillations.

Conventionally, to tune the PSS parameters, equations of the nonlinear model of the system are linearized around the operating point and the linear control techniques are then applied. The PSS parameters are then set to certain values corresponding to given operating conditions. It is important to remember that the parameters of the generator vary with the load: the behavior dynamics of the machine varying according to the operating points. The PSSs must therefore be tuned and coordinated so that the overall stability of the system is guaranteed for a wide variety of operating points.

In the beginning, the design of PSS was based on the model of a machine connected to an infinite buse, single Machine to Infinite Bus (SIMB), with the use of the concept of damping torque and synchronism coefficients.

Phillips and Heffron, were the first to present the small perturbations in terms of k-constant of a SMIB system, to explain the stability at small perturbations and the effect of the excitation system. Larsen and Swann present the application of PSS using speed, frequency or power as input signals. Guidelines have been presented for tuning the PSS to allow the user to achieve the desired dynamic performance with less effort.

In the literature, several researches on heuristic techniques and artificial intelligence have been proposed and successfully implemented to improve the dynamic stability of the power system. Nature-inspired stochastic optimization (NISO) algorithms (Both as model and as metaphor) gain wide attention from the research community for decades. These algorithms either mimic individual or social behavior of a group of animal or natural phenomena, such as biological processes (e.g., reproduction, mutation, and interaction), or take advantages from species which have had adapted their physical attitude, structure, and learning to fit the environment over millions of years. Crow search algorithm (CSA) is a recent proposed algorithm proposed by Askarzadeh. CSA performs based on the idea that crows save their unneeded food in concealing places and retrieve it when it becomes in state of shortage. Therefore, crows turn into researcher in their environment for the best food source hidden by one of them, CSA algorithm has a simple mechanism controlled only by two parameters and is able to provide optimal or near-optimal solutions for large scale optimization problems.

The objective of our work is to ensure a maximum damping of low frequency oscillations by the use of PSS. This ensures satisfactory damping of rotor oscillations and guarantees the overall stability of the system for different operating points. To achieve this goal, we propose an optimal tuning of the PSS parameters by developing a new improved version of the conventional CSA called dynamic crow search

algorithm (DCSA). DCSA is proposed to overcome the drawbacks of the conventional CSA. In the proposed DCSA, two modifications of the conventional algorithm are made. The first modification concerns the continuous adjustment of the CSA parameters leading to a DCSA. This will provide more global search capability as well as more exploitation of the pre-final solutions. The second modification concerns the improvement of CSA's swarm diversity in the search process. This will lead to high convergence accuracy, and fast convergence rate.

With the liberalization of the electricity generation market in many countries, the fall in the cost of photovoltaic modules and the maturity of photovoltaic technology, some countries have adopted a policy of development and integration of photovoltaic power plants (CPV) in their national power systems. The development and integration of these photovoltaic power plants in a sub-Saharan network characterized for the most part by its weak mesh, its low installed power and above all its instability suggests many technical problems and unforeseeable technological consequences. At first sight, these problems will be induced by the interaction of these CPVs with the power system, not initially designed to accommodate them. These potential problems include:

• Alteration of the power systems voltage plan,

• Changes to the power systems service warranty conditions

• Uncontrollable overflow of capacity

• Difficulty of forecasting production,

• Malfunctioning of the protections...

It is very likely that the proliferation and dispersion of these sources, of an intermittent nature, will lead to a review of the structures and nature of current power systems. In order to analyze the interaction of these photovoltaic power plants on the distribution and high voltage power systems where they operate, it is necessary to develop suitable models for their behavioral analysis. It is for this reason that the objective pursued in this thesis is to analyze the impacts of photovoltaic production in transmission power systems in order to propose optimal solutions adapted to the development of the integration of PV power plants into existing public power systems.

This thesis is organized around four chapters which deal with all the questions raised:

In the first chapter, a reminder of the power system stability is discussed. The different methods of stability evaluation are presented.

The second chapter of this work concerns the general modeling of a power system adjusted to the study of small-signal stability. Two models are presented, a nonlinear

model and a linear model. Next, the power stabilizers (PSSs) are discussed in details as well as their parameters adjustment.

Third chapter presents the principle of photovoltaic conversion. Moreover, the constitution and the electric characteristics of a PV generator, its modeling and its simulation are treated there. A second part of this chapter deals in particular with network interface power converters and their classification. Thus, the problems of coupling a photovoltaic power plant to the power system are analyzed.

We present in the fourth chapter the development of dynamic crow search algorithm and we prove its superiority against basic CSA and other well known algorithms. Afterwards, the results of the application of DCSA to the optimization of the PSS parameters installed in the study system are presented, as well as a comparative study of the results obtained by other optimization methods. In other hand, the integration effect of a photovoltaique PV generators on the power system stability (test system) is presented, as well as provide some solutions to increase the amount of PV generator integration without losing the system stability. Finally, we end this essay with a conclusion and perspectives to complete this work.

Chapter I

Power System Dynamics
And Stability

I. 1. Introduction

Power system stability has been recognized as a vital and important issue for a reliable and secure interconnected power system operation as far back as the 1920s. The importance of stability problem associated with power system operation arises from increasing power exchange between the constituent parts of a large interconnected power system [1]. In a free deregulated market, utilities are allowed to participate in the market without mandatory upper or lower limits. Thus, a number of highly publicized blackouts happened in the early years. The blackouts illustrate the necessity of assessing the stability of large power systems and maintaining an adequate level of system security to minimize the risk of major blackouts resulting from cascading outages emanating from a single disturbance [2]. The main requirement of system stability is to keep the synchronous operation of power system with adequate capacity and fast reaction to meet the fluctuations in electric demand and changes in system topology. Successful operation of a power system depends largely on the engineer's ability to provide reliable and uninterrupted service to all loads and supply the required amount of loads by the available facilities [3].

Distance between the current state and a hypothetical state wherein units may lose synchronization evaluated after each state of estimation and after each new power flow [4, 5]. In the evaluation, the concern is the behavior of the power system when it is subjected to transient disturbances. If the oscillatory response of a power system during the transient period following a disturbance is damped within acceptable time and the system can settle in a finite time to a new steady state, it is considered stable [6]. The depicted Figure (I.1) presents the sequence of operation states to assure a secure and reliable power system operation. As seen in the figure, the system state evaluated continuously to assure reliable and steady state operating condition and necessary actions, which need to be ready to anticipate such abnormal sates [7, 8]. The steady state operating condition of a power system is an operating condition in which all the physical quantities that characterize the system are considered constant for the purpose of analysis [9].

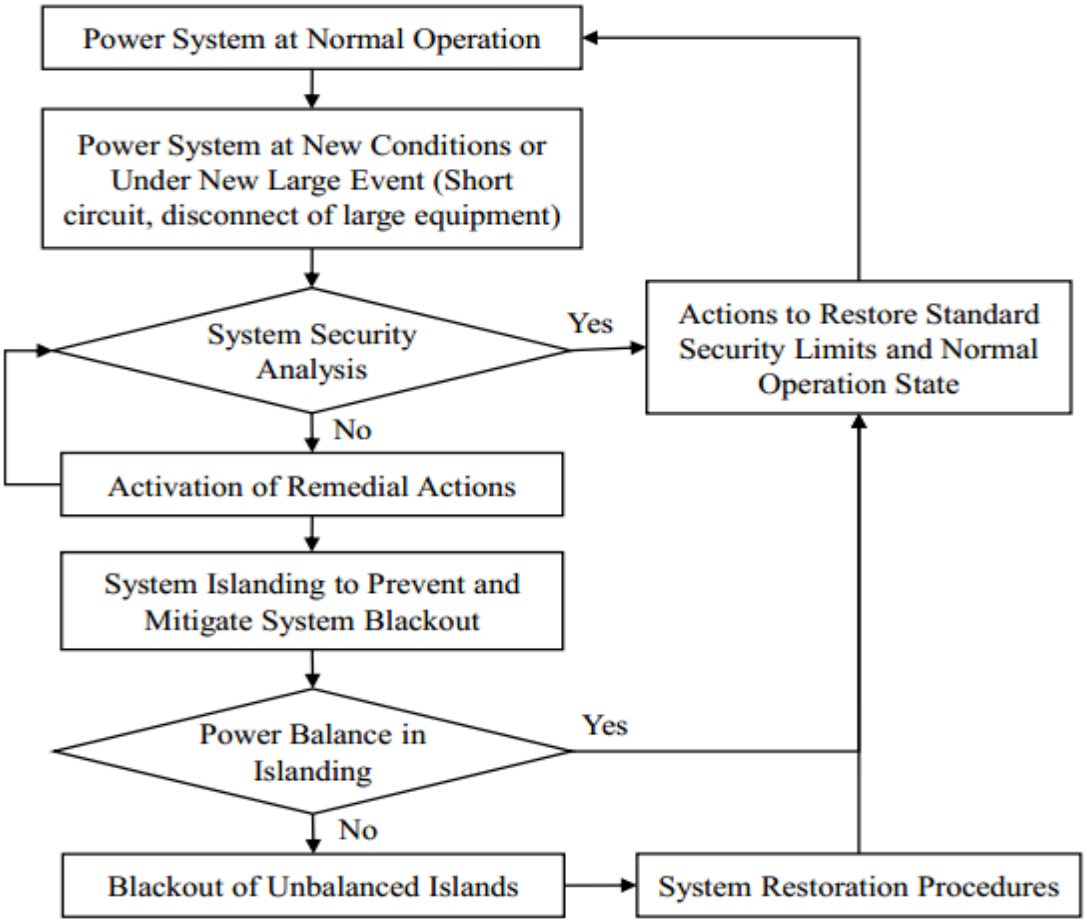

Figure I. 1. Sequence of operation states to assure system security

I. 2. Definition and Classification of Power System Stability

Power system stability is the ability of an electric power system, for a given initial operating condition, to regain a state of operating equilibrium after being subjected to a physical disturbance, with most system variables bounded so that practically the entire system remains intact [10]. Stability phenomenon is a single problem associated with various forms of instabilities affected on power system due to the high dimensionality and complexity of power system constructions and behaviors. For properly understood of stability, the classification is essential for significant power system stability analysis. Stability classified based on the nature of resulting system instability (voltage instability, frequency instability…), the size of the disturbance (small disturbance, large disturbance) and timeframe of stability (short term, long term). In the other hand, stability broadly classified as steady state stability and dynamic stability [11]. Steady state stability is the ability of the system to transit from one operating point to another under the condition of small load changes. Power system dynamic stability appears in the literature as a class of rotor angle stability to describe whether the system can maintain the stable operation after various

disturbances or not. Figure (I.2) shows the classification of power system stability in IEEE/CIGRE joint task force on stability terms and definitions.

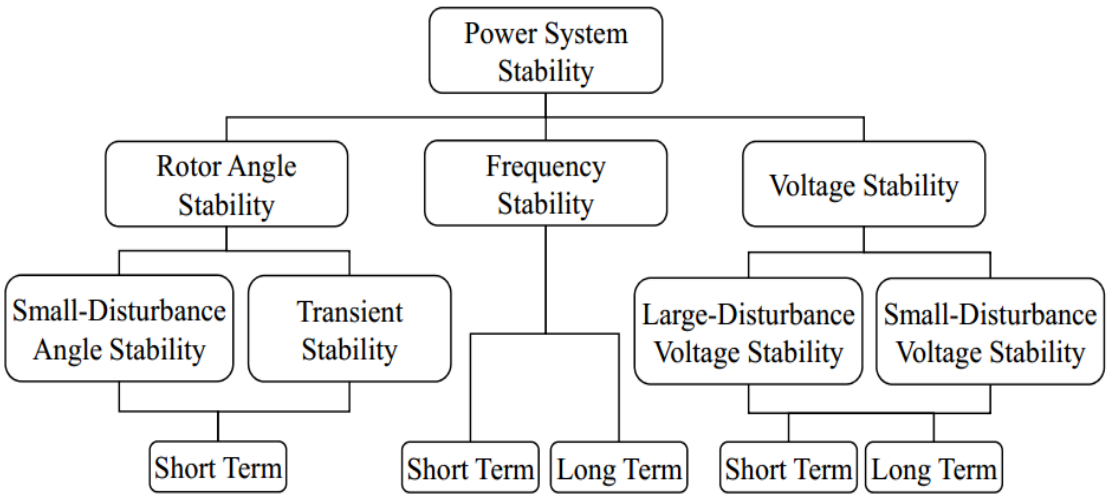

Figure I. 2. Classification of stability based on IEEE/CIGRE joint task force on stability

I. 2. 1. Rotor Angle Stability

Rotor angle stability is concerned with the ability of interconnected synchronous machines of a power system to remain in synchronism under normal operating conditions and after being subjected to a disturbance [10]. The stability of synchronous machines depends on the ability of restoring the equilibrium between their electromagnetic outputs torques and the mechanical input torques and keeping at synchronize with other machines following a major disturbance such as short circuit. Under steady state conditions, there is equilibrium between the input mechanical torque and the output electromagnetic torque of each generator, and the speed remains constant [9]. If the system is perturbed, this equilibrium is upset and instability may occur in the form of increasing or decreasing angular swings of some generators leading to their loss of synchronism with other generators. The change in electrical torque ΔT_e of a synchronous machine following a perturbation can be resolved into two components as follows:

$$\Delta T_e = T_S \, \Delta\delta + T_D \, \Delta\omega \qquad (I.1)$$

Where, $T_S \, \Delta\delta$ is the component of torque change in phase with the rotor angle perturbation $\Delta\delta$ and it is referred to as synchronizing torque component. T_S is the synchronizing torque coefficient. $T_D \, \Delta\omega$ is the component of torque change in phase with the speed deviation $\Delta\omega$ and it is referred to damping torque component. T_D is the damping torque coefficient.

Stability of each machine in the system depends on the existence of both components. Lack of sufficient synchronizing torque produces instability through aperiodic or non-oscillatory drift in the rotor angle, whereas lack of damping

torque results in oscillatory instability causes rotor oscillating with increasing amplitude. Rotor angle stability depends on the initial operating state and the severity of the disturbance on synchronous machines. Commonly, rotor angle stability are classified into small disturbance-rotor angle stability and large disturbance-rotor angle stability for gaining more understanding and insights into the nature and characteristics of stability problem [12].

I. 2. 1. 1. Small Disturbance Rotor Angle Stability

Small-disturbance rotor angle stability (oscillatory stability) is concerned with the ability of the power system to maintain a steady state operating point when subjected to small disturbances. Oscillations have been recognized as a consequence of parallel operation of alternative current generators which are connected to provide more power capacity and more reliability [7]. Thus electromechanical oscillations are understandable because of the change in kinetic energy of rotating parts (rotor) in electrical machines due to their moment of inertia and the synchronizing torque, which acts to keep the generators in synchronism during disturbances [13].

Oscillations can also arise in the power system due to any sudden change in a power system such as high power flows over weak tie lines, which can become heavily loaded if many generators oscillate towards another group at the same time. Fast and powerful voltage regulators or other types of controls may produce oscillations in the network. If the disturbance is small, the synchronizing torque keeps the generators in synchronism with generators relative angles oscillation [14]. These oscillations should decay for small signal stable system operation otherwise; the system is a small signal unstable. Critical oscillatory modes can be triggered by a small disturbance because of the weak interconnection and stress. These oscillations limit the amount of power that can be transferred among system areas at peak load and may lead to power system break-up and outage.

Oscillatory stability problems are usually due to insufficient damping for power system oscillations. The system mode parameters can be investigated using two basic approaches; namely modal analysis of complete state spaces or time response analysis of collected synchronized measurements. Table 1 shows the complete summary of the various oscillation types. The oscillation modes are mainly classified into local and inter-area modes [15].

Local modes are associated with the swinging of units at generating station with respect to the rest of power system at 1.0 to 2.0 Hz. When a generator tied to a power system via a long radial line, it is susceptible to local mode oscillations. Local modes affected by the strength of the transmission system at the plant, the generation level and excitation control system. The oscillation may be removed with a single or dual input power system stabilizer that provides modulation of the voltage reference of the automatic voltage regulator with proper phase and gain compensation circuit.

Inter-area modes are associated with the swinging of many machines in one area of an interconnected power system against machines in other areas and have major impact on the global stability of the complete power system. It involves two coherent groups of generators swinging against each other at 0.05-1.0 Hz. Poorly damped inter-area oscillation affecting every part of interconnected power system and coordinated analysis are required to check the small signal stability of the whole power system. Inter-area modes depend on various reasons such as weak ties between interconnected areas, voltage levels, and the nature of the load [16].

Additionally, other types of oscillations have been recorded such as intraplant modes, torsional modes and control modes.

Intraplant modes is associated with machines on the same power generation site oscillate against each other at 2-3 Hz depending on the unit ratings and the reactance connecting them. Usually the rest of the system is unaffected because the oscillations manifest themselves within the generation plant.

Torsional modes are associated with the turbine generator shaft system rotational components due to the interaction between generator exciter control and prime mover control, and HVDC controls in the frequency range 10-46 Hz. Usually these modes are excited when a multi-stage turbine generator connected to the grid through a series compensated line. A mechanical torsional mode of the shaft system interacts with the series capacitor at the natural frequency of the electrical network. The shaft resonance appears when network natural frequency equals synchronous frequency minus torsional frequency.

Control modes are associated with generating units and other equipments control such as poorly tuned controls of excitation systems, speed governors, FACTs devices controls, HVDC converters. Loads and excitation system can interact through control modes. Transformer tap-changing controls can also interact in a complex manner with nonlinear loads giving rise to voltage oscillations.

I. 2. 1. 2. Large Disturbance Rotor Angle Stability

Large-disturbance rotor angle stability (transient stability) is concerned with the studying of the ability of power system to maintain synchronization among synchronous machines when subjected to a server transient disturbance e.g. a three-phase short circuit [17]. Transient stability depends on the current operating conditions of the system and the severity of the contingency on connected generators. The angles between each pair of generator rotor angles will change continuously by small amounts as power distribution change [6, 18]. Transient instability phenomenon is usually in the form of uncontrollable significant increase and separation of the relative angles between two or more rotors due to insufficient synchronizing torque. The resulting system response involves large excursions of generator rotor angles and influences by the nonlinear power angle relationship. Small-disturbance rotor angle stability as well as transient stability is categorized as short-term phenomena.

I. 2. 2. Voltage Stability

Voltage stability refers to the ability of a power system to maintain steady voltages at all buses in the system after being subjected to a disturbance from a given initial operating condition [19]. The voltage deviations need to maintain within predetermined ranges. A voltage stability problem occurs in heavily stressed systems, which associated with long transmission lines. Voltage stability depends on the active and reactive power balance between load and generation in the entire power system and the ability to maintain/restore this balance during normal and abnormal operation [20]. The main contributor in voltage instability is the increase of reactive power requirements beyond the sustainable capacity of the available reactive power resources when some of the generators hit their field or armature current time-overload capability limits. The other contributor is the extreme voltage drop that occurs when active and reactive power flow through inductive reactance of the transmission network; this limits the capability of the transmission network for power transfer and voltage support.

A typical scenario of voltage instability is unbalance reactive power in the system resulting in extended reactive power transmission over long distances. As long as the load increases, the power transmitted to supply load also increases while bus voltages on transmission line will drop in inductive network. Close to the maximum transmission capability, a small increase of the load implies a great decrease in the voltage level of the network that may lead to cascaded outages (under-voltages protective devices) while instability occurs in the form of a progressive fall of some bus voltages (voltages collapse) [21]. Generally, the voltage collapse mainly affected by the large distances between generation and load, under load tap changing transformers performance during low voltage conditions, unfavorable load characteristics, and poor coordination between various control and protective systems. In addition, the system may experience uncontrolled over-voltage instability problem at some buses due to the capacitive behavior of the network and under excitation limiters that preventing generators and synchronous compensators from absorbing excess reactive power in the system [22]. This can arise if the capacitive load of a synchronous machine is too large. Examples of excessive capacitive loads that can initiate self-excitation are open-ended high voltage lines, shunt capacitors, and filter banks from HVDC stations.

The phenomena of voltage stability can be classified into small disturbance and large disturbance voltage stability. Small-disturbance voltage stability refers to the system's ability to maintain steady voltages when subjected to small perturbations such as incremental changes in system load [12, 23]. A criterion for small-disturbance voltage stability in that, at a given operating condition for every bus at the system, the bus voltage magnitude increases as the reactive power injection at the same bus increased. A system is voltage-unstable if, for at least one bus in the system, the bus voltage magnitude decreases as the reactive power injection at the same bus increased. Large-disturbance voltage stability refers to the power system ability to

maintain steady voltages following large system disturbance such as loss of generation, loss of critical lines, system faults, or protection system failures. Investigation of this form of stability requires the examination of the dynamic performance of the system over a time sufficient to capture the interactions of such devices as under load tap changing transformers and generator field current limiters [24].

The voltage stability can be classified in terms of time into short-term stability and long-term voltage stability. Short-term voltage stability involves the dynamics of fast acting load component such as induction motors and electronically connected devices with study period of interest in the order of several seconds [25]. Long-term voltage stability involves the slower acting equipment such as tap-changing transformers and generator current limiters with study period extend several minutes [7, 26]. There are many methods can be used to mitigate voltage instability problem including operation of uneconomic generators to change power flows or provide voltage support during emergencies, using reactive power control and compensation devices, under-voltage load shedding to avoid voltage collapse or control of network voltage and generator reactive output.

I. 2. 3. Frequency Stability

Frequency stability refers to the ability of a power system to maintain steady frequency following a severe system upset resulting in a significant imbalance between generation and load. A typical cause for frequency instability is the loss of generation, which results in sudden unbalance between the generation and load. The control schemes of frequency deviation used to recover the system frequency without the need for customer load shedding by instantaneously activating the spinning reserve of the remaining units to supply the load demand in order to raise the frequency [8, 27]. In case of an incident with a large frequency deviation, the primary control (in the first 30 minutes) is activated where the partly loaded or carry spinning reserve units selected to initiate an automatic rapid increase of their outputs within a few seconds. The controllers of all activated generators alter the power delivered by the generators until a balance between power output and consumption is re-established. Spinning reserve to be utilized by the primary control should be uniformly distributed around the system. Then the reserve will come from a variety of locations and the risk of overloading some transmission corridors will be minimized. The frequency stabilization obtained and maintained at a quasi-steady state value, but differs from the frequency set point [4]. The Secondary control, in the portion of the system contains power unbalance, will take over the remaining frequency and power deviation after 15 to 30 seconds to return to the initial frequency and restore the power balance in each control area. Load shedding used as last option to minimize the risk of further uncontrollable system separation, loss of generation, or system shutdown. Automatic load shedding initiated using under-frequency relays expected to be able to shed the required amount of load during low frequency events. These

relays detect the onset of decay in the system frequency and shed appropriate amount of system load until the generations and loads are in balance [16, 28].

I. 3. Factors Affected on Power System Stability

Stability of a nonlinear system depends on the type and magnitude of inputs, and the initial state [29]. Power system stability is affected by many factors including the behavior and characteristics of system equipment, system control and protection schemes. The most important factors can be summarized by:

- Pre-and-post-disturbance system state such as the generators loading before the fault and the generator outputs during the fault. The higher the loading before the fault is the more likely to be less stable during faults.
- The duration, location and type of the fault determine the amount of kinetic energy will be gained. Longer fault duration allows generator rotors to gain more kinetic energy during the fault. At certain limit, the gained energy may not be dissipated after the fault clearance. This gained energy may lead to instability.
- Synchronous machine parameters such as the inertia constant H (stored kinetic energy at rated speed per rated power), and the generator terminal voltage. The increase of generators inertia constant tends to reduce the swings of rotor angle and hence improve system stability. The generator bus voltages specify the profile of the power angle curve and hence effects on the delivered power into the entire system.
- Excitation system and governor characteristics of synchronous machines have important role in damping of power oscillations. The automatic voltage regulator (AVR) senses the terminal voltage and helps to control it by acting within the excitation system. Fast valves for rapidly opening and closing steam valves of the turbine used to control the generators accelerating power during faults.
- Transmission reliability margin greatly effect on stability where a transmission outage may take place due to overloading during system abnormal conditions, which may lead to uncontrolled loss of a sequence of additional network elements.
- System relaying and protection have a great importance in system stability. The power system has a finite capacity to absorb such energy and as majority of fault are transient in nature, rapid switching and isolation of unhealthy lines followed by rapid reclosing improves the stability margins. Special protection schemes can be used to split the grid at predetermined points in the network to quickly avoid cascading actions.

I. 4. Power System Security Analysis

Power system security describes the ability of a power system to withstand and survive plausible contingencies without interruption of the customers. Security

requires detection of dangerous operating conditions and contingencies as well as the associated actions to steer the system away from any such situations. Security analysis can be divided into static and dynamic security. Static security analysis is the ability of the system to supply load without violating operating conditions and load curtailment, which mainly includes the pre- and post-contingency states [30]. Pre-contingency states determine the available transfer capability of transmission links and identify network congestion. Post-contingency states verify the bus voltages and limits of lines power flow.

Dynamic security analysis measures the ability of power system to withstand a defined set of contingencies and survive by the transition to an acceptable steady state condition, which includes methods to evaluate stability and quality of the transition from the pre- to post-contingency state [13]. Dynamic security analysis should be constantly in operation to detect when the security level falls below an adequate safety level to make proper preventive measures for a secure operation.

Figure (I.3) shows an example of such analysis architecture according to CIGRE Report No. 325. The collected data and database are used to model the system using the identification of the power system configuration and state estimation. After that, the system model validation and security assessment evaluated using a number of computer programs executing voltage stability analysis, small signal analysis and transient stability analysis. Based on the system state, a scientific report describe how close the system is to an insecure state created which should also include information about preventive and corrective action. The tripping of the overloaded equipment can be achieved immediately within the admissible overload duration which detected by overload or distance protection systems and a warning should be given to the dispatchers.

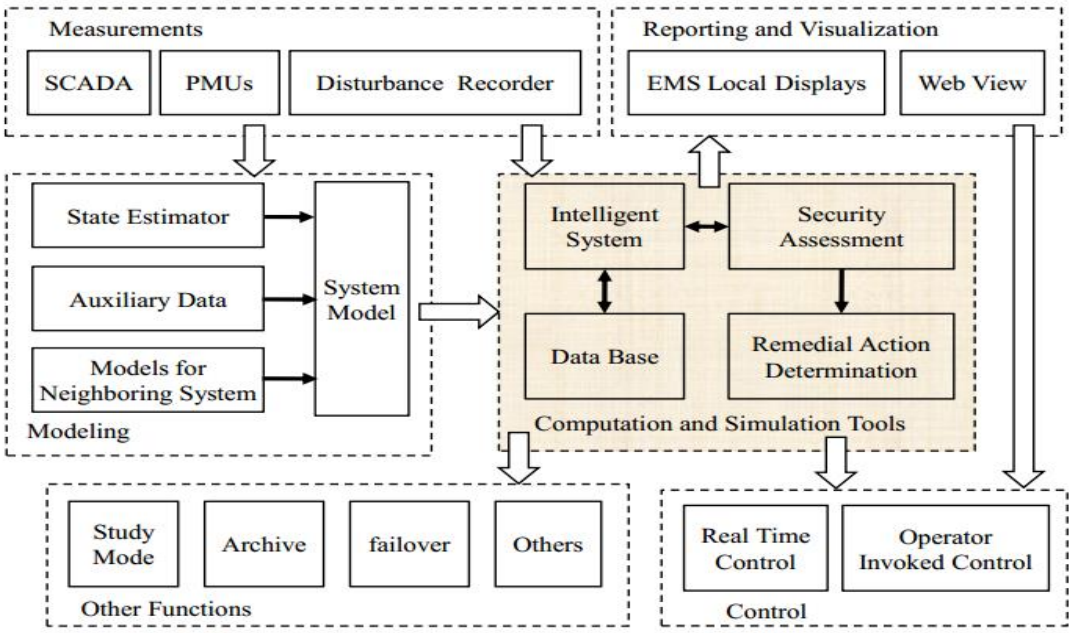

Figure I. 3. Components of dynamic security analysis according to CIGRE Report No. 325.

I. 5. Dynamic Stability Assessment

Dynamic stability assessment deals with the analysis of the system in the transition from the initial to the final operation condition following a disturbance or a changing power demand. A power system is dynamically stable for a particular steady state operating condition and for a particular disturbance if, following that disturbance; it reaches an acceptable steady state operating conditions. An important requirement was the ability to determine the risk of blackout, which can be computed by quantifying the distance between the current state and the steady-state stability limit rather than just characterizing it as stable or unstable [31]. This required a fast and accurate online security assessment tools and special actions to prevent system instability, which commonly defined as remedial actions. The remedial actions include curative and preventive actions that should be prepared in the operational planning stage. Curative remedial actions should be prepared in advance and immediately activated after any credible contingency or abnormal conditions to relieve system constraints. Preventive remedial actions should be designed in advance at steady state to anticipate the events and restore the security level in case curative remedial actions which are not sufficient to face the expected contingencies [15].

The security analysis and recommended actions are investigated in the computation block in Figure 1.3, which includes a number of computer programs to execute voltage stability analysis, small-signal stability analysis, transient stability analysis and any other important phenomenon to evaluate the system state. Based on the system state the system operator should design or execute the proper preventive and corrective actions [32]. After occurrence of the contingency, if there is a delay or insufficient of remedial actions to anticipate the new situation, the system falls at risk. Therefore, in a short while the ISO has to coordinate future remedial actions with neighbors to search about convenient remedial action. These actions should be able to secure the system and to be ready for the occurrence of new emergencies, which includes load shedding and generation rescheduling. Beside the remedial actions, the automatic N-1 contingency simulation should be evaluated periodically, at least every 5-15 minutes in real time operation. This highlights the importance of fast DSA tools to evaluate the system dynamics during contingencies.

I. 5. 1. Dynamic Stability Assessment Methods

I. 5. 1. 1. Transit Stability Assessment

It relates to the power system ability to maintain synchronism after having undergone a severe transient disturbance such as a short circuit on a transmission line or a loss of a significant part of the load or generation. The response of the system involves large variations in rotor angles. It depends on the non-linear couples-angles relationship.

The concept of transient stability can be explained by a simple graphical approach, namely the Equal Area Criterion. This approach combines the equation of motion and the traditional (P-δ) curve representing the relationship between the power produced by the generator and the rotor angle [31].

To explain this approach, we take a simple power system consisting of a synchronous generator connected to an infinite bus via a transmission line, Fig (I. 4). The generator is modeled by an ideal voltage source E_g in series with a reactance X_g (classic model). The line and the transformer are represented by the reactance X_E.

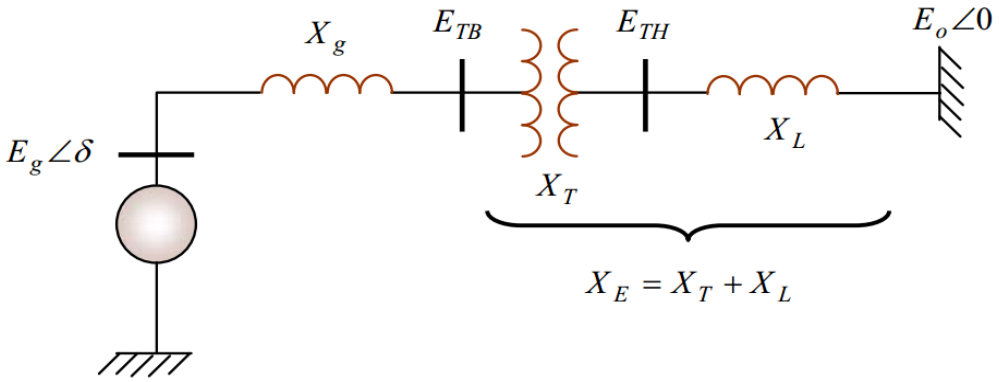

Figure I. 4. Synchronous machine connected to an infinite bus.

In the balanced state, the power produced by the generator P_e is given by the following equation:

$$P_e = \frac{E_g E_0}{X_g X_E} \sin \delta \qquad \text{(I. 2)}$$

Where, δ the rotor angle (said here, the power angle), is the phase shift between the internal generator voltage (E_g) and the infinite bus voltage (E_0). Eq (I. 2) is shown graphically in Fig (I. 5).

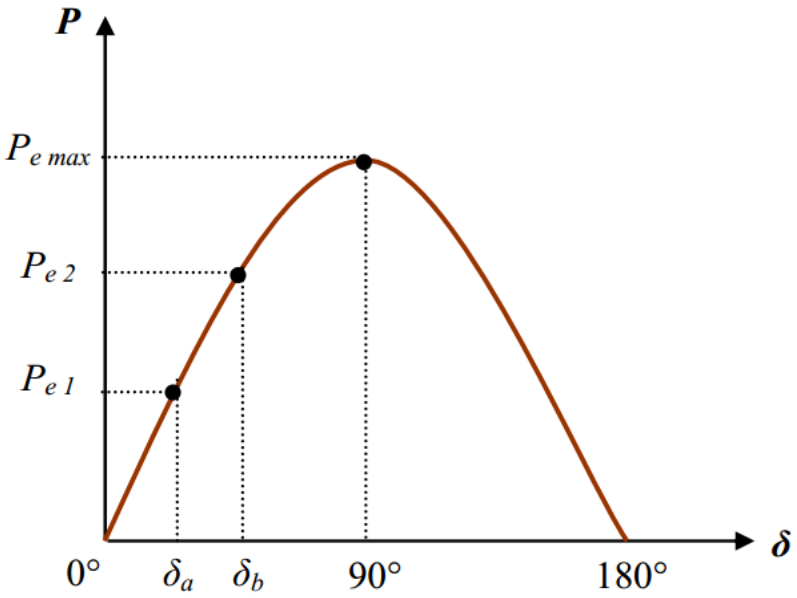

Figure I. 5. Power-rotor angle relationship.

During equilibrium, the electrical power P_{e1} is equal to the mechanical power applied for the corresponding angle δ_a.

A sudden change in the generator load causes a variation in the mechanical power, and consequently in the electrical power, for example from P_{e1} to P_{e2}, Fig (I. 5). The rotor will therefore accelerate so that the power angle increases, from δ_a to δ_b, to be able to provide additional power to the load. However, the rotor acceleration cannot stop instantly. Thus, although the power developed for angle δ_b is sufficient for the load, the rotor will exceed angle δ_b until sufficient opposite torque is developed to stop this acceleration. The extra energy will cause the rotor to slow down and decrease the power angle. Depending on the inertia and the damping of the system, the oscillations of the resulting rotor angle will either dampen, and the machine will remain stable (case 1, Fig (I. 6)), or diverge, and the machine will become unstable by losing synchronism with the system (case 2, Fig (I. 6)).

I. 5. 1. 1. 1. Equal Area Criterion

Consider a fault, such as a fault on the transmission line, applied to the previous system that disappears after a few periods. This will change the power flow and hence the rotor angle δ. Let us retrace the curve (P-δ) taking this defect into account, Fig (I. 7). Below this curve, we can consider two areas.

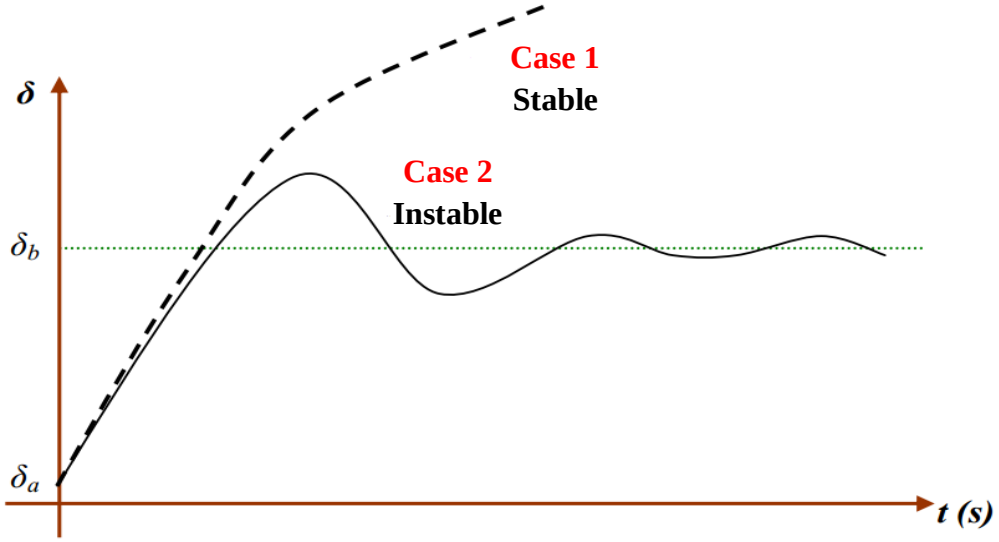

Figure I. 6. Rotor angle variation.

- The first area (area A_1, acceleration area) is located below the horizontal line corresponding to the initial operating point (the load line). It is limited by the two rotor angles (δ_0 and δ_1) corresponding to the appearance and disappearance of a fault. This zone is characterized by the kinetic energy stored by the rotor due to its acceleration: $P_m > P_e$.
- The second area (area A_2, deceleration zone), which begins after the fault elimination, is located above the load line: it is characterized by the deceleration of the rotor: $P_m < P_e$.

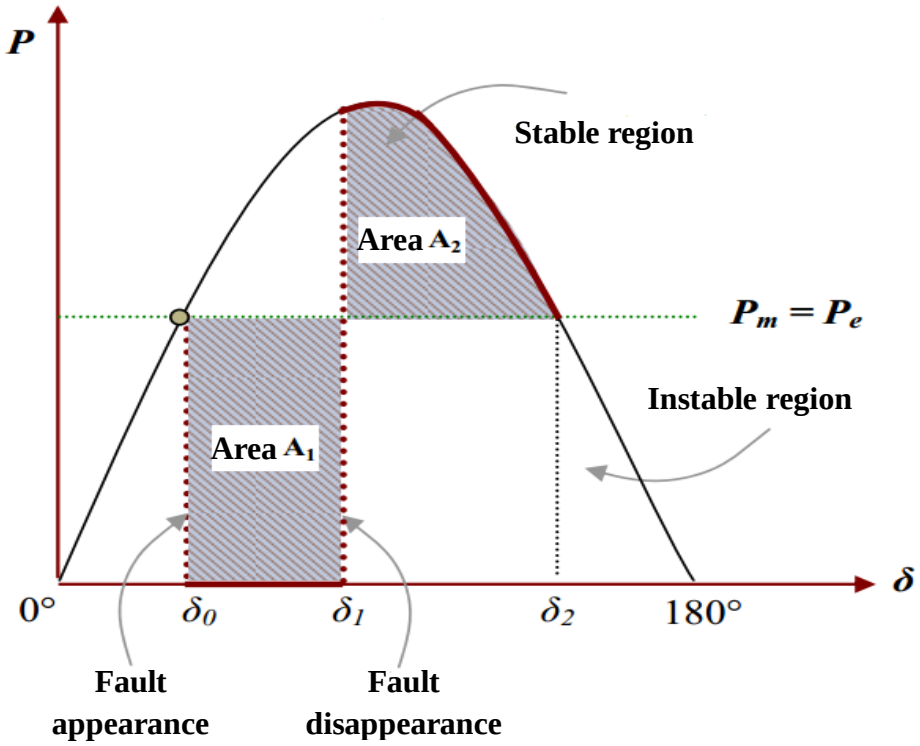

Figure I. 7. Power-angle curve of the generator following a transmission fault.

If the rotor can return in zone A2 all the kinetic energy acquired during the first phase, the generator will regain its stability. But if the A2 zone does not restore all the kinetic energy, the deceleration of the rotor will continue until the loss of synchronism.

The relation between the areas (A_1 and A_2) and the transient stability can be mathematically explained as follows:

Recall first of all that the equation of the generator motion is given by the following relation:

$$\frac{d^2\delta}{dt^2} = \frac{w_0}{2H}(P_m - P_e) \qquad \text{(I. 3)}$$

w_0: The speed of synchronism.

H: The inertia constant.

P_m: The mechanical power supplied to the generator.

P_e: The electric power of the generator

By multiplying this equation by $\frac{d\delta}{dt}$, and integrating with respect to time and making, we get:

$$\left(\frac{d\delta}{dt}\right)^2 + cte = \int_{\delta_0}^{\delta_2} \frac{\omega_0}{H}(P_m - P_e)\,.\,d\delta \qquad \text{(I. 4)}$$

δ_0: the initial rotor angle at the time of the fault application.
δ_2: the rotor angle at the end of the transitional period.

So when: t = 0 $\Rightarrow$ δ = 0, $\frac{d\delta}{dt} = 0$ $\Rightarrow$ the constant cte = 0.

After the fault has been eliminated, the angle δ will stop varying and the generator will return to its synchronous speed, when $\frac{d\delta}{dt} = 0$

Therefore, Eq (I. 4) is written as follows:

$$\int_{\delta_0}^{\delta_2}(P_m - P_e)\,.\,d\delta = 0 \qquad \text{(I. 5)}$$

$$\Rightarrow \qquad \int_{\delta_0}^{\delta_1}(P_m - P_e).d\delta + \int_{\delta_1}^{\delta_2}(P_m - P_e).d\delta = 0 \qquad \text{(I. 6)}$$

$$\Rightarrow \qquad A_1\text{-}A_2=0 \qquad \text{(I. 7)}$$

Thus, the transient stability restoration limit is expressed mathematically by the equality of the areas A_1 and A_2: this condition is called Equal Area Criterion.

Therefore, transient stability controllers can improve stability either by decreasing the acceleration area (area A_1) or by increasing the deceleration area (area A_2). This can be achieved either by increasing the electrical power or by decreasing the mechanical power.

I. 5. 1. 2. Small-Signal Stability Assessment Methods

Stability can be assessed by different methods. Eigenvalue analysis and modal analysis of the linearized power system are "powerful" tools to study the dynamic properties of the system. These methods are techniques that are used to determine whether the system is stable or unstable [23]. The following sections describe these techniques in detail.

I. 5. 1. 2. 1. Power System Linearization

The power system linearization method is suitable for analyzing small-signal stability disturbance. Any power system can be described by a set of differential and algebraic equations expressed as follows:

The generalized state equations are presented as follows:

$$\dot{x} = f(x, u) \tag{I. 8}$$

$$y = g(x, u) \tag{I.9}$$

Which:

$$\dot{x} = \begin{bmatrix} \dot{x}_1 \\ \dot{x}_2 \\ . \\ . \\ . \\ \dot{x}_n \end{bmatrix} \quad x = \begin{bmatrix} x_1 \\ x_2 \\ . \\ . \\ . \\ x_n \end{bmatrix} \quad u = \begin{bmatrix} u_1 \\ u_2 \\ . \\ . \\ . \\ u_r \end{bmatrix} \quad y = \begin{bmatrix} y_1 \\ y_2 \\ . \\ . \\ . \\ y_m \end{bmatrix} \quad f = \begin{bmatrix} f_1 \\ f_2 \\ . \\ . \\ . \\ f_n \end{bmatrix} \quad g = \begin{bmatrix} g_1 \\ g_2 \\ . \\ . \\ . \\ g_m \end{bmatrix}$$

x= state vector of the system of n variables.

$\dot{x}$= derived state vector of the system with respect to time.

u= vector of r input signals to the system.

y= vector of m system output signals.

f= vector of n non-linear functions connecting the state variables x_i and the input signals u_i to the derivatives of the state variables.

g = vector of m nonlinear functions relating the input signals u_i and the state variables to the output variables y_i.

Linearization of equations (I. 8) and (I. 9) is as follow:

Define that:

$$\dot{x}_0 = f(x_0, u_0) \tag{I. 10}$$

Where:

$\dot{x}_0$= derived state vector corresponding to the equilibrium point.

x_0= vector of the state variables corresponding to the equilibrium point.

u_0= input vector corresponding to the equilibrium point.

By applying a small disturbance to the equilibrium values

$$x = x_0 + \Delta x \tag{I. 11}$$

$$u = u_0 + \Delta u \tag{I. 12}$$

We find

$$\dot{x} = \dot{x}_0 + \Delta\dot{x} = f(x_0 + \Delta x, u_0 + \Delta u) \tag{I.13}$$

Since these perturbations are small, equation (I. 13) can be developed in Taylor series.

So, we get for each state variable:

$$\dot{x}_i = \dot{x}_{i0} + \Delta\dot{x}_i = f_i(x_0, u_0) + \frac{\partial f_i}{\partial x_1}\Delta x_1 + \cdots + \frac{\partial f_i}{\partial x_n}\Delta x_n + \frac{\partial f_i}{\partial u_1}\Delta u_1 + \cdots + \frac{\partial f_i}{\partial u_r}\Delta u_r \tag{I. 14}$$

With i=1,2,....,n

Given that, $f_i(x_0, u_0) = \dot{x}_{i0}$

$$\Delta\dot{x}_i = \frac{\partial f_i}{\partial x_1}\Delta x_1 + \cdots + \frac{\partial f_i}{\partial x_n}\Delta x_n + \frac{\partial f_i}{\partial u_1}\Delta u_1 + \cdots + \frac{\partial f_i}{\partial u_r}\Delta u_r \tag{I. 15}$$

We apply the same linearization steps to the equation (I. 9).

$$\Delta y_i = \frac{\partial g_j}{\partial x_1}\Delta x_1 + \cdots + \frac{\partial g_j}{\partial x_n}\Delta x_n + \frac{\partial g_j}{\partial u_1}\Delta u_1 + \cdots + \frac{\partial g_j}{\partial u_r}\Delta u_r \tag{I. 16}$$

With j=1,2,....,m

So, the linear state model of equations (I.8) and (I.9) are:

$$\Delta\dot{x} = A\,\Delta x + B\,\Delta u \tag{I. 17}$$

$$\Delta y = C\,\Delta x + D\,\Delta u \tag{I. 18}$$

With:

$$A = \begin{bmatrix} \frac{\partial f_1}{\partial x_1} & \cdots & \frac{\partial f_1}{\partial x_n} \\ \vdots & \ddots & \vdots \\ \frac{\partial f_n}{\partial x_1} & \cdots & \frac{\partial f_n}{\partial x_n} \end{bmatrix} \quad , \quad B = \begin{bmatrix} \frac{\partial f_1}{\partial u_1} & \cdots & \frac{\partial f_1}{\partial u_r} \\ \vdots & \ddots & \vdots \\ \frac{\partial f_n}{\partial u_1} & \cdots & \frac{\partial f_n}{\partial u_r} \end{bmatrix} \tag{I. 19}$$

$$C = \begin{bmatrix} \frac{\partial g_1}{\partial x_1} & \cdots & \frac{\partial g_1}{\partial x_n} \\ \vdots & \ddots & \vdots \\ \frac{\partial g_m}{\partial x_1} & \cdots & \frac{\partial g_m}{\partial x_n} \end{bmatrix} \quad , \quad D = \begin{bmatrix} \frac{\partial g_1}{\partial u_1} & \cdots & \frac{\partial g_1}{\partial u_r} \\ \vdots & \ddots & \vdots \\ \frac{\partial g_m}{\partial u_1} & \cdots & \frac{\partial g_m}{\partial u_r} \end{bmatrix} \tag{I. 20}$$

Where:

A: state matrix (n × n).

B: input matrix (n × r).

C: output matrix (m × n).

D: control matrix (m × r).

Matrix A is called the state matrix or evolution matrix, because it contains the description of the dynamic behavior of the system. It also reports on the evolution of the system in free regime, i.e. at zero command. Matrix B is called the control matrix or input matrix. It reports on the dynamic behavior of the system in response to a command. The matrix C is called the observation matrix. It connects the output to the state. The matrix D is finally called the direct action matrix which directly links the control to the output. It is generally zero in physical systems.

I. 5. 1. 2. 2. Eigen-values Analyses

After having established the linear state model, the characterization of the system stability can be done from the dynamic matrix A and its eigenvalues (first Lyapunov method).

Consider a linear system defined by the state model (I. 17), (I. 18) By the use of the Laplace transform, the above equations in the frequency domain can be obtained:

$$s\Delta x(s) = A\,\Delta x(s) + B\,\Delta u(s) \tag{I. 21}$$

$$\Delta y(s) = C\,\Delta x(s) + D\,\Delta u(s) \tag{I. 22}$$

So, the formal solution of the state system is:

$$\Delta y(s) = C(sI - A)^{-1}B\,\Delta u(s) + D\,\Delta u(s) \tag{I. 23}$$

Where I is the identity matrix

Thus, the dynamic response of the system is determined by the characteristic equation of the state matrix A defined by:

$$\det(\lambda I - A) = 0 \quad \text{(I.24)}$$

The values λ which satisfy the preceding equation are called the eigenvalues of the system. An eigenvalue defines the movement of the system linked to an eigenfrequency.

An eigenvalue -a mode- is characterized by an oscillation frequency and damping. It is generally represented by the following complex number:

$$\lambda = \sigma \pm j\omega \quad \text{(I. 25)}$$

This relation is equivalent to the relation defining the eigenvalues of a second order system. As a result:

$$\lambda = -\omega_n \varepsilon \pm j\omega_n \sqrt{1 - \varepsilon^2} \quad \text{(I. 26)}$$

Where: σ is the real part of the eigenvalue (abscissa of convergence).

ω is the proper oscillation pulsation (rad / s).

ω_n: is the natural oscillation pulse (rad / s).

ε :is the oscillation damping factor.

An n × n state matrix is associated with n eigenvalues.

The analysis of the eigenvalues makes it possible to first obtain the oscillation frequency and the damping factor.

The natural frequency of oscillation (Hz) is given by the following relation:

$$f = \frac{\omega}{2\pi} \quad \text{(I. 27)}$$

The damping factor determines the decrease in the amplitude of oscillation. It is given by:

$$\varepsilon = \frac{-\sigma}{\sqrt{\sigma^2 + \omega^2}} \quad \text{(I. 28)}$$

In a linear model, the solution of the system linear equations describes the exponential evolution over time of the disturbance. Thus, this solution can be represented by a combination of exponential functions $e^{\lambda,t}$representing the temporal characteristics associated with each eigenvalue λ_i. The time constants $\tau = \frac{1}{\sigma_i}$ generally characterize the damping of the system.

The physical interpretation of the signals corresponding to the functions of the form $e^{\lambda i,t}$ is simple. It is illustrated by Fig (I. 4) which represents in the complex plane the shape of the variations of such signals as a function of time, according to the position of the representative point of λ_i.

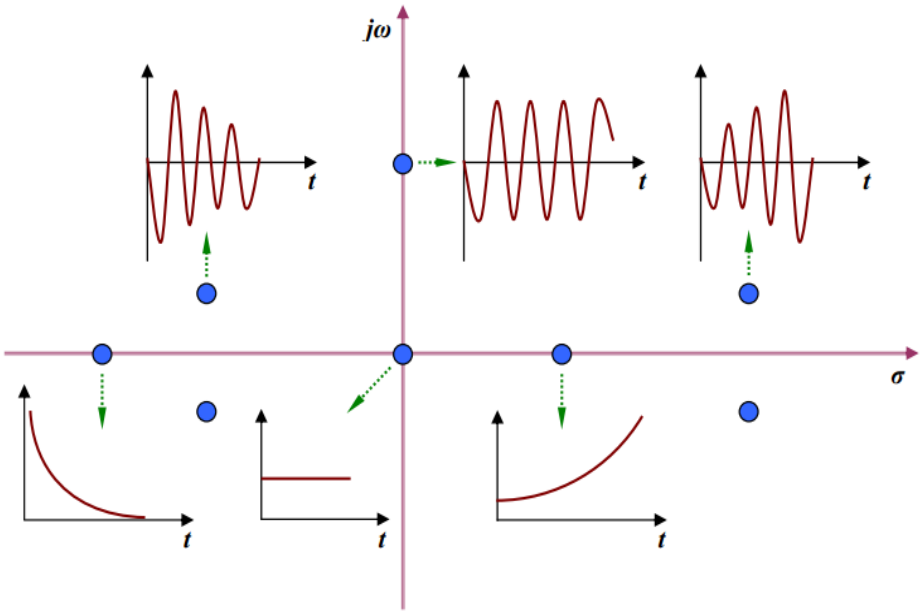

Figure I. 8. Analysis of the system stability by poles location.

A real eigenvalue corresponds to a non-oscillatory mode. If the real eigenvalue is negative, the exponentials appearing in the temporal response are decreasing functions of time. The decay rate is related to the damping time constant. The greater is the value of the convergence abscissa σ, the faster is the damping time constant. On the other hand, if the real eigenvalue is positive, the mode presents an aperiodic instability.

On the other hand, the complex eigenvalues, in conjugate pairs, correspond to the oscillatory modes. The oscillatory mode can be divergent (unstable), if the real part of the eigenvalue is positive, it is on the contrary damped (stable), if the real part is negative.

This analysis reveals that it is possible to determine the nature (stable or unstable) of a linear system from an "inspection" of the system transfer function poles position in the complex plane. In addition, knowledge of the poles position can provide information on the system behavior during typical transient conditions such as the response to an impulse, to a step,….

In power system, it is obviously necessary that all modes of the system are stable i.e. placed in the left part of the complex plan.

I. 5. 1. 2. 3. Modal analysis (Residues)

This method arose from the relationship between the transfer function and the state model. To determine the relationship between the transfer function and the state model, we take equations (I. 21) and (I. 22) for a mono-variable system, and we consider the transfer function between the variables y and u.

Suppose that D = 0, the state equations are written as follows:

$$\Delta \dot{x} = A\,\Delta x + B\,\Delta u \quad \text{(I. 29)}$$

$$\Delta y = C\,\Delta x \quad \text{(I. 30)}$$

The transfer function $\frac{\Delta y(s)}{\Delta u(s)}$ is written as follows:

$$G(s) = \frac{\Delta y(s)}{\Delta u(s)} = C(sI - A)^{-1}B \quad \text{(I. 31)}$$

For an open loop system, the function G (s) can be broken down into simple elements as follows:

$$G(s) = \frac{R_1}{s-\gamma_1} + \frac{R_2}{s-\gamma_2} + \cdots + \frac{R_n}{s-\gamma_n} = \sum_{i=1}^{n} \frac{R_i}{s-\gamma_i} \quad \text{(I. 32)}$$

Where:

s: Laplace operator.

$\gamma_1, \gamma_2, \ldots, \gamma_n$: Poles of G (s) - the eigenvalues of the system.

$R_1, R_2, \ldots, R_n$: residues of G (s).

The figure (I.4) shows a system G (s) equipped with a transfer function feedback controller H (s).

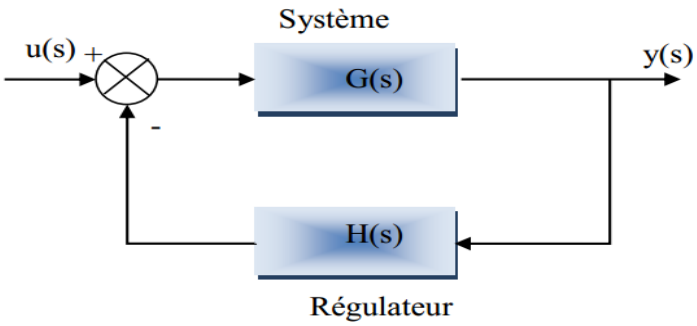

Figure I. 9. The closed loop system-controller assembly.

When the loop is closed by a regulator H (s), the eigenvalues of the initial system G (s) will move. The displacement of these eigenvalues can be calculated by the following equation:

$$\gamma_i = R_i H(\gamma_i) \quad \text{(I. 33)}$$

This equation shows that the displacement of the eigenvalues, created by the controller, is proportional to the amplitudes of the corresponding residues.

I. 5. 1. 2. 4. Simulation analysis

It is a method of analysis in the time domain. Oscillations in the power system can be directly observed, this provides more accurate information on the amplitude of the oscillations and their damping than other methods.

However, this method requires a large number of modeling work, information and data of the studied power system.

I. 6. Preventive Measures to Avoid System Instability

In power system design and preparation stage, a wide number of disturbances have to be assessed by system operators. If the system is found to be unstable (or marginally stable) following any contingency, variety of actions can be taken to improve the system stability [9]. These preventive actions can be classified mainly into Offline and online preventive actions. Offline preventive measures: Improvement of system stability can be achieved by many actions including:

- Organizing the system configuration and maintenances in such that being suitable for the particular operating conditions without overloading during abnormal conditions.
- Reduction of transmission system reactance which can be achieved by adding additional parallel transmission circuits, providing series compensation on existing circuits and by using transformers with lower leakage reactance.
- Activating new generation facilities for reactive power support and voltage control service such as power system stabilizers, FACTs, distributed generation technologies, and rapid thermal units with fastvalving capability and fast acting automatic excitation systems.
- Connecting dynamic breaking resistors at the generator and substation terminals in order to break the acceleration of the rotor of generators during faults. Shunt resistors can be switched in to create an artificial load following a fault, in order to improve the damping of accelerated generators.
- Installing efficient protective devices and coordinating between the interconnected system operators for faster fault clearing and initiating proper corrective actions during abnormal conditions.

Online remedial and preventive measures: The operation of interconnected power system is economically oriented based competitive manner in the most cases. This complicates the ability of Offline preventive measures to keep the power system away from the stability limits. This produces the importance of system operators to use online DSA and operating the power system within these limits. There are many online preventive measures can be used to safeguard and enhance system stability such as:

- Changing the system topology such as tripping of critical generator to ensure that the other generators maintain in synchronism. In addition, generation rescheduling/re-dispatching can be used to reallocate power generation in order to avoid system overloads and relieve constraints.
- Using of high-speed protective schemes such as transmission line protection with single-pole tripping and adaptive reclosing capabilities to minimizes system disturbance. High-speed automatic reclosing system is effective methodology to restore power continuity.
- Effectively use of online transformer tap-changers and phase shifting transformers to control the power flow across transmission system by continuous control of voltage regulator set points and changing the phase using taps.
- Automatic load shedding of interruptible consumers is an effective corrective counter-measure to maintain the frequency at nominal value during abnormal conditions. In the simple implementation, under-frequency relays installed at fixed points and with fixed settings can be made adaptive by adjusting the location and level of shedding in accordance with power flow and voltage conditions on the transmission network.
- Implementation of high-speed excitation systems to rapidly boosts field voltage in response to disturbances. Increasing of the internal voltage of a generator has the effect of proving transient stability.

I. 7. Conclusion

Stability must be carefully studied because it allows continuity of service on power system after possible disturbances. Stability depends on the type of disturbance, the duration of the disturbance, the operating point before the fault, the protection systems and the dynamic characteristics of the network elements (generators, loads, regulators, etc.). Depending on the simulation techniques used, the stability can be analyzed and evaluated by various methods.

Chapter II

Power System Modeling For Stability Analysis

II. 1. Introduction

To study the stability of a power system we need a fairly representative mathematical model. Furthermore, to establish a power system model for dynamic studies, we only take into account equipments in operation during the time range of the dynamic phenomenon considered [33]. The result is therefore a model composed of algebraic and non-linear differential equations. Thus, modern power systems are characterized by increasing size and complexity. More the dimension of power system increases, more the dynamic processes and analysis of the underlying physical phenomena complexity will be. In addition to their size and complexity, power systems exhibit non-linear and time-varying behavior. Non-linearity can be introduced by elements with discontinuous operation such as relays, thyristors,… , and by elements with hysteresis or saturation,….. .Nowadays, this structural complexity increasingly impacts the evolution of stability problems and dynamic phenomena in interconnected power systems [34-36].

The major components of a power system can be represented by a block diagram as shown in figure (II.1). This representation does not show all the dynamic interactions between elements and their controls, but it can be used as a general description for dynamic structures. Study of the power system dynamic performance is very important for the system operators (economic point of view) and the society in general (reliability point of view). An essential step in this type of study is to understand physically and mathematically the dynamic phenomena of interest. Then, the modeling and simulation performed of the system can reflect its critical behavior.

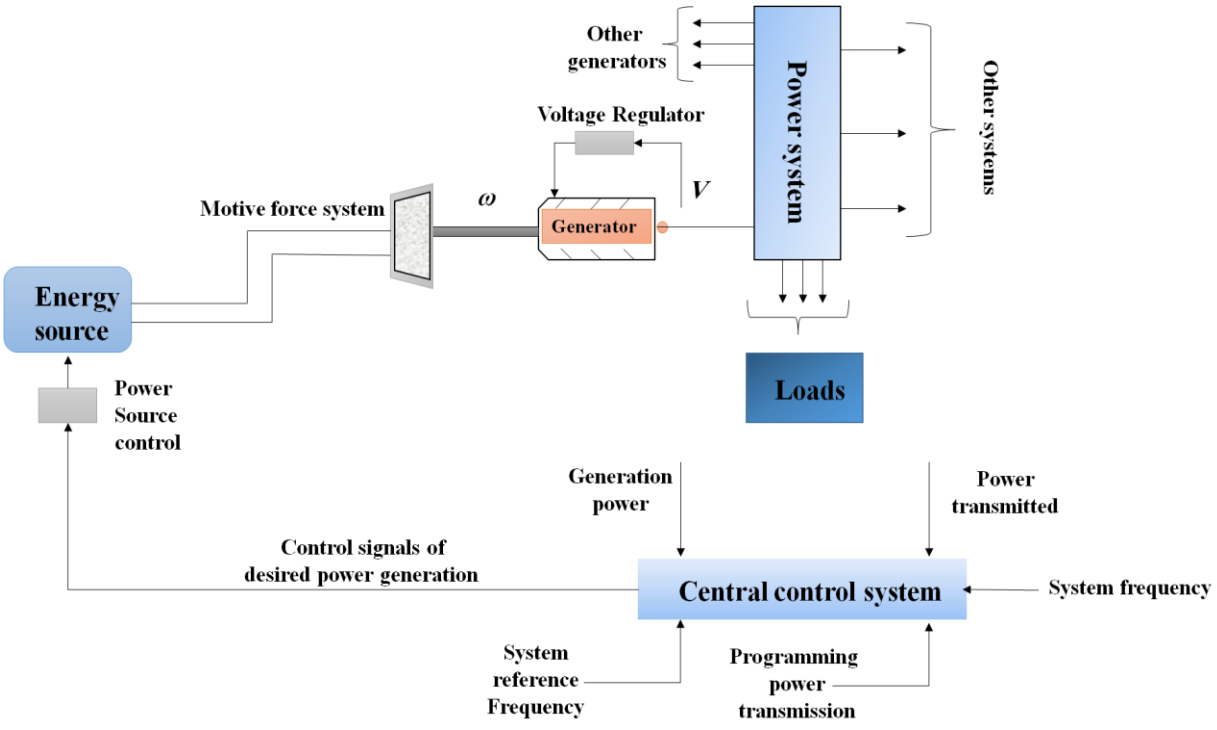

Figure II. 1. General structure of a power system.

II. 2. General power system nonlinear model

II. 2. 1. Simplifying assumptions of the model

In order to simplify the mathematical representation, we have adopted the following assumptions.

- The frequency remains constant which makes it possible to preserve the network reactance elements notion [37].
- The three-phase network behavior is balanced and therefore it is possible to work with the network single-phase representation.
- The network elements do not show mutual impedance with each other.
- The transmission lines are represented by circuits in π, and transformers by a series circuit (linear admittances).
- We admit that the loads supplied by the network are all passive and linear, similar to impedances [38, 39].

II. 2. 2. Generator model

Electrical energy is generally produced by synchronous machines. The latter are characterized by a rotational speed of the machine shaft equal to the rotational speed of the rotating field. To obtain such an operation, a mechanical torque resulting from a primary source of energy, such as hydraulic energy, nuclear energy or chemical energy, is applied to the axis of the synchronous machine via an intermediate mechanical link, that is depends on the turbine [40, 41]. The rotor magnetic field is usually generated by an excitation circuit powered by direct current. The position of the rotor magnetic field is then fixed with respect to the rotor: this imposes in normal operation an identical rotation speed between the rotor and the rotating stator field. Thus, the stator windings are subjected to magnetic fields which vary periodically. An emf AC current is therefore induced in the stator [42].

Synchronous generators play an extremely important role in dynamic phenomena and in the overall quality of the power supply. It is therefore necessary to develop practical and realistic models of synchronous machines. In this chapter, we will present and discuss a model suitable for the analysis of dynamic stability [43].

II. 2. 2. 1. Synchronous machine model in the Park's reference

In the ideal machine, the stator has three windings marked a, b and c, shifted by 120 degrees. The rotor has a number of windings, distributed over two axes: the d-axis (direct axis) which coincides with that of the excitation winding and the q-axis (quadratic axis) located in advance quadrature with respect to the direct axis as shown in Fig (II. 2).

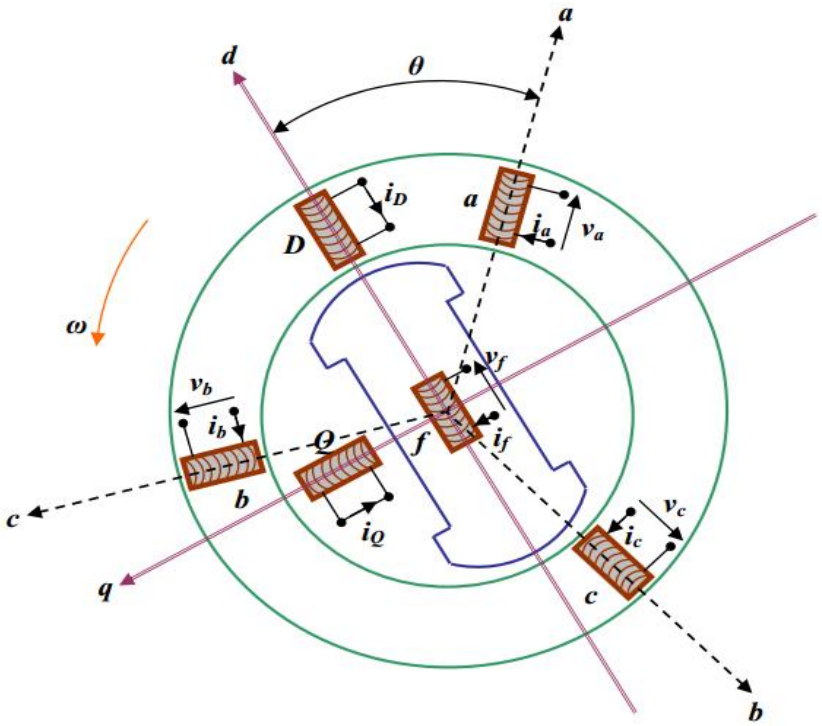

Figure II. 2. Modeling of the idealized synchronous machine.

To eliminate the non-linearity between the magnitudes of the stator and those of the rotor, the windings of the machine must be ordered along two perpendicular axes, each machine is modeled in its local reference (d-q) rotating with its rotor [44]. To formalize the coupling between the system equations and establish the equations describing the behavior of the overall system, all the voltages and currents must be represented in a single reference common to all machines. Usually, a reference rotating at synchronous speed is used as a common reference. Such an approach can be achieved by Park transformation [45, 46].

Fig (II. 3) gives the equivalent model in the Park coordinate system (d-q). The different windings in the two representations are as follows:

- The three stator windings denoted a, b and c, and their equivalent windings denoted d_s and q_s.
- The direct axis includes the excitation winding noted f, and a damping winding noted d_a.
- The quadrature axis comprises a damping winding denoted q_a.

Finally, note that the excitation winding is subjected to a voltage V_f while the circuits d_a, q_a are permanently short-circuited.

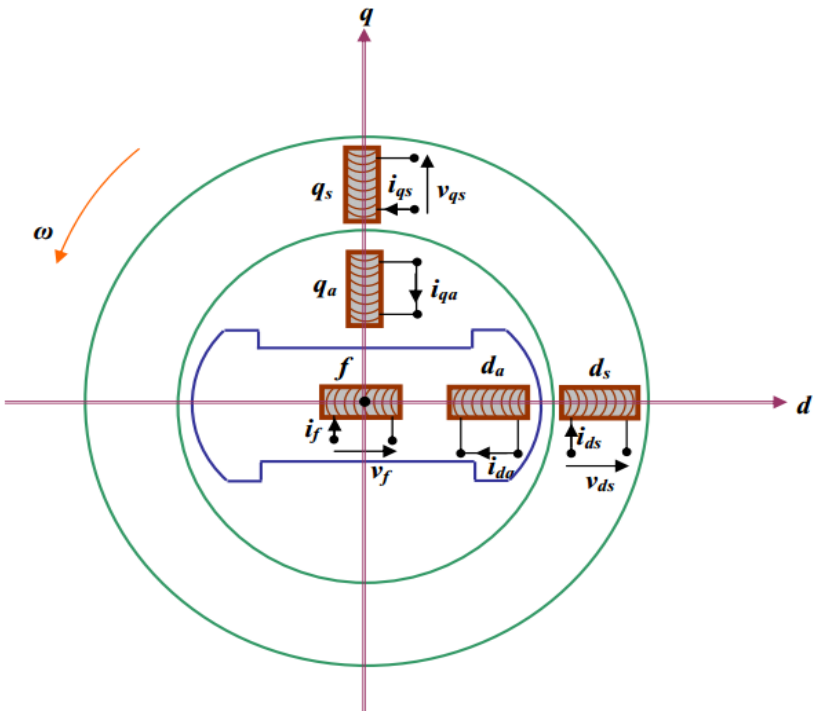

Figure II. 3. Synchronous machine model in the Park's reference.

II. 2. 2. 2. Assumptions of the model

The generator model and its controls are usually limited to ordinary differential equations coupled together via the power system algebraic equations. Each differential equation expresses the derivative of a state variable (such as rotor angle, excitation voltage, ...) as a function of other state variables and algebraic variables. The number of differential equations describing the generator model defines the order of the model [47]. There are several models, ranging from the simplest, the classic model representing only the electromechanical characteristics of the generator, to the more complex, namely the eighth order model taking into account all rotor, stator, damping and field circuits saturation. In studies of electromechanical oscillations, the generator model must represent two fundamental characteristics: the electrical characteristics of the excitation windings and the mechanical characteristics of the generator shaft [48].

The assumptions considered to establish this model are based on neglecting the influence of:

- Rotor and stator resistors.
- Damping windings.
- Saturation field.
- Transient phenomena in the stator.
- The speed variation in the stator voltage equations (thus, $\omega_r = \omega_0 = 1$ [p.u]), (this assumption is made to compensate for the effect of the cancellation of transient phenomena in the stator).

This model also neglects the damping produced by Foucault currents in the rotor body (the transient emf following the d axis, namely E'_d, is assumed to be constant). So, since there is no winding on the quadrature axis to represent the rotor body, we will have:

$E'_d = 0, \quad X'_q = X_q$

E'_d: induced emf of the generator along the d axis, in p.u.

X'_q: q axis synchronous reactance, in p.u.

X_q: q axis transitory reactance, in p.u.

Finally, we assume that the rotor angle δ (angular position of the rotor with respect to the rotating reference at synchronism) coincides with the angle of the internal voltage of the generator.

The resulting model is the third order model. It is described by the following state variables [37]:

E'_q: Induced emf of the generator along the q axis, in p.u.

ω: Angular speed of the rotor, in p.u.

δ : rotor angle, in rad.

This model, well suited for the study of dynamic stability, is the simplest. It is widely used in eigenvalue analysis and parameter setting of power stabilizers [39].

II. 2. 2. 3. Electrical equations

In this section we take an i^{th} machine of a multimachine power system to determine the algebraic equations of the synchronous machine stator, which are equations concerning the voltages along the d and q axes and the electric powers.

The electrical quantities of this machine are shown in Fig (II. 4). Before starting the calculation, we can make the following remarks:

- The reference (d_i, q_i) concerns the i^{th} machine alone, while the reference (D, Q) is common to all machines of the system.
- The torque angle δi between D and qi, represents the position of the i^{th} machine frame reference (d, q) with respect to the common frame reference (D, Q): it varies constantly over time and can be positive or negative.

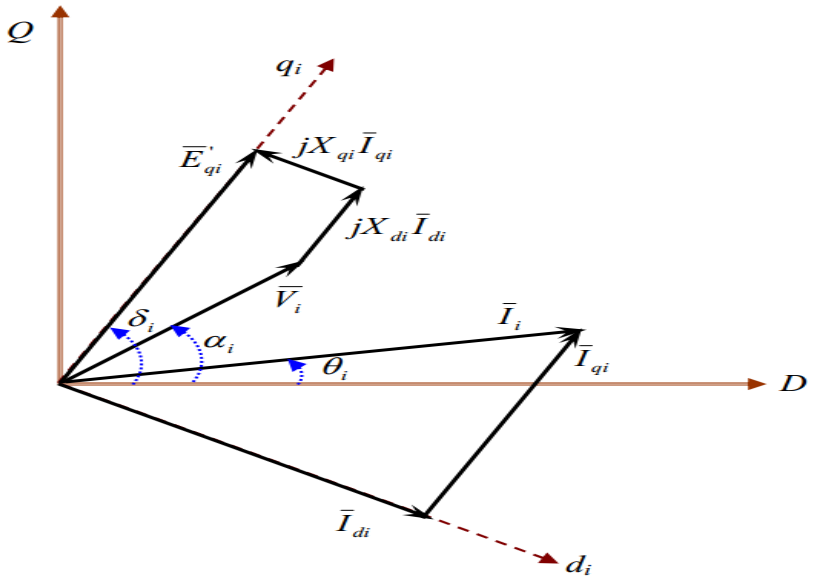

Figure II. 4. Phasors relating to the i[th] machine of a multi-machine system.

From Fig (II. 4), the terminal voltage V_i of the i[th] machine can be determined by the following equation:

$$\overline{V_i} = \overline{E'_{qi}} - jX'_{di}\,\overline{I_{di}} - jX_{qi}\,\overline{I_{qi}} \qquad \text{(II. 1)}$$

Let us note in the common reference (D-Q) the following expressions:

$$\overline{E'_{qi}} = E'_{qi}\,e^{j\delta_i} \qquad \text{(II. 2)}$$

$$\bar{I}_{qi} = I_{qi}e^{j\delta_i} \qquad \text{(II. 3)}$$

$$\bar{I}_{di} = I_{di}e^{j(\delta_i - 90°)} \qquad \text{(II. 4)}$$

$$\overline{V_i} = V_i e^{j\alpha_i} \qquad \text{(II. 5)}$$

By introducing Eq (II. 2,3) into Eq (II. 1), we obtain:

$$V_i e^{j\alpha_i} = E'_{qi}e^{j\delta_i} - X'_{di}I_{di}e^{j\delta_i} - jX_{qi}I_{qi}e^{j(\delta_i + 90°)} \qquad \text{(II. 6)}$$

After arrangement:

$$V_i e^{-j(\delta_i - \alpha_i)} = E'_{qi} - X'_{di}I_{di} - jX_{qi}I_{qi} \qquad \text{(II. 7)}$$

$$V_i\cos(\delta_i - \alpha_i) - jV_i\sin(\delta_i - \alpha_i) = E'_{qi} - X'_{di}I_{di} - jX_{qi}I_{qi} \qquad \text{(II. 8)}$$

By separating real part and imaginary part, we obtain the following expressions of V_d and V_q:

$$\begin{cases} V_{di} = X_{qi} I_{qi} \\ V_{qi} = E'_{qi} - X'_{di} I_{di} \end{cases} \quad \text{(II. 9)}$$

Considering Eq (II. 2,3) and the following relation: $\overline{I_i} = \overline{I_{di}} + \overline{I_{qi}}$, Eq(II. 1) can therefore be rewritten as follows:

$$\bar{V}_i = E'_{qi} e^{j\delta_i} - jX'_{di} \bar{I}_i + jX'_{di} e^{j\delta_i} - jX_{qi} I_{qi} e^{j\delta_i} \quad \text{(II. 10)}$$

For n machines in a multi-machine system, Eq (II. 10) can be written in the following matrix form:

$$[\bar{V}] = [E'_q][e^{j\delta}] - j[X'_d][\bar{I}] + j[X'_d - X_q][I_q][e^{j\delta}] \quad \text{(II. 11)}$$

In this last equation, the terms: $[\bar{V}]$, $[E'_q]$, $[\bar{I}]$ and $[I_q]$ are column vectors of dimension n and the coefficients $[e^{j\delta}]$, $[X'_d]$ and $[X'_d - X_q]$ are diagonal matrices.

The electrical powers (apparent, active and reactive) of the ith machine are given by:

$$\overline{S_i} = P_{ei} + j\, Q_{ei} = \overline{V_i}\, \overline{I_I^*} = (V_{di} + jV_{qi})(I_{di} - jI_{qi}) \quad \text{(II. 12)}$$

Therefore,

$$\begin{cases} P_{ei} = V_{di} I_{di} + V_{qi} I_{qi} \\ Q_{ei} = V_{qi} I_{qi} - V_{di} I_{qi} \end{cases} \quad \text{(II. 13)}$$

Since the transient phenomena in the stator are neglected, the electric torque is therefore equal to the active electric power in per-unit. So $T_{ei} = P_{ei}$.

II. 2. 2. 4. Mechanical equations

The equation of rotor motion describes the mechanical properties of synchronous machines. This equation is fundamental in the study of electromechanical oscillations. In steady state operation, all synchronous machines in the system rotate at the same angular speed. The mechanical torque Tm is the same as the rotation direction of the generator axis. The electric torque Te is in the opposite direction to rotation and this torque balances the mechanical torque [49], Fig (II. 5). During a disturbance, one or more generators can be accelerated or slowed down and there is therefore a risk of losing synchronism. This can have a big impact on the stability of the system and the generators losing synchronism must be disconnected, otherwise they could be severely damaged.

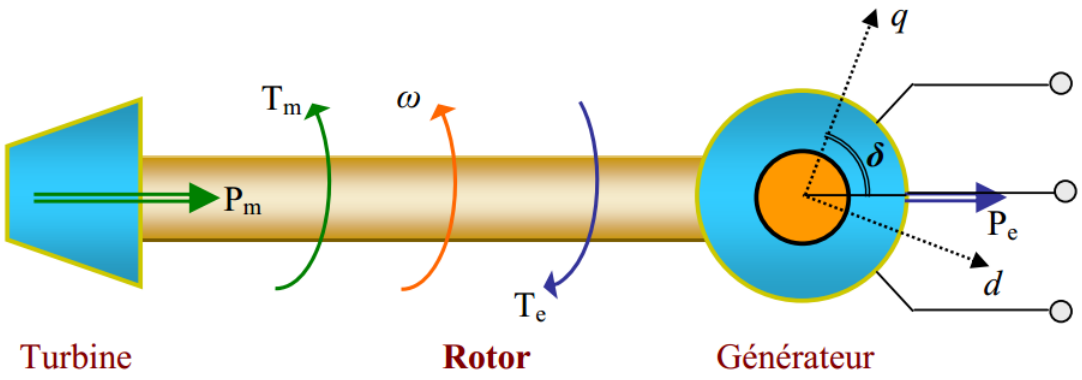

Figure II. 5. Mechanical and electrical couples acting on the axis of a generator.

For a multi-machine system, if there is an imbalance of the torques acting on the rotor of the i[th] machine, the latter will accelerate or slow down according to the following equation of motion:

$$\Delta\dot{\omega}_i = \frac{1}{2H_i}(T_{mi} - T_{ei}) \qquad \text{(II. 14)}$$

H_i is the inertia constant (in seconds) representing the total inertia of all rotating masses connected to the generator shaft.

For oscillations at low frequencies, the current induced in the damping windings is negligible. Therefore, the damping windings can be completely neglected in the modeling of the system. If the damper windings are ignored, the damping torque produced by them is also negligible. To take into account the neglected component of the torque, we introduce in the equation of motion a compensation term D (also called damping coefficient) in p.u, [41, 50]. This coefficient represents the natural damping of the system: it prevents the increase of oscillations, unless a negative damping source is introduced (such as the voltage regulator of the excitation system). The equation of motion can therefore be rewritten as follows:

$$\Delta\dot{\omega}_i = \frac{1}{2H_i}(T_{mi} - T_{ei} - D_i(\Delta\omega_i - 1)) \qquad \text{(II. 15)}$$

The equation for the rotor angle of the i[th] machine is given by:

$$\dot{\delta}_i = \omega_0\,(\Delta\omega_i - 1) \qquad \text{(II. 16)}$$

Where,

$\Delta\omega_i$: Angular speed deviation of the i[th] machine rotor, in p.u.

ω_0 : Synchronism speed (basic speed), in rad / s.

($\omega_0 = 2\pi f$, f: nominal frequency, in Hz).

T_{mi}: Mechanical torque supplied by the turbine, in p.u.

T_{ei}: Electromagnetic torque associated with the electrical power P_{ei} produced by the generator, $T_{ei} = \frac{P_{ei}}{W_i}$ (en p.u).

D_i: Generator damping coefficient, in p.u.

δ_i: Rotor angle, in rad.

II. 2. 2. 5. Generator regulation

Synchronous machines in the system must be able to maintain the balance (generation/ demand) of active and reactive powers under various operating conditions. Moreover, balanced sinusoidal voltages must be guaranteed with constant amplitudes and frequencies.

If the active power balance is not assured, the synchronism frequency in the system will be affected, while a reactive power imbalance will cause some buses voltage disturbances from their reference values [51].

To ensure satisfactory generation of electrical energy, for a large number of operating points, the mechanical torque T_m applied to the rotor and the excitation voltage E_{fd} must be systematically adjusted to accommodate any variation in the system.

The system responsible for generating the mechanical torque and thus driving the generator rotor is called the "motive power system". The frequency control (or active power control) associated with this system maintains the nominal speed of the generators. Thereby, ensuring a constant frequency. Furthermore, the excitation system is responsible for the excitation voltage supplied to the generator. The associated voltage regulator (or reactive power regulator) modifies the values of the excitation system to finally obtain the desired voltages at the terminals of the generator [52].

II. 2. 2. 5. 1. Frequency regulator

A motive power system Fig (II. 6), consists of the primary power source, the turbine (fitted with a servomotor) and the frequency regulator (governor) [53].

The turbine converts the potential energy of the source into rotational energy of the shaft (rotor) on which the alternator is placed. The alternator converts the mechanical power supplied by the turbine into electrical output power. The speed of the turbine shaft is measured precisely and compared to the reference speed. The frequency (speed) regulator then acts on the servomotor to open and close the control valves and therefore change the speed of the generator. Thus, the role of the turbine is to drive the rotor of the generator at the synchronous speed corresponding to the frequency of the power system.

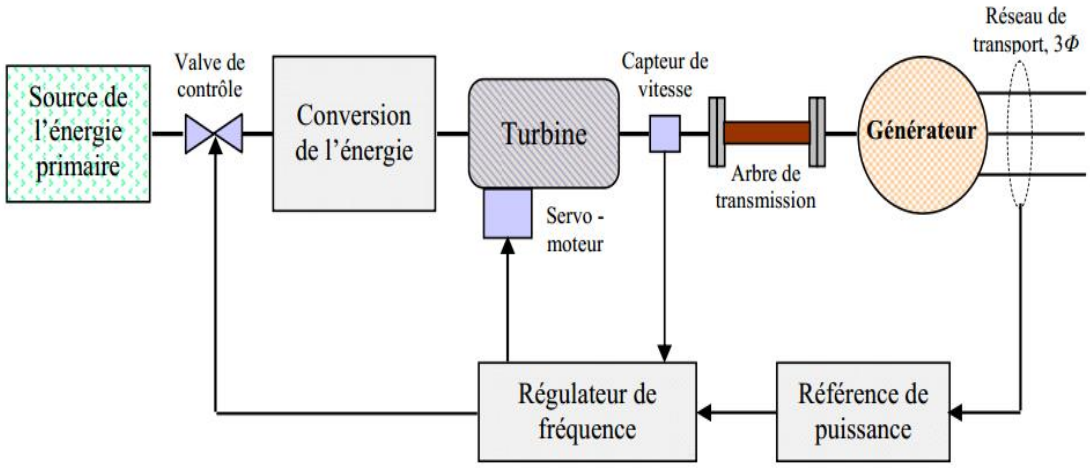

Figure II. 6. General structure of a motive power system - generator.

The governor forms a feedback loop which monitors the speed of the rotor at all times. Consider for example a disturbance of the active power balance. In the first seconds, the corresponding energy will be taken from the kinetic energy of the rotating masses of the production units. This will cause a disturbance in the speed of rotation of these units. This speed deviation must be detected and corrected automatically by the governors. These governors must change the inlet of fluid (steam, gas or water) in the turbines in order to bring the speeds and therefore the frequency of the network, around their nominal values.

In any power system, it is very important to keep the frequency within a narrow range around its nominal value (50 or 60 Hz). Strict compliance with this value is not only necessary for the correct functioning of the loads, but it is also an indicator of the balance between active power produced and consumed [42].

In the analysis of transient or dynamic stability, the temporal response of the driving force system to a disturbance is considered slower than the study range of the stability concerned (typically between 10 and 20 seconds). Thus, the model of the motive power system can be greatly simplified. For a transient stability analysis lasting a few seconds, the model of the driving force system can be deleted considering that the mechanical torque of the turbine remains constant [44]. Its weak influence on the behavior of electromechanical oscillations associated with stability at small disturbances can also be neglected. Thus, it is not used when establishing the linear model of the power system associated with this type of stability.

II. 2. 2. 5. 2. Voltage regulator and model of the excitation system

The excitation system is an auxiliary system that powers the excitation windings of the synchronous machine so that the latter can provide the required level of reactive power. In steady state, this system provides direct current and voltage, but it must also be able to vary the excitation voltage rapidly in the event of a disturbance on the network [47].

Currently, various excitation systems are employed. Three main types can be identified (IEEE, 2005):

1- Direct current excitation systems -DC-:
They use a DC generator with collector as a power source for the excitation system.

2- Alternating current excitation systems -CA-:
They use an alternator and static or rotating rectifiers to produce the direct current needed in the synchronous machine excitation winding.

3- Static excitation systems (ST systems):
In this case, the excitation current is supplied by a controlled rectifier. Its power is supplied either directly by the generator through a transformer giving the appropriate level of voltage, or by auxiliary windings mounted in the generator.

The excitation systems are equipped with controllers, usually called automatic voltage regulators (AVR), Fig (II. 7). These controllers are very important for the balance of reactive power that will be supplied or absorbed according to the needs of the loads. In addition, these controllers represent a very important means of ensuring the transient stability of the power system. The voltage regulator acts on the excitation current of the alternator to regulate the magnetic flux in the machine and "return" the output voltage of the machine to the desired values. A very important characteristic of a voltage regulator is its ability to vary the excitation voltage rapidly.

The IEEE task forces group periodically presents recommendations for the modeling of power system components including excitation systems. Several models are suggested for each type of excitation system (IEEE, 2005). Static excitation systems are the most widely installed today, we therefore chose in our study to use the IEEE-ST1A system model, the model most used in the literature. This type of excitation system is characterized by its speed and sensitivity (IEEE, 2003):

- Its time constant Ta is low, normally of the order of a few milliseconds.
- Its Ka gain is high, generally between 200 and 400 per-unit.

Fig (II. 8) shows the model of the excitation system and its voltage regulator used in our study.

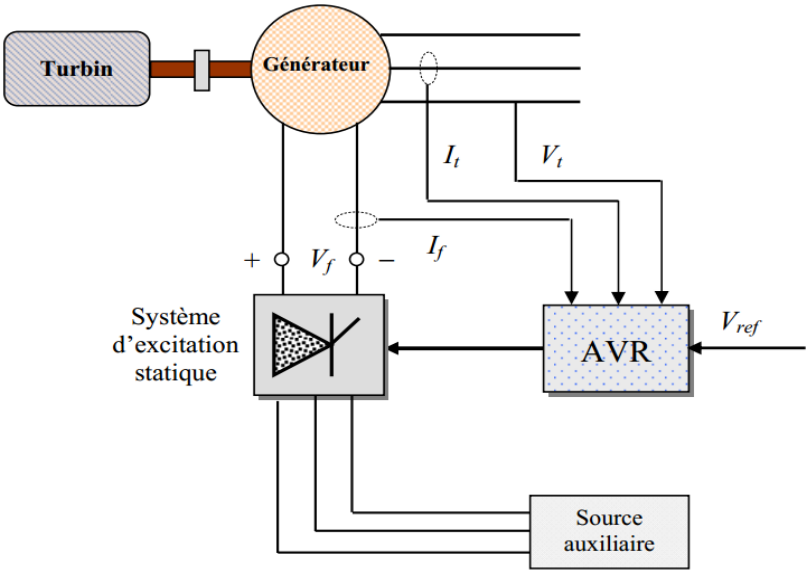

Figure II. 7. General structure of a static excitation system with its AVR.

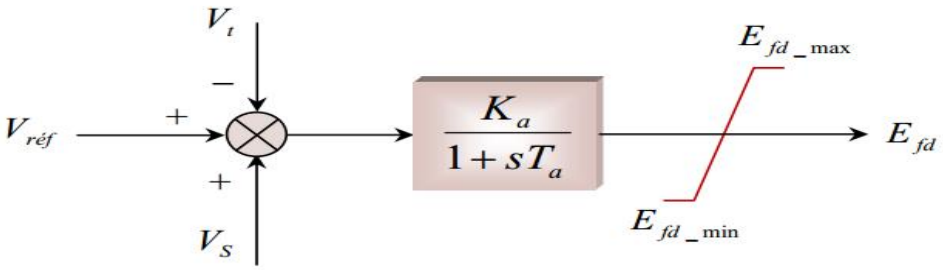

Figure II. 8. Simplified model of the IEEE-type ST1A excitation system.

The quantity V_{ref}, is the voltage set point determined to meet the conditions of the balanced state. The voltage regulator compares the signal V_t (a continuous signal proportional to the rms value of the alternating voltage of the generator) with the set point voltage V_{ref}. A complementary signal V_S can be added to the comparison node: this is a signal from certain specific control devices such as power stabilizers (PSS). Then the error signal is amplified to give the requested excitation voltage E_{fd}. The time constant and the gain of the amplifier are T_a and K_a respectively. The extreme values of the excitation voltage (E_{fd_max}, E_{fd_min}) are set by a limitation system.

The following relation describes, all calculations done, the functioning of the model:

$$\dot{E}_{fd} = \frac{1}{T_a}(K_a(V_{réf} - V_t + V_s) - E_{fd} \qquad \text{(II. 17)}$$

The relationship between the excitation voltage E_{fd} and the internal voltage of the generator E'_q is given as follows:

$$\dot{E}'_q = \frac{1}{T'_{do}}\left(E_{fd} - (X_d - X'_d)I_d - E'_q\right) \qquad \text{(II. 18)}$$

II. 2. 3. Transmission power system

The electrical transmission system connects all the power plants in a power system and distributes the power to the different consumers. The main elements of the transmission power system are high voltage overhead lines, underground cables, transformers and buses. Auxiliary elements can be found like: series capacitors, shunt reactors, compensation systems and protection systems…, [35].

II. 2. 3. 1. Transformers model

The transformer is used to increase the amplitude of the alternating voltage available at the output of the production unit to bring it to the levels required for transport. At the other end of the chain, on the consumer side, transformers are used to lower the voltage and bring it back to the values used in the -BT- distribution networks.

Besides the transmission of electrical energy with modification of the voltages, transformers can be used to control the power system buses voltage [40]. This voltage control uses the number variation of transformer turns. Fig (II. 9) shows the equivalent diagram of the transformer (without magnetic circuit): it is equipped with several taps (high voltage side) allowing the primary turns number modification. The ZT impedance corresponds to the total equivalent impedance at primary view.

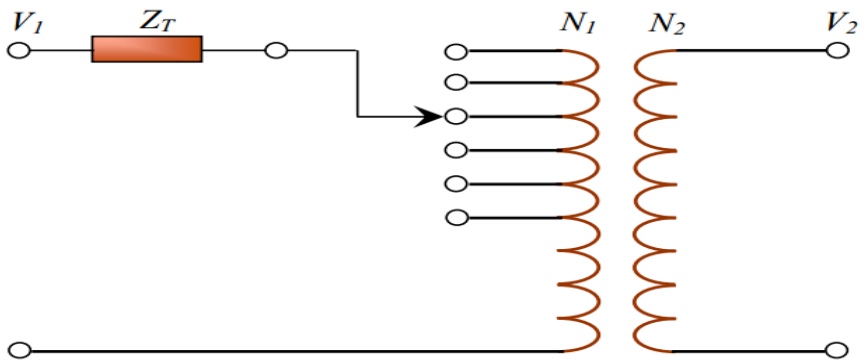

Figure II. 9. Simplified transformer model.

If N_1 is the high voltage turns number and N_2 is the low voltage turns number, the transformation ratio M is defined by:

$$M = \frac{N_1}{N_2} \quad \text{(II. 19)}$$

The relationship between the voltage on the primary side V_1 and the voltage on the secondary side V_2 when it's not loaded is:

$$V_2 = \frac{V_1}{M} \quad \text{(II. 20)}$$

Fig (II. 10) represents the equivalent diagram in π of the transformer without magnetic circuit (Milano, 2005). In our study, the on-load regulators are not modeled: thus the transformation ratio remains fixed during the dynamic simulations. However, we take this into account when calculating the power flow, so that the voltages remain within their allowable limits and the convergence of the power flow algorithm remains assured [33].

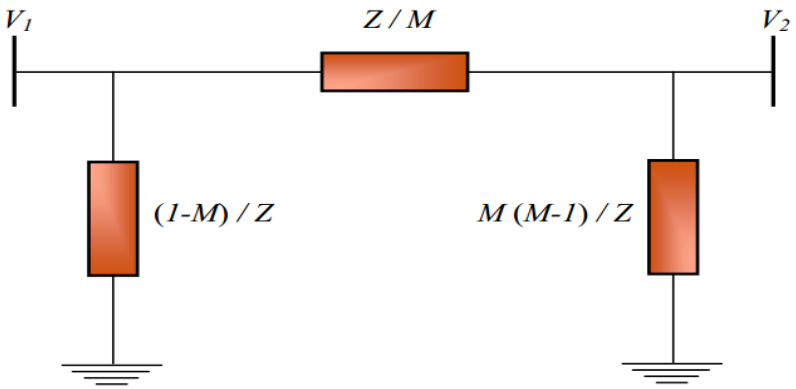

Figure II. 10. Simplified transformer model.

II. 2. 3. 2. Transmission lines model

The transmission power lines provide a link between the power plants and the consumption areas. They also allow power to be exchanged across interconnection lines, between countries or large areas under different grid operators [41].

Transmission line models used in dynamic analysis of power system are usually classified into three groups, based on line lengths, (long, medium, short). Taking into account the lengths and the operating frequency, typically 50-60 Hz, a transmission line is characterized by a model with localized constants (the propagation phenomena are neglected because $L << \lambda / 2\pi$, where λ is the length wave associated with frequency f. The structure most used for this model is the equivalent diagram in π, Fig (II. 11). It is characterized by three main parameters [54]:

- A series resistor R.
- An inductive reactance X
- A capacitive reactance B

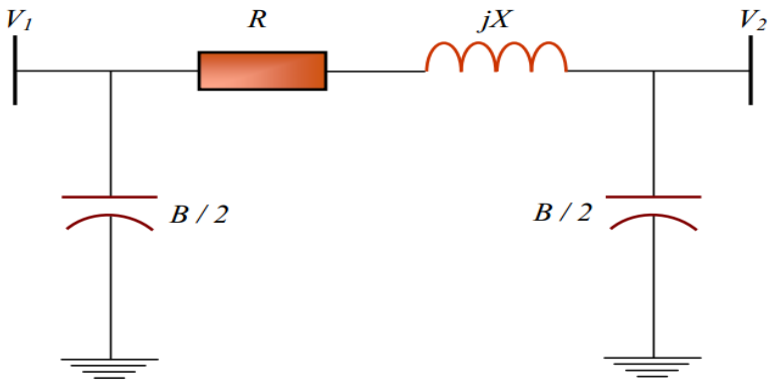

Figure II. 11. Model of the transmission line.

II. 2. 4. Loads model

The loads characteristics have an important influence on the stability and dynamics of the system. Due to the complexity and continual variation of loads and the difficulty of obtaining accurate data on their characteristics, accurate modeling of loads is very difficult. Thus, simplifications are essential depending on the purpose of the requested study. For stability studies in which the time range considered is of the order of 10 seconds after the disturbance, the most used load models are generally static models. The static character is linked to the description of the charge by purely algebraic equations [43].

Let be a voltage node VL, to which a load consuming a power $P_L + jQ_L$ is connected. This load can be represented by static admittances $G_L = P_L / V_L^2$ and $B_L = Q_L / V_L^2$ as shown in Fig (II. 12) [39].

The equivalent load admittance is calculated after determining the necessary data from the power flow study:

$$G_L = \frac{P_L}{V_L^2} \; ; \; B_L = -\frac{Q_L}{V_L^2} \qquad \text{(II. 21)}$$

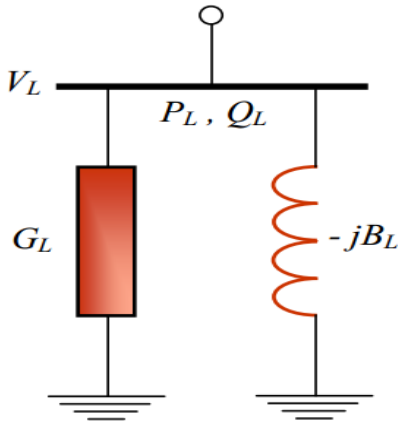

Figure II. 12. Modeling of a load by its equivalent admittance.

II. 2. 5. Transmission power system equations

Establishment of the transmission power system generalized model and loads involves determining the algebraic equations representing the interconnections between the circuits of the generators and all of the transformers, transmission lines and loads of the system. The problem is thus to determine and to put into equations the functioning of the macro-model of the transmission power system. The power system can be described in the following matrix form:

$$[\bar{I}] = [\bar{Y}].[\bar{V}] \quad \text{(II. 22)}$$

$[\bar{I}]$: Currents vector injected at the power system buses.

$[\bar{V}]$: Voltages vector of the power system buses.

$[\bar{Y}]$: Power system admittance matrix.

Let's start with the "construction" of the admittance matrix$[\bar{Y}]$. This matrix consists of diagonal terms $[\bar{Y}]_{ii}$ and non-diagonal terms and $[\bar{Y}]_{ij}$

- Terms $[\bar{Y}]_{ii}$, (self admittance), represent the sum of all admittances connected to node i.
- Terms $[\bar{Y}]_{ij}$ (mutual admittance), represent the sum of all admittances joining nodes i and j.

Starting from the idea that all the power system buses except the ones of the generators have no current injection, the principle of the Kron method can thus be applied for the reduction of the network.

Knowing that the sum of all currents in each load node is zero, the load nodes in Eq (II. 22) can therefore be eliminated. Eq (II. 22) is then written as follows [42]:

$$\begin{bmatrix} \bar{I}_n \\ \dots \\ 0 \end{bmatrix} = \begin{bmatrix} \bar{Y}_{nn} \vdots \bar{Y}_{nr} \\ \cdots \cdots \dots \\ \bar{Y}_{rn} \vdots \bar{Y}_{rr} \end{bmatrix} . \begin{bmatrix} \bar{V}_n \\ \dots \\ \bar{V}_r \end{bmatrix} \quad \text{(II. 23)}$$

Where,

n: Is the index of generator buses.

r: Is the index of the remaining buses.

m: Is the index of all the power system buses.

By decomposing the matrix Eq (II. 23), we obtain the following system of equations:

$$[\bar{I}_n] = [\bar{Y}_{nn}].[\bar{V}_n] + [\bar{Y}_{nr}].[\bar{V}_r] \quad \text{(II. 24)}$$

$$0 = [\bar{Y}_{rn}].[\bar{V}_n] + [\bar{Y}_{rr}].[\bar{V}_r] \quad \text{(II. 25)}$$

This system of equations can be reformulated as follows:

$$[\bar{I}_n] = [\bar{Y}_{bus}].[\bar{V}_n] \quad \text{(II. 26)}$$

$$[\bar{Y}_{bus}] = [\bar{Y}_{nn}] - [\bar{Y}_{nr}].[\bar{Y}_{rr}]^{-1}.[\bar{Y}_{rn}] \quad \text{(II. 27)}$$

Where: $[\bar{Y}_{bus}]$ is the power system reduced admittance matrix, because the dimension of this matrix has been reduced from m × m to n × n.

By introducing Eq (II. 11) into Eq (II. 26), we obtain:

$$[\bar{I}] = [\bar{Y}_m].\left[\left[E'_q\right]\left[e^{j\delta}\right] + j\left[X'_d - X_q\right]\left[I_q\right]\left[e^{j\delta}\right]\right] \quad \text{(II. 28)}$$

With,

$$[\bar{Y}_m] = \left[[\bar{Y}_{bus}]^{-1} + j[X'_d]\right]^{-1} \quad \text{(II. 29)}$$

Where, $[\bar{Y}_m] = [Y_m]\left[e^{j\beta}\right]$ represents the total admittance matrix of the reduced power system.

The current of the ith machine in the n-machine power system is written in the (D-Q) reference as follows:

$$\bar{I}_i = \sum_{j=1}^{n} Y_{mij} e^{j\beta ij} (E'_{qj}\, e^{j\delta j} + j(X'_{dj} - X_{qj}) I_{qj} e^{j\delta j}) \quad \text{(II. 30)}$$

Including the term j = i.

By breaking down Eq (II. 30), we obtain the expressions for the ith machine current along the direct and quadrature local axe (d,q):

$$I_{di} = \sum_{j=1}^{n} Y_{mij} \left(-S_{ij} E'_{qj} + (X_{qj} - X'_{di}) C_{ij} I_{qj})\right) \quad \text{(II. 31)}$$

$$I_{qi} = \sum_{j=1}^{n} Y_{mij} \left(C_{ij} E'_{qj} + (X_{qj} - X'_{di}) S_{ij} I_{qj})\right) \quad \text{(II. 32)}$$

With:

$$C_{ij} = \cos(\beta_{ij} + \delta_{ij}) \quad \text{(II. 33)}$$

$$S_{ij} = \sin(\beta_{ij} + \delta_{ij}) \quad \text{(II. 32)}$$

$$\delta_{ij} = \delta_j - \delta_i \quad \text{(II. 33)}$$

The set of these current equations supplemented by the corresponding voltage equations represent the algebraic part of the general state model presented later.

II. 2. 6. Generalized state equations of the model

As we presented in the first chapter, a power system is a nonlinear dynamic system, which can be described by a set of coupled nonlinear ordinary differential

equations of the first order and a set of algebraic equations, where the general forms of these sets of differential and algebraic equations can be expressed as Eq(I. 2) and Eq(I. 3). Differential equations correspond to the dynamic operations of generators, excitation systems and other elements of the system. The algebraic equations correspond to the transmission power system and the generators stators. The solution of these two groups of equations determines the electromechanical state of the system at all times.

We recall below the non-linear equations describing the power system model:

$$\Delta\dot{\omega}_\iota = \frac{1}{2H_i}(T_{mi} - T_{ei} - D_i(\Delta\omega_i - 1)) \quad \text{(II. 34)}$$

$$\dot{\delta}_\iota = \omega_0\,(\Delta\omega_i - 1) \quad \text{(II. 35)}$$

$$\dot{E}_{fd} = \frac{1}{T_a}(K_a\big(V_{réf} - V_t + V_s\big) - E_{fd} \quad \text{(II. 36)}$$

$$\dot{E}'_q = \frac{1}{T'_{d0}}\big(E_{fd} - (X_d - X'_d)I_d - E'_q\big) \quad \text{(II. 37)}$$

$$T_{ei} = E'_{qi}I_{qi} + (X'_{qi} - X'_{di})I_{di}I_{qi} \quad \text{(II. 38)}$$

$$V_{di} = X_{qi}I_{qi} \quad \text{(II. 39)}$$

$$V_{qi} = E'_{qi} - X'_{di}I_{di} \quad \text{(II. 40)}$$

$$V_{ti} = \sqrt{V_{di}^2 + V_{qi}^2} \quad \text{(II. 41)}$$

$$I_{di} = \sum_{j=1}^{n} Y_{mij}\left(-S_{ij}E'_{qj} + (X_{qj} - X'_{di})C_{ij}I_{qj})\right) \quad \text{(II. 42)}$$

$$I_{qi} = \sum_{j=1}^{n} Y_{mij}\left(C_{ij}E'_{qj} + (X_{qj} - X'_{di})S_{ij}I_{qj})\right) \quad \text{(II. 43)}$$

When the derivatives of the state variables x are zero, (i.e. $\dot{x} = 0$), the system is at equilibrium. Thus, this equilibrium point is the point at which all state variables are constant and the operation of the system around this point is linear. Fig (II. 13) represents the elements of the power system model with their interactions.

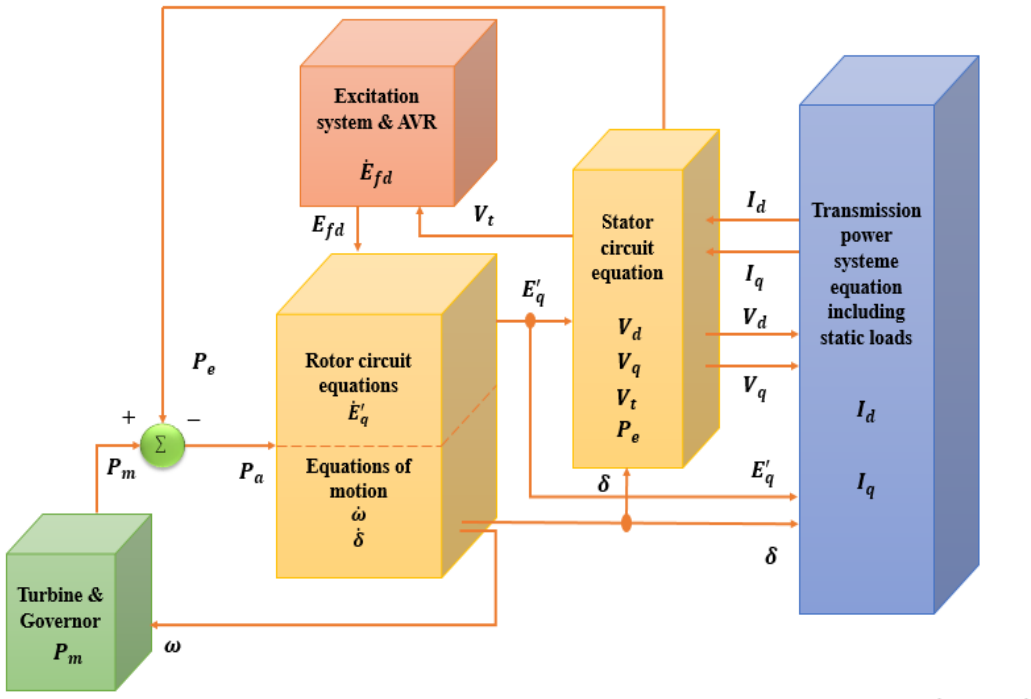

Figure II. 13. Diagram of all the blocks of the power system.

II. 3. Linear model of the power system

When the power system is subjected to a small disturbances, the system state variables remain in the vicinity of their initial values and the system linearization can be easily applied [55].

The state variables proposed for our power system of n machines, represented by a set of equations as follows:

$$\Delta x_i = \left[\Delta\omega_i \ , \ \Delta\delta_i \ , \ \Delta E'_{qi} \ , \ \Delta E'_{fdi}\right]^T \quad \text{i} = 1, \ldots, \text{n} \qquad \text{(II. 44)}$$

Where,

$$\Delta\dot{\omega}_\iota = \frac{1}{2H_i}\left(-D_i\Delta\omega_i - \sum_{j=1}^{n}(K_{1ij}\,\Delta\delta_j) - \sum_{j=1}^{n}(K_{2ij}\,\Delta E'_{qj})\right) + \frac{1}{2H_j}\Delta T_{mi} \qquad \text{(II. 45)}$$

$$\Delta\dot{\delta}_\iota = \omega_0\Delta\omega_i \qquad \text{(II. 46)}$$

$$\Delta\dot{E'_{q\iota}} = \frac{1}{T'_{doi}}\left(-\sum_{j=1}^{n}\left(K_{4ij}\Delta\delta_j\right) - \sum_{j=1}^{n}\left(\frac{1}{K_{3ij}}\Delta E'_{qj}\right) + \Delta E_{fdi}\right) \qquad \text{(II. 47)}$$

$$\Delta\dot{E'_{fd\iota}} = \frac{1}{T_{ai}}\left(-K_{ai}\sum_{j=1}^{n}(K_{5ij}\,\Delta\delta_j) - K_{ai}\sum_{j=1}^{n}(K_{6ij}\,\Delta E'_{qj}) + \Delta E_{fdi}\right) + \frac{K_{ai}}{T_{ai}}\Delta U_{si} \qquad \text{(II. 48)}$$

The linearization constants K_{1ij}… K_{6ij} are square matrices of order n. The values of these constants depend on the parameters of the generators, the transmission network and the initial conditions of the system. The diagonal elements of the matrices of the constants determine the dynamic properties of machines, while non-diagonal elements represent dynamic interactions between machines.

This linear state model will therefore be used to analyze the stability of the system.

II. 4. Introduction to PSS Controller

The additional control of the AVR excitation system, known as the PSS (Power System Stabilizer) has became the most widespread means for improving the damping of low frequency oscillations in power system. The output power of a generator is determined by the mechanical torque. However, the latter may vary by the action of the generator excitation field. The PSS being added, it detects the electrical output power variation and controls the excitation system so as to quickly dampen the power oscillations.

A PSS allows adding a voltage signal proportional to the change in rotor speed to the input of the generator's voltage regulator (AVR) Fig (II. 14). Therefore, the entire excitation control system (AVR and PSS) must ensure the following points.

- Support the first oscillations before a large disturbance; i.e. ensuring the transient stability of the system.
- Maximize the damping of electromechanical oscillations associated with local modes. As well as interregional modes without negative effects on other modes.
- Minimize the probability of adverse effects, namely: local instabilities in the desired action band of the control system and be robust enough to allow the control system to meet its targets for various likely operating points.

A good result can be obtained if the input of the PSS is the rotor variation speed ($\Delta\omega$), the variation of the generated power (ΔPe) or the output frequency (Δf). Since the PSS is used to produce an electric torque proportional to the speed variation, it therefore appears more suitable to use the speed variation ($\Delta\omega$) as an input to the PSS. However, regardless of the input signal, the transfer function of the PSS must compensate the phase characteristics of the excitation system, electrical parts of the generator, and other electrical parts of the system. All of these determine the transfer function between the input of the excitation system (ΔVer) and the generator electrical torque (ΔTe) [36]. This transfer function is denoted GEP (s).

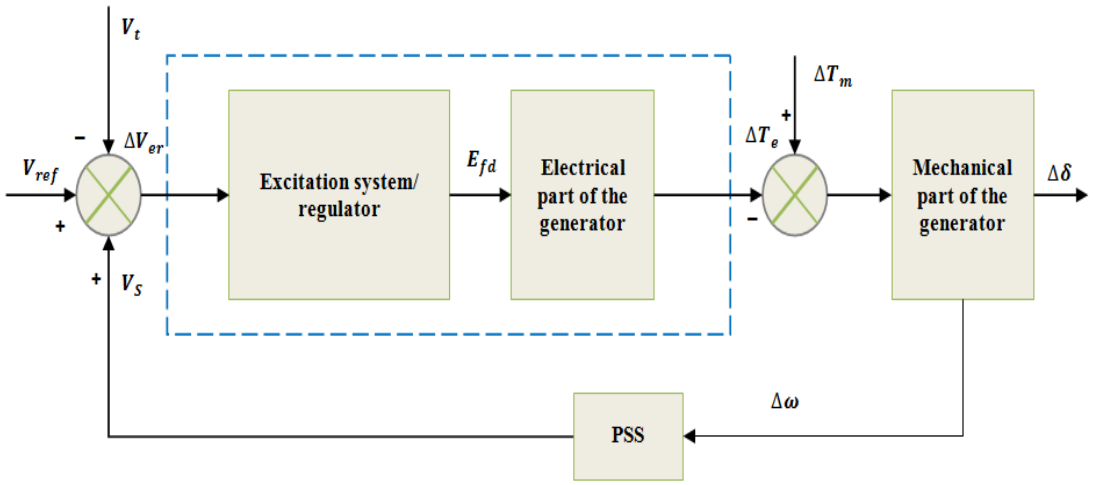

Figure II. 13: Simplified model of connection between a PSS and the AVR

The most widely used type of PSS is known as conventional PSS (or lead / lag PSS). This type has shown its high efficiency in maintaining stability at small disturbances. This PSS uses the rotor speed variation as input. It generally consists of four blocks: an amplifier block, a high pass "washout filter" block, a phase compensation block and a limiter. Fig (II. 14):

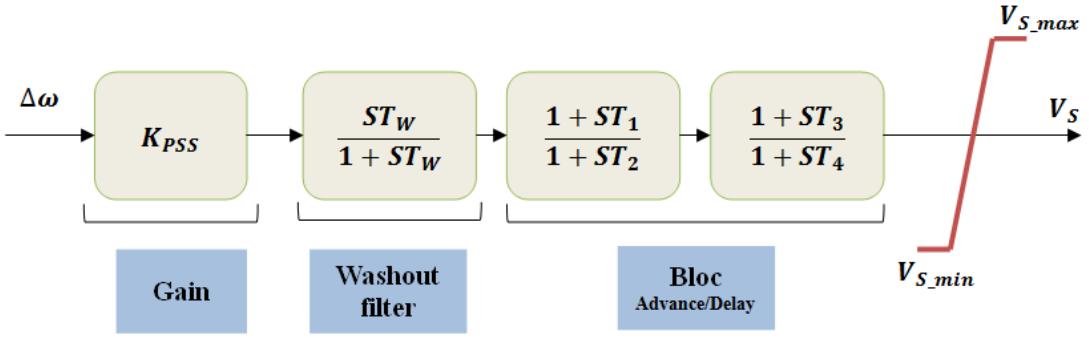

Figure II. 13: conventional PSS model.

II. 4. 1. PSS composition blocks

II. 4. 1. 1. Amplifier

It determines the damping value introduced by the PSS. Theoretically, its value (K_{PSS}) should correspond to the maximum damping. However, the value of the gain must satisfy the damping of the system dominant modes without risking degrading the stability of the other modes or the transient stability [34]. Generally, KPSS generally ranges from 0.01 to 50 [49].

II. 4. 1. 2. High pass filter "washout filter"

It eliminates very low frequency oscillations (less than 0.2 Hz) presented in the input signal. It also removes the DC component of the speed (the "DC" component corresponding to the static regime): the PSS therefore only reacts when there are

variations in speed. The time constant of this filter (T_W) must be large enough to allow signals which are in the useful band, to be transmitted without attenuation. However, it should not be too large to avoid leading to unwanted generator voltage variations during islanding conditions. Typically, T_W range is from 1 to 20 seconds [49].

II. 4. 1. 3. Phase compensation filter

The origin of the negative damping is associated with the phase delay introduced between the generator electric torque (ΔTe) and the input of the excitation system (ΔVer). Therefore, the PSS provides the necessary phase advance to compensate the phase delay of the GEP(s) transfer function. In practice, a pure advance phase block is not sufficient to achieve the necessary phase compensation. Thus, a phase (advance / delay) block is often used. To better guarantee the stability of the system, two stages (at least) of phase compensations are necessary. The transfer function of each stage is a simple combination of pole-zero, with the lead (T_1, T_3) and lag (T_2, T_4) time constants adjustable. The range of each time constant generally extends from 0.01 to 6 seconds [35]. But for considerations of physical realization, the delay time constants (T_2, T_4) are considered fixed and generally around the value of 0.05 seconds.

II. 4. 1. 4. Limiter

The PSS is designed to improve the damping of the system in the event of small variations around an equilibrium point. Its goal is not to restore system stability to severe disturbances (transient stability). The PSS sometimes has a tendency to disrupt the proper functioning of the voltage regulator by saturating it when the latter tries to maintain the voltage during transient conditions. Thus, the PSS must be equipped with a limiter in order to reduce its undesirable influence during the transient phases. The minimum and maximum values of the limiter range from ± 0.02 to 0.1 per-unit [35].

II. 4. 2. Adjusting PSS Parameters

The problem in designing a PSS is to determine the values of its parameters to increase the damping of the target modes and ensure robust stabilization. The minimization of the probable risks of unfavorable interactions between the oscillatory modes concerned by the PSS and the other modes of the system also represents an important critical point which influences its adjustment. In addition, PSS parameters should be adjusted without adversely affecting the restoration of transient stability.

Many methods are proposed in the literature for adjusting PSS parameters. Generally, most of these methods are based on the analysis of the system eigenvalues.

II. 4. 2. 1. Phase compensation method

To explain the setting of the PSS parameters by the phase compensation method, we take a simple system consisting of a generator connected to an infinite bus. The linear model of this system can be graphically illustrated by the Heffron-Philips representation, as shown in Fig (II. 14). The terms K1,…, K6 are the linearization constants.

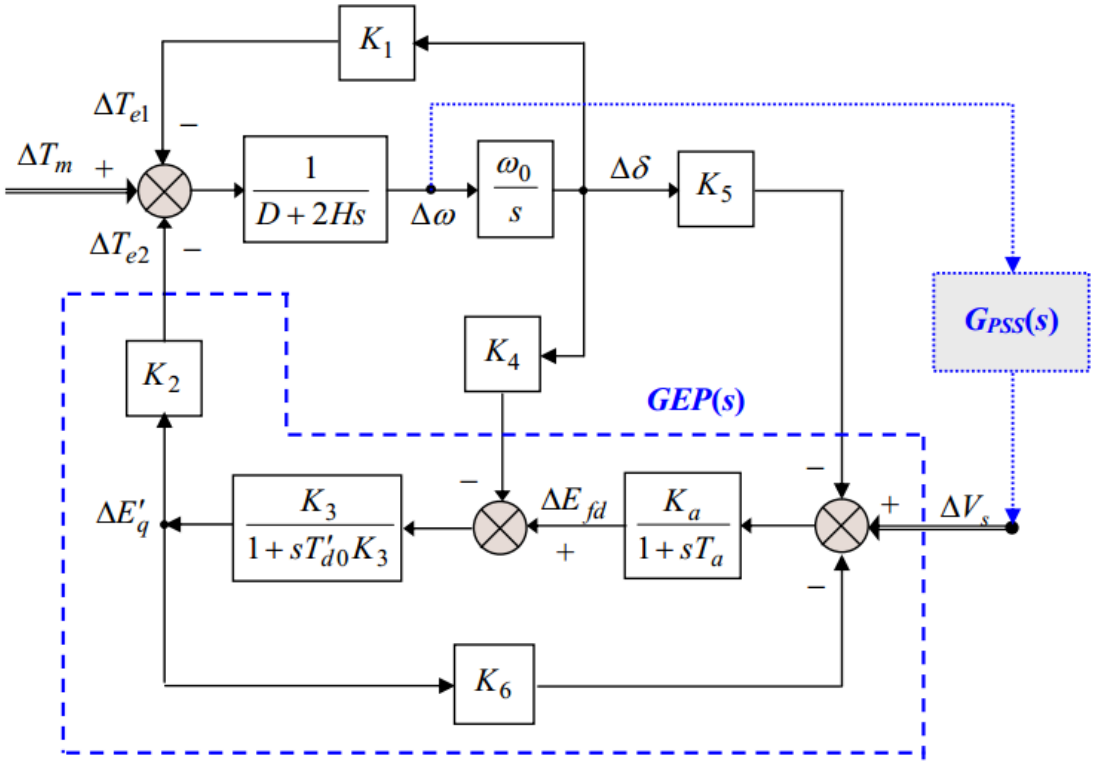

Figure II. 14: Heffron-Phillips model (single-machine - infinite bus).

The main objective of a PSS is to introduce an electrical torque component to the rotor of the synchronous machine; this torque is proportional to the difference between the current speed of the rotor and the speed of synchronism. When the rotor oscillates, this torque acts as a damping torque to dampen oscillations.

The GEP (s) transfer function and the phase delay of the electrical loop can be derived from the Heffron-Philips model. They are given by the following two relations.

$$GEP(s) = \frac{K_a K_3 K_2}{(1+sT_a)(1+sT'_{do}+K_a K_3 K_6)}\Big|_{s=\lambda=\sigma+j\omega} \quad \text{(II. 49)}$$

$$Phi_{GEP} = \arg(GEP(s)|_{s=\lambda=\sigma+j\omega}) \quad \text{(II. 50)}$$

With $\lambda = \sigma + j\omega$ is the eigenvalue calculated for the system without stabilization signal.

To simplify, we consider that the PSS parameters to be adjusted are the gain K_{pss} and the time constants T_1 and T_3 (with $T_1 = T_3$); the other parameters are fixed (with $T_2 = T_4$). Thus, the transfer function of PSS can be rewritten as follows:

$$G_{PSS}(s) = K_{PSS} \frac{sT_w}{1+sT_w}\left(\frac{1+sT_1}{1+sT_2}\right)^2 = K_{PSS}.G_f(s) \quad \text{(II. 51)}$$

Since the phase advance of the PSS (Phi_{PSS}) is equal to the phase Phi_{GEP}, the time constant T_1 is given, after all calculations, by the following relation:

$$T_1 = T_3 = \frac{\tan(\beta)}{\omega - \sigma \cdot \tan(\beta)} \quad \text{(II. 52)}$$

With,

$$\beta = \frac{1}{2}\left(-Phi_{GEP} - \tan^{-1}\left(\frac{\omega}{\sigma}\right) + \tan^{-1}\left(\frac{\omega T_w}{1+\sigma T_w}\right) + 2\tan^{-1}\left(\frac{\omega T_2}{1+\sigma T_2}\right)\right) \quad \text{(II. 53)}$$

PSS gain, for its part, is given by the following relation:

$$K_{PSS} = \frac{4\omega_n \xi H}{K_2 |GEP(s)||G_f(s)|}\Bigg|_{s=\lambda=\sigma+j\omega} \quad \text{(II. 54)}$$

With, $$\omega_n = \sqrt{\frac{\omega_0 K_1}{2H}} \quad \text{(II. 55)}$$

ω_0: is the synchronism speed of the system (rad / s).
ω_n: is the natural oscillation pulse (rad / s).

The value ω_n represents the solution of the characteristic equation of the mechanical loop Fig (II. 11). It is defined by the following equation (neglected damping coefficient D).

$$2Hs^2 + \omega_0 K_1 = 0 \quad \text{With, } s = \pm j\omega_n \quad \text{(II. 56)}$$

II. 4. 2. 2. Residue method

We have seen that the PSS advance / delay filter is used to compensate for the phase delay of the GEP (s) transfer function. By determining the value of the phase delay, we can thus calculate the time constants (lead / lag) necessary to ensure the requested compensation. To do this, the residue phase angle can be used [35]. Consider the following form of the PSS transfer function for a one-input / one-output system:

$$H(s) = K_{PSS} . \frac{sT_W}{1+sT_W} . \left[\frac{1+sT_1}{1+sT_2}\right]^m \quad \text{(II. 57)}$$

Where: m is the number of compensation stages (generally m = 2).

Fig (II. 15) shows the residue effect on the eigenvalue shift to the left part of the complex plane.

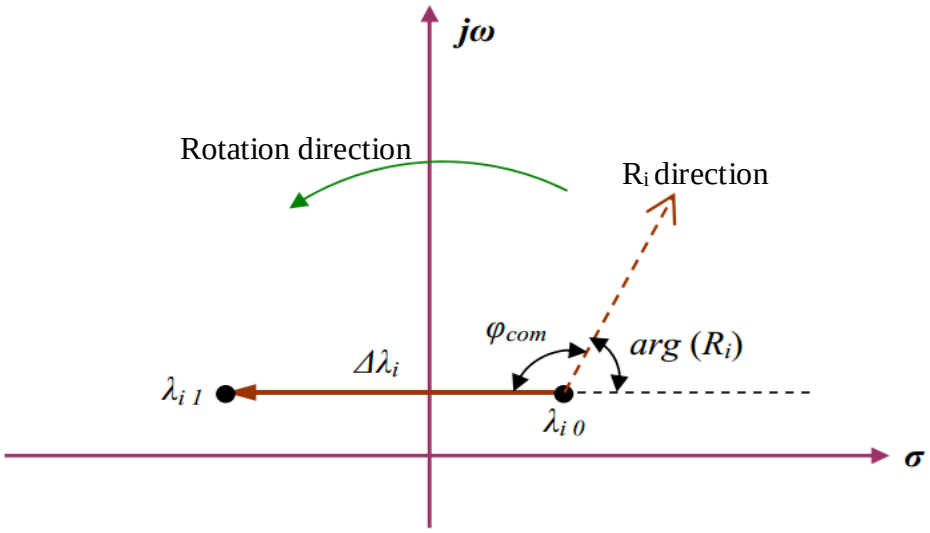

Figure II. 15: Displacement of eigenvalue by the rotation of the associated residue.

The phase angle φ_{com}, necessary to direct the direction of the residue Ri so that the associated eigenvalue λi moves parallel to the real axis, can be calculated by the following equation:

$$\varphi_{com} = 180° - \arg(R_i) \quad \text{(II. 58)}$$

Where: arg (R_i) is the phase angle of the residue R_i.

Therefore, the time constants T_1 and T_2, of the lead / lag block necessary to obtain the angle φcom, can be calculated as follows.

$$T_1 = \alpha \,.\, T_2 \;, \quad T_2 = \frac{1}{\omega \,.\sqrt{\alpha}} \quad \text{(II. 59)}$$

With:
$$\alpha = \frac{1-\sin\left(\frac{\varphi_{com}}{m}\right)}{1+\sin\left(\frac{\varphi_{com}}{m}\right)} \quad \text{(II. 60)}$$

Where: ω_i is the frequency of the λ_i mode in (rad / sec).

To calculate the K_{PSS} gain, we can rewrite the transfer function of the PSS as follows:

$$H(s) = K_{PSS} \,.\, H_f(s) \quad \text{(II. 61)}$$

The displacement of the eigenvalues is given by Eq (I. 27) which we recall below:

$$\Delta\lambda_i = |\lambda_{i1} - \lambda_{i0}| = R_i H(\lambda_i) \quad \text{(II. 62)}$$

By replacing Eq (II. 61) in the last equation, we obtain for K_{PSS} gain the following literal value [49]:

$$K_{PSS} = \left|\frac{\lambda_{i1}-\lambda_{i0}}{R_i \,.H_f(\lambda_i)}\right| \quad \text{(II. 63)}$$

II. 4. 2. 3. Pole placement method

This method consists in determining the PSS parameters so that all the closed-loop system poles would be placed in previously specified positions in the complex plane.

This method can be mathematically described by considering the following representation of the system, Fig (II. 16).

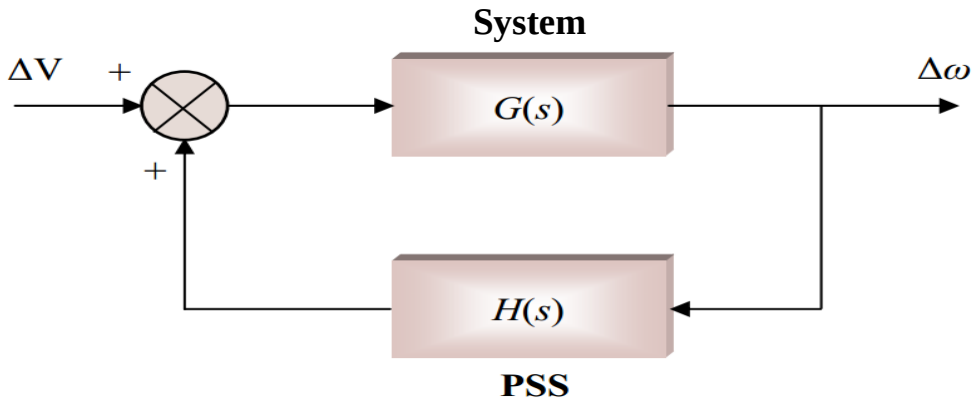

Figure II. 16: The whole (system-PSS) in closed loop.

Where: G (s) is the system transfer function between the reference signal ΔV from the generator voltage regulator, where the PSS is to be installed, and the change in rotor speed Δω.

H (s) is the transfer function of PSS.

The poles of G (s) are precisely the eigenvalues of the linearized system in open loop. The transfer function of the entire closed-loop system F (s) becomes:

$$F(s) = \frac{G(s)}{1-G(s).H(s)} \quad \text{(II. 64)}$$

The eigenvalues of the closed loop system are the poles of the transfer function F (s); they must satisfy the following characteristic equation:

$$1 - G(s).H(s) = 0 \quad \text{(II. 65)}$$

$$H(s) = \frac{1}{G(s)} \quad \text{(II. 66)}$$

If λi =1,2, ..., n are the eigenvalues specified previously, Eq (II. 66) can thus be rewritten as follows:

$$H(\lambda_i) = \frac{1}{G(s)} \quad \text{(II. 67)}$$

$$K_{PSS} \cdot \frac{\lambda_i T_W}{1+\lambda_i T_W} \cdot \frac{1+\lambda_i T_1}{1+\lambda_i T_2} \cdot \frac{1+\lambda_i T_3}{1+\lambda_i T_4} = \frac{1}{G(\lambda_i)} \quad \text{(II. 68)}$$

Therefore, we get a set of linear algebraic equations. By solving these equations, we can determine the values of the desired PSS parameters that ensure the precise placement of the eigenvalues.

II. 4. 2. 4. Optimal location of PSS

All generators in the system do not participate in the dominant modes: therefore not all generators need to be equipped with PSSs. In addition, it is necessary to take into account the negative interactions between the PSSs which increase with the number of the latter. Finally, economic criteria must be taken into account.

Thus, the first step in the implementation of PSSs, is to find the optimal locations of the necessary PSSs and to determine their number. This problem has been the subject of a great deal of research over the past ten years [34, 49]. The most efficient approaches proposed are based on the modal analysis of the linearized system: the shape mode, the participation factors and the residues.

As we have seen, the amplitudes of the residuals associated with the dominant modes of the transfer function of the open-loop system can be used to determine the most efficient placements for installing PSSs. The amplitudes of the participation factors or the shape mode make it possible to determine the influence of each state variable in the associated oscillatory modes. These methods can therefore provide us with important indications on the optimal location of PSSs in the system to achieve better damping against given criteria.

Knowing that different locations of the PSSs result in totally different oscillations, "badly placed" PSSs may therefore not meet the objectives. To do this, you have to choose the method you need to determine the right locations for the PSSs. The above-mentioned methods generally give good results, but the search for more efficient methods is still ongoing.

II. 5. Conclusion

In this chapter, we have presented the power system modeling for small disturbance stability studies. We also presented the power system linearization. The main study points from this chapter are presented below:

- The model chosen for each synchronous machine in the system is of the third order. The differential equations of the machine are described by the three state variables: δ, ω and E'_q. This model is well suited for angular stability studies at small disturbances.
- The excitation system and its regulator are also modeled.

- The generalized transmission power system model and loads is determined. In this model, the stator circuits of machines, transformers, transmission lines, and loads are represented as algebraic equations.
- The system is represented by a set of differential and algebraic equations coupled together. This model describes the non-linear behavior of the power system.
- The power system is often subjected to small disturbances which occur continuously under the influence of small variations in loads and sources. These disturbances are considered to be small enough to allow the general model equations linearization. The state representation of the system is then deduced.

Chapter III

Solar Power Plant Characteristics and Integration Problems

III. 1. Introduction

Today, electricity is an essential and vital resource for the sustainable development of mankind. Access to electrical energy and its reliable supply are key elements that support the economic development of a country or region. Thus, in developing countries, there has been a strong demand for electrical energy in recent decades, which they try more or less to satisfy through the use of thermal power stations, mainly given their relatively low investment cost.

It is obvious that fossil fuels will not disappear overnight but a scarcity or simply an inability of supply to keep up with demand will cause, by the simple effect of the inelasticity of demand, a skyrocketing cost production of electricity from these fuels.

With the rising cost of electricity production and the search for energy independence coupled with environmental problems, energy policies must be put in place to support growth, especially in developing countries. Some possible solutions are:

- Rational use of electricity (energy efficiency).
- Interconnection of regional power systems.
- Development of alternative sources of renewable electrical energy to constitute an energy mix with conventional production systems.

If the first two avenues are necessary for reducing the rate of increase in consumption and reducing unsatisfactory energy demand, the third avenue seems best suited for sustainable and environmentally friendly electrical energy production. Renewable energies are therefore an alternative to fossil fuels, some of the advantages of which we recall here:

- Renewable energies are generally less harmful to the environment (no greenhouse gas emissions) and inexhaustible over the lifespan of humanity.
- A possibility of autonomous or decentralized production adapted to both local resources and needs.

The production of solar electricity is based on two distinct technologies:

- **Concentrated solar power plant or thermodynamic solar power plant**: This technology consists of using mirrors to concentrate direct solar radiation on a focal point in order to obtain very high temperatures (from 200°C to 1000°C). This temperature heats a medium to produce steam which is used to drive a turbine coupled to an alternator and produce electricity. The schematic diagram of the thermal solar power plant in Figure (III. 1).

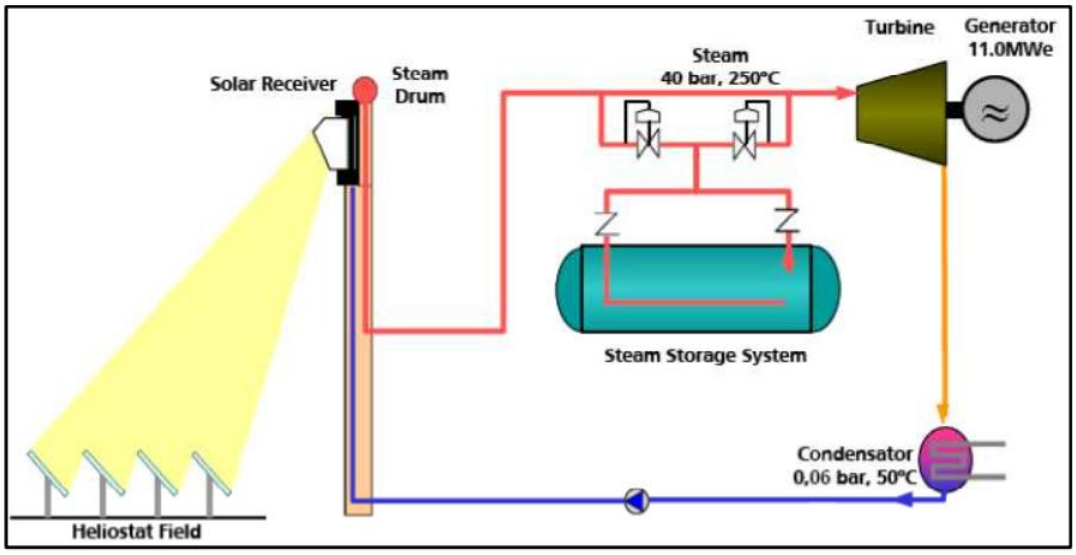

Figure III. 1. Block diagram of the thermodynamic plant

- **Photovoltaic technology (PV)**: It uses one of the properties of semiconductors which consist in generating an electric current when it is exposed to light. The photovoltaic effect therefore makes it possible to directly transform sunlight into electrical energy. One of the main advantages of PV technology is the absence of moving parts leading to long life (>20 years) and low operating cost. The main disadvantages are the high cost of the first investment and a low return (15-20%) which is constantly improving. Photovoltaic technology is the renewable energy source that has shown the strongest growth in recent years.

Between these two technologies, the photovoltaic sector seems to be well suited for integration into urban or rural areas when we take into account the importance of (global) sunshine, the real but slow prospect of reducing the cost of the technology thanks to the maturity of the sector, the ease of deployment and operation, the modularity of the system and the increased performance observed in recent years in terms of power electronics. This justifies the choice of work for this thesis, which essentially concerns issues related to the injection of electricity from photovoltaic systems into public power system.

Photovoltaic systems can be classified according to their application as below [56]:

- **Autonomous residential-type systems**: essentially group together low-power systems for domestic applications or for systems not connected to the power system. They power lighting systems, small refrigeration and more. Their capacity is less than 10 kWp. They are more economical in places without or far from public electricity networks.
- **Autonomous commercial-type systems**: PV systems used for commercial purposes, for example for water pumping, energy production for powering

telecommunication systems, battery charging, etc. The energy needs in these remote locations make PV systems an economically viable alternative.

- **Systems connected to low voltage LV power systems**: Systems installed on the roofs of houses or on the terraces of buildings and connected to the LV network. In countries where tariff regulations exist for the connection of renewable energy systems to the LV network (Feed-in tariff, Net-metering), smart meters are installed to quantify the energy consumed (by the owner) where sold (to the electricity company). The capacity of these systems varies according to the useful surface available for the photovoltaic installation but also the percentage of energy that the owner would like to save annually and of course his financial capacity.
- **Centralized Systems**: Utility-scale systems capable of reaching hundreds of megawatts of peak power under favorable climatic conditions. Installed on the ground and occupying a large area, these systems are usually connected to high voltage distribution or transmission power systems depending on their installed power.

The construction of grid-connected PV systems requires the use of several pieces of equipment to perform the production and conversion function as shown in Figure (III. 2).

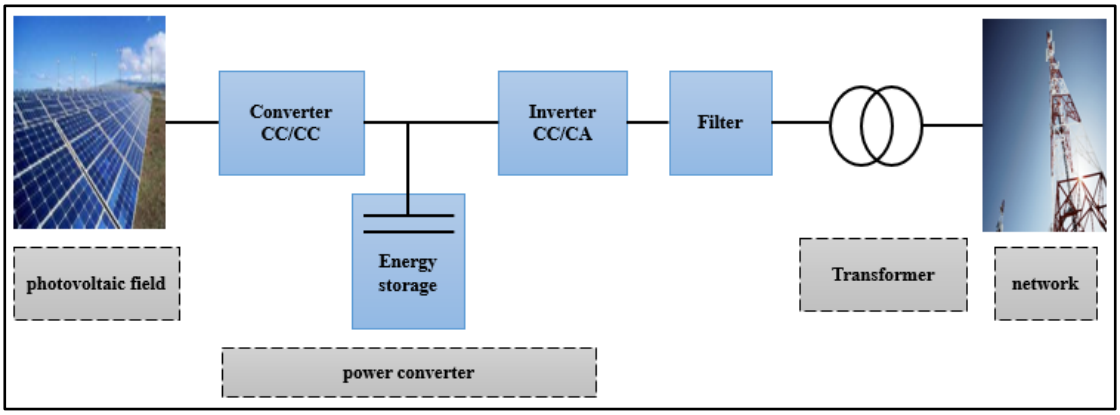

Figure III. 2. Components of a grid-connected photovoltaic system.

A photovoltaic field is used for the direct conversion of solar radiation into direct current (DC). A DC/DC converter may or may not be connected to the PV array in order to step up the voltage and also operate the PV generator at its maximum power point. A large capacitor smoothes the voltage before the DC/AC conversion which is performed by a three-phase inverter synchronized with the power system for energy injection. A harmonic filter is added after the inverter to reduce harmonics resulting from the power conversion process. The interface between the PV system and the network is very often made by a step-up transformer to adapt the output voltage of the inverter to that of the network and at the same time ensure galvanic separation. In addition to all the equipment mentioned above, there are all the protection, sectioning and monitoring devices necessary for the protection and management of the system.

We will present in the following paragraphs the main components of a photovoltaic system connected to the network.

III. 2. Photovoltaic cell

PV cells are semiconductor devices, usually made from silicon in different forms. They do not use any fluids and do not contain corrosive substances or any moving parts [57]. They require practically no maintenance, they do not pollute and produce no noise. PV modules would therefore be one of the ecologically efficient alternatives for producing electricity.

III. 2. 1. Brief History

In 1839, Edmond Becquerel, a French experimental physicist, discovered the photovoltaic effect while experimenting with an electrolytic cell consisting of two metal electrodes placed in an electrically conductive solution, he found an increase in electricity production when the cell was exposed in the light.

In 1904, Albert Einstein, publishing a document explaining the photovoltaic phenomenon and received for this occasion the Nobel Prize in Physics in 1921. At that time, the photovoltaic effect was not applicable to the production of electricity because of its low yield (<0.5%), the need to use rare and expensive materials and the lack of industrial production processes. It was in 1954 that the laboratories of the Bell company manufactured a silicon photovoltaic cell with an efficiency reaching 4.5% and thus giving an interest in the production of electricity from photovoltaic cells. Early applications were primarily for powering space vehicles, where it is expensive to supply power to onboard electronic equipment for a long period of time. Only four years later, the first satellite powered by photovoltaic cells, the US-Vanguard, was launched.

Since then, new records for photovoltaic efficiency have been constantly announced. For laboratory prototypes, the record is now above 30%, for space applications, the yield is well over 25%, while the efficiency of commercial terrestrial photovoltaic cells varies from 8 to 20% [58].

Nowadays, a strong acceleration is observed at the level of the photovoltaic modules market. It is mainly due to the growth in the installed power of systems connected to the network. This market relies heavily on government incentive policies (Europe, America, China, Japan, India, etc.) for the acquisition of grid-connected PV installations. However, the costs of the photovoltaic modules as well as the other components of the PV system are currently experiencing a continuous decline. The improvement in yields and the continual reduction in the cost of equipment could lead very quickly in very sunny regions to parity between the photovoltaic kWh and that of conventional production and thus accelerate the installation of PV systems connected to the power system.

III. 2. 2. PV cells Operation

The PV cell, or PN-type junction, absorbs light energy and transforms it directly into electric current. The operating principle of this cell calls on the properties of radiation, the physics of wave-matter interactions and those of doped semiconductors [59]. Figure (III. 3) shows a cross section of a PN junction (A) and the energy band diagram (B).

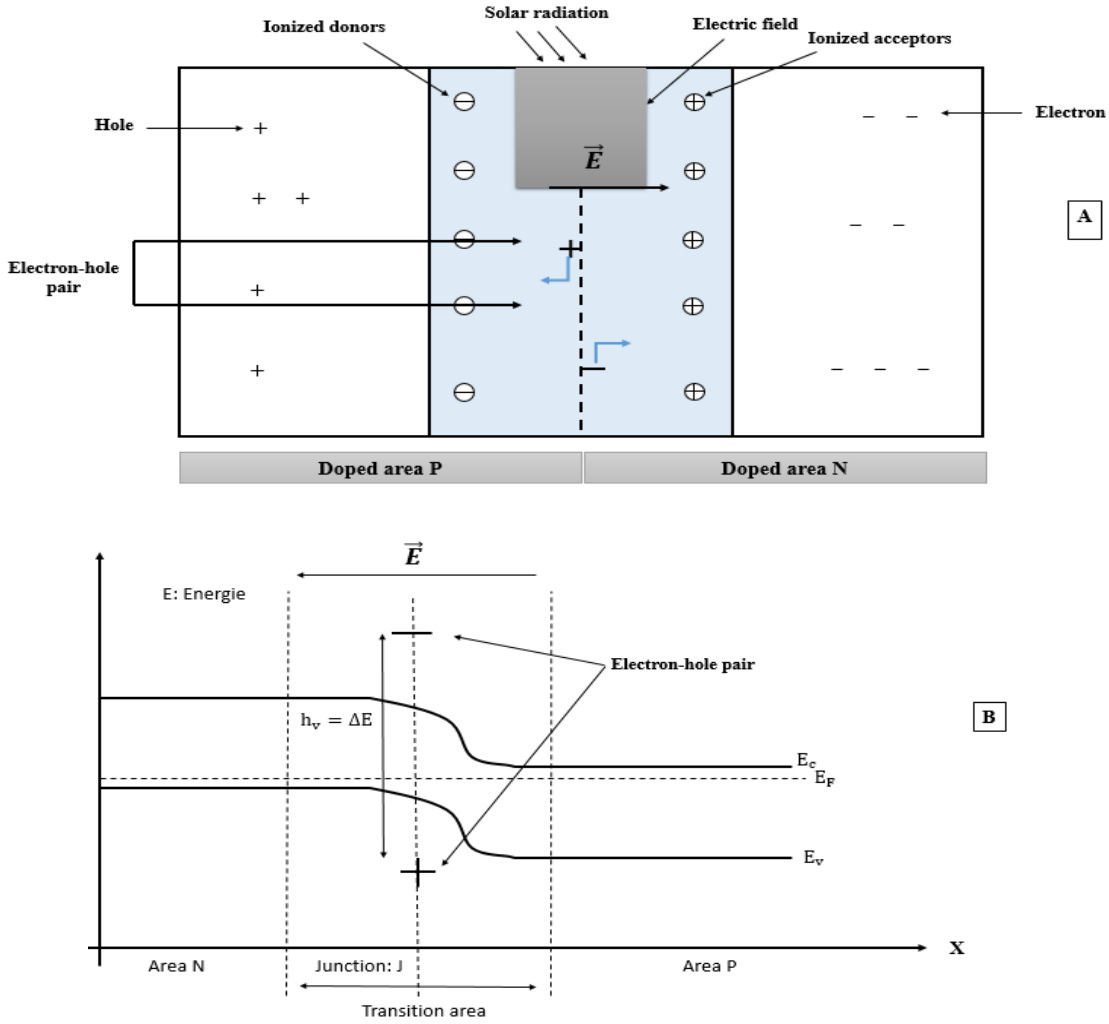

Figure III.3. Split PN junction: A) Cross section B) Energy band diagram.

In the depletion zone of the PV cell, when the energy of the absorbed photon contained in the incident radiation is greater than that associated with the forbidden band (Eg) of the semiconductor, free electron-hole pairs are created in this zone. (Figure III. 3. B). Under the effect of the electric field E which reigns in the depletion zone [60], these free carriers are drained towards the metallic contacts of the P and N regions. If the circuit is closed, an electric current then results in this circuit under a potential difference (0.6 V to 0.8 V) depending on the materials used.

III. 2. 3. Electric model

There are several electrical models of PV cells in the scientific literature. The most used models are those with two diodes and with one diode. We present here the model with a diode which combines simplicity and satisfaction from the simulation point of view.

This model consists of a perfect current generator in parallel with a diode, a series resistor and a shunt resistor as shown in Figure III. 4. The series resistance represents the base and edge contribution of the junction and the front and back face contacts. Shunt resistance is a consequence of the surface condition along the cell periphery, it is reduced following the penetration of metallic impurities into the junction during the deposit of the metallic grid or contact points on the diffused face of the cell [61].

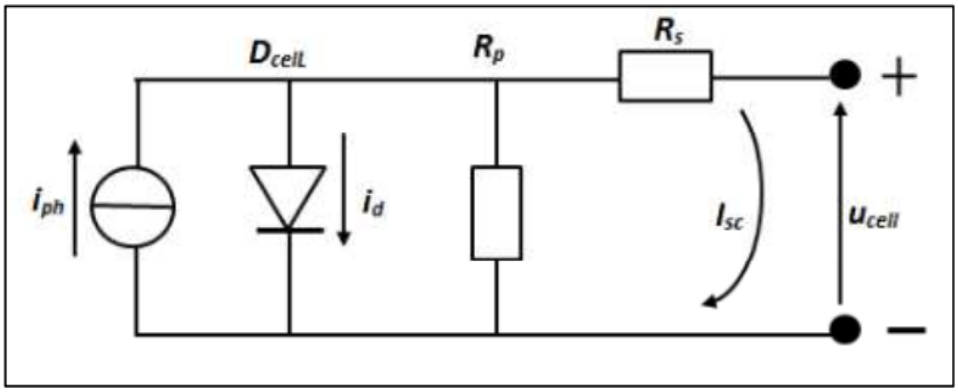

Figure III. 4. Electrical model of a single diode PV cell.

III. 2. 3. 1. Current source depending on the illumination

In the current source of Figure (III. 4), i_{sc} is proportional to the irradiation, and linear with respect to the temperature of the photovoltaic cell. According to Eq (III. 1), an increase in temperature leads to a decrease in bandgap energy, which leads to more current generated by incident photons. The expression of the current given by:

$$i_{sc} = \left(i_{sc,STC} + K_c\left(T_{cell} - T_{cell,STC}\right)\right)\frac{G}{G_{STC}} \qquad \text{(III. 1)}$$

Where i_{sc} and $i_{sc,STC}$ respectively represent the short-circuit current at a given temperature at standard test conditions (STC). Kc is the temperature coefficient of the short-circuit current. T_{cell} and $T_{cell,STC}$ are respectively the temperature in the real working conditions and that in STC of the PV cell. Finally, G and G_{STC} respectively represent the illuminance in real working conditions and at STC conditions.

III. 2. 3. 2. Diode

The current flowing through the diode, described by Eq (III. 2) is very well known:

$$i_d = i_{rs}\,.\left(exp\left(\frac{q.u_d}{k.A.T_{cell}}\right) - 1\right) \qquad \text{(III. 2)}$$

Where $i_{rs,}$ is the inverse saturation current of the diode, A is its quality factor (between 1 and 5), k is the Boltzmann constant (k= 1.38x10-23 Joule/°K), q the charge of 1 ' electron (1.602x10-19 coulomb), and u_d (V) the voltage across the diode. The reverse saturation current increases with temperature. This aspect must be taken into account in order to integrate the thermal effects in the module. The reverse saturation current can be expressed by Eq (III. 3) below:

$$i_{rs} = i_{rs,STC} \cdot \left(\frac{T_{cell}}{T_{STC}}\right)^3 . exp\left(\frac{E_{gap(.q)}}{k.A} \cdot \left(\frac{1}{T_{STC}} - \frac{1}{T_{cell}}\right)\right) \quad \text{(III. 3)}$$

Where, $i_{rs,STC}$ is the reverse saturation current at STC conditions.

III. 2. 3. 3. Resistors

The shunt resistance R_p has a high value, its influence is then negligible on the characteristics of the PV cell. The measurements made in [62] and [63] give approximately 1Ω for a module composed of 72 cells which corresponds to 14 mΩ per cell.

The impedance per PN junction is determined by neglecting the resistive components, by Eq (III. 4):

$$R_{PN} = -\frac{du_{PV}}{di_{PV}} = \frac{k.A.T_{cell}}{q.(I_d + i_{rs})} = \frac{k.A.T_{cell}}{q.((i_{SC} - i_{cell}) + i_{rs})} \approx \frac{k.A.T_{cell}}{q.(i_{SC} + i_{cell})} \quad \text{(III. 4)}$$

Which corresponds to the $\frac{U_{MPP}}{I_{MPP}}$, at the maximum power point.

III. 2. 3. 4. Electrical circuit

The current at the output of the PV cell is given by Eq (III. 5), assuming infinite shunt resistance. The voltage across the PN junction is given by Eq (III. 6) and finally, the power produced by the PV cell is given by formula (III. 7).

$$i_{cell} = i_{ph} - i_d \quad \text{(III. 5)}$$

$$u_d = u_{cell} + R_s . i_{cell} \quad \text{(III. 6)}$$

$$P_{cell} = u_{cell} . i_{cell} \quad \text{(III. 7)}$$

The characteristics of photovoltaic cells strongly depend on external factors such as temperature and the level of solar irradiation. Temperature has a significant effect on the reverse saturation current given by Eq (III. 3). Eq (III. 8) gives the relationship between temperature and voltage across the cell:

$$V_{PV} = V_{PV,STC} - K_V(T_{cell} - T_{cell,STC}) \quad \text{(III. 8)}$$

Where, V_{PV} and $V_{PV,STC}$ is the cell output voltage respectively at the given operating point and at STC conditions. K_V is a constant representing the voltage temperature coefficient of the cell. Tcell and $T_{cell,STC}$ are the respective cell temperatures under

actual working and standard test (STC) conditions. With Eq (III. 8), we understand that the voltage at the terminals of the cell decreases with the increase in temperature and this decrease is proportional to the increase in temperature.

III. 3. Photovoltaic module

III. 3. 1. PV cell array

The photovoltaic cell constitutes the basic element of a photovoltaic generator with a low voltage of the order of 0.6 V for silicon-based cells. For current applications, the need to obtain a higher voltage leads to putting n cells in series as illustrated in Fig (III. 5).

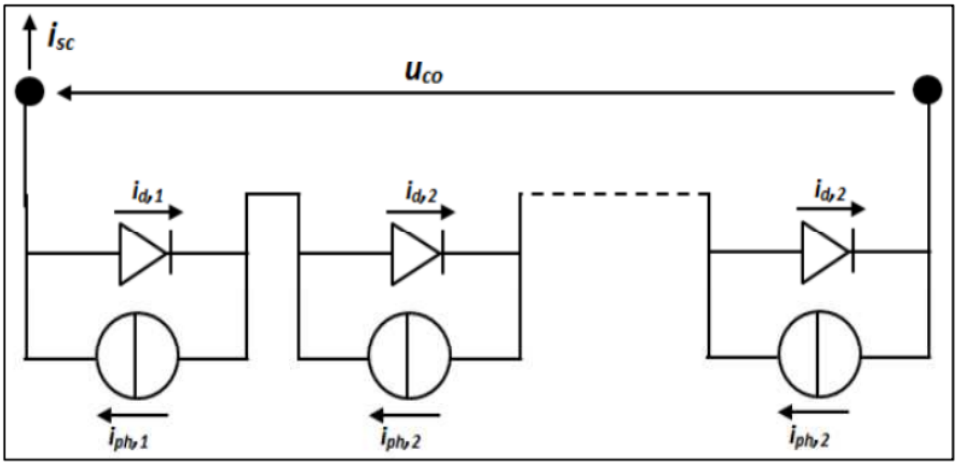

Figure III. 5. Serialization of cells to form a module.

The problems of serialization of cells (or modules) belonging to the same string under conditions of non-homogeneous illumination widely discussed in [64, 65] underline not only a drop in power at the level of the string but also highlight the phenomenon of “hot spots” observed on poorly lit cells. The "hot spot" effect, which is due to the power dissipation of poorly lit cells now operating as receivers, can damage the affected area and permanently degrade the performance of the photovoltaic module. To avoid these undesirable effects, one of the solutions is to associate bypass diodes with a sub-network of cells, as proposed in [64, 65]. The diagram in Fig (III. 6) illustrates the configuration made on two sub-branches of 18 cells each. Its traditional operating environment includes the connection of two bypass diodes and one anti-reverse diode. The physical connection makes it possible to work with or without the diodes depending on the desired conditions.

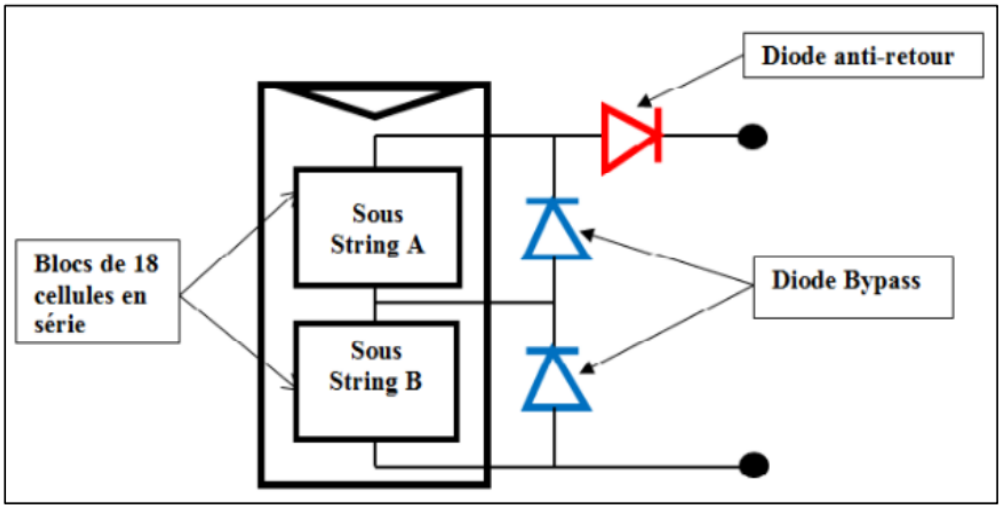

Figure III. 6. Diagram of a module with bypass diodes and anti-return diode.

The module being the basic element of a photovoltaic installation, by extension the protection of a PV generator in order to increase its lifespan against the destructive effect of the "hot spot" must include:

- Protection in case of parallel connection of PV modules to avoid negative currents in the PV generator (anti-return diode)
- Protection during the series connection of PV modules in order to avoid “hot spots” and total or partial loss of the string (bypass diode).

III. 3. 2. Behavioral study of a PV module

The photovoltaic cell constitutes the basis of the photovoltaic module and all other things being equal, the behavior of the PV module can be assimilated to that of the PV cell.

The behavioral study is made on the ET Solar module of reference ET-M53685 85W whose diagram is given in Fig (III. 7). The electrical characteristics of a cell under STC conditions are: V_{oc} = 0.6 V and I_{sc} = 5A. The simulation tool used is the Simulink/Simpower software.

Simpower has in its SimElectronics library a photovoltaic cell block comprising an input for lighting and two output terminals for connection to the external circuit as shown in Fig (III.7). This block is designed by default for operation in Standard Test Conditions (STC) but the possibilities of testing it under other climatic conditions exist.

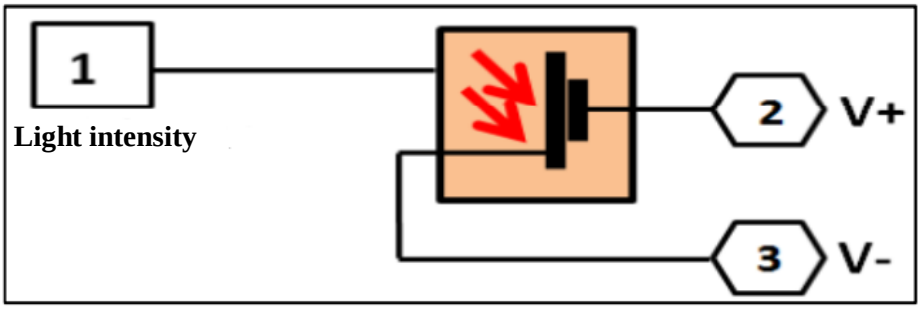

Figure III. 7: General structure of the Simpower photovoltaic cell block.

The realization of the module from this block was made by series association of PV cells.

For the simulation, the module was modeled by grouping 6 cells in series to form a string and the 6 strings put in series as shown in Fig (III. 8).

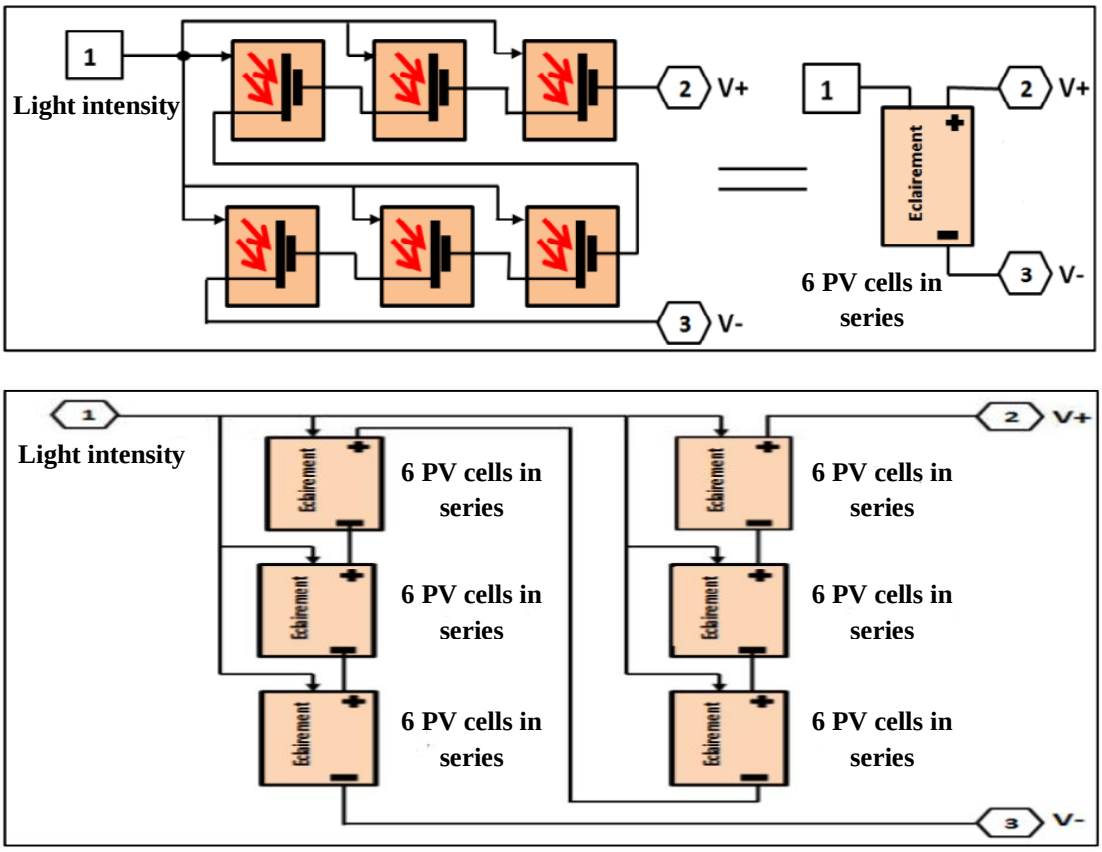

Figure III. 8. PV module made using Simpower.

Simulation of the module thus produced under various conditions to observe its behavior from its current-voltage and power-voltage characteristics. The results are illustrated in Fig (III.9).

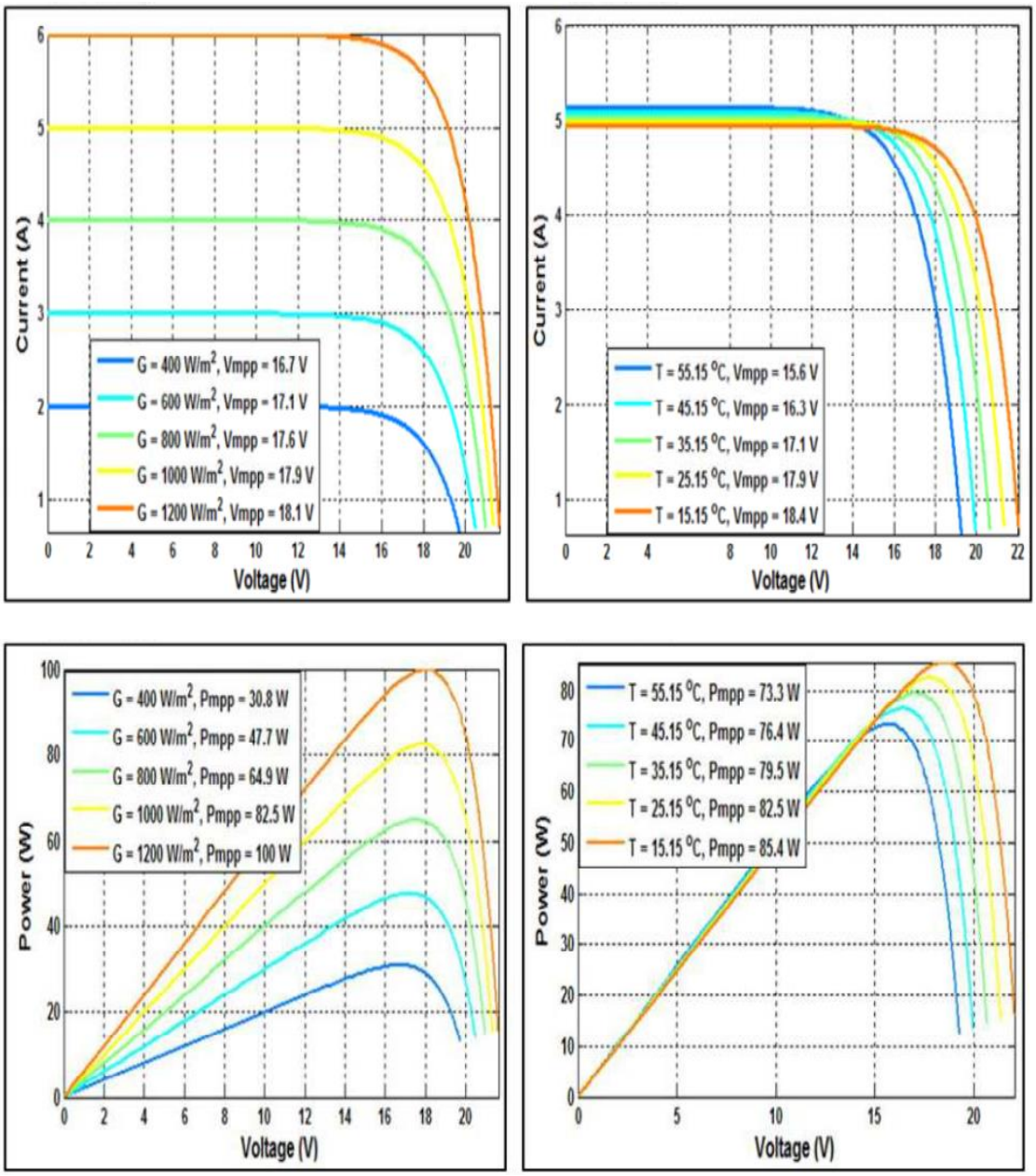

Figure III. 9. Characteristic curves illustrating the effects of sunlight and temperature on the performance of the photovoltaic module.

The results of the various simulations Fig (III. 9) make it possible to conclude, for all proportions kept, that the effects of illumination and temperature on the performance of the PV module are identical to those of a photovoltaic cell in the sense that:

- The short-circuit current I_{SC} varies with the intensity of the illumination G.
- The open circuit voltage V_{oc} (I_{SC} = 0) varies little with illumination. It can be considered as a constant for a given PV module.
- The power supplied by the PV module depends on the intensity of the lighting and the voltage at the terminals of the PV module. Thus, the optimal power P_{mpp} is very sensitive to illumination: when illumination decreases by 50%

(1200W/m2 to 600 W/m2), the optimal power P_{mmp} decreases by 52.3% (100W to 47.7W) in this case.

- The optimal power P_{mpp} is degraded when the temperature increases. For example, if the temperature increases by about 55% (from 25°C to 55°C), the optimum power P_{mmp} decreases by about 11% (82.2W to 73.3W).

Results of the simulations prove that the PV module (PV generator) is a source of nonlinear electric energy and this property constitutes one of the major problems of the modeling of the photovoltaic systems as written in [66, 67].

III. 4. Choice of interface converters

III. 4. 1. Electrical constraints

The connection of a PV generator to the power system is done by power converters which play the role of interface between these two energy sources. These conversion and grid connection interfaces must be able to perform the functions below despite the intermittent nature of solar energy.

III. 4. 1. 1. Maximum photovoltaic power extraction

An important relationship in the PV generator is the Power-Voltage characteristic (P(V)). The power P is calculated at each point of the curve I(V) which makes it possible to plot the curve P(V) represented in Fig (III. 10). Initially, the power increases with the increase in voltage until it reaches a certain point corresponding to the maximum power (P_{mpp}) developed by the generator under given lighting and temperature conditions, this point is called Maximum Power Point (PPM), generally adopted by PV module manufacturers. After this point, the power developed by the PV generator decreases with the increase in voltage until it reaches the zero value corresponding to the open circuit voltage (Voc).

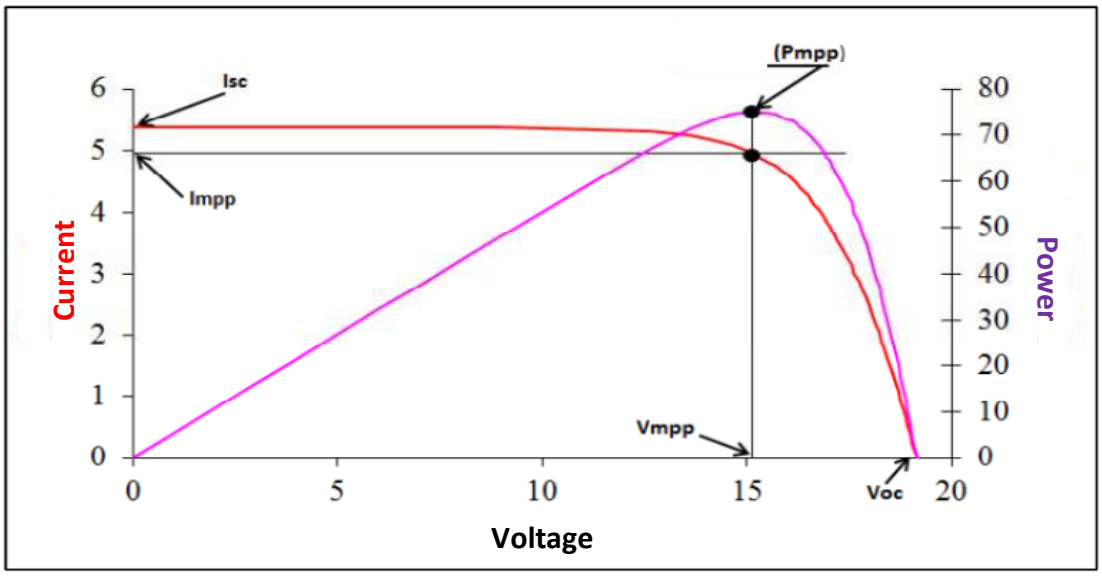

Figure III. 10: Current/voltage/power characteristic of a photovoltaic module.

It becomes obvious that if the impedance of the load connected to the terminals of the PV generator is not equal to the impedance necessary to extract the maximum power, the PV generator will then be under-exploited. In order to overcome these difficulties, use is commonly made of a static converter equipped with a control function whose role is to operate the PV generator around its maximum power despite variations in climatic conditions and possible variations in powered load. The maximum power extraction technique is known as "Maximum Power Point Tracking" (MPPT), the general principle is illustrated in the diagram of Fig III. 11.

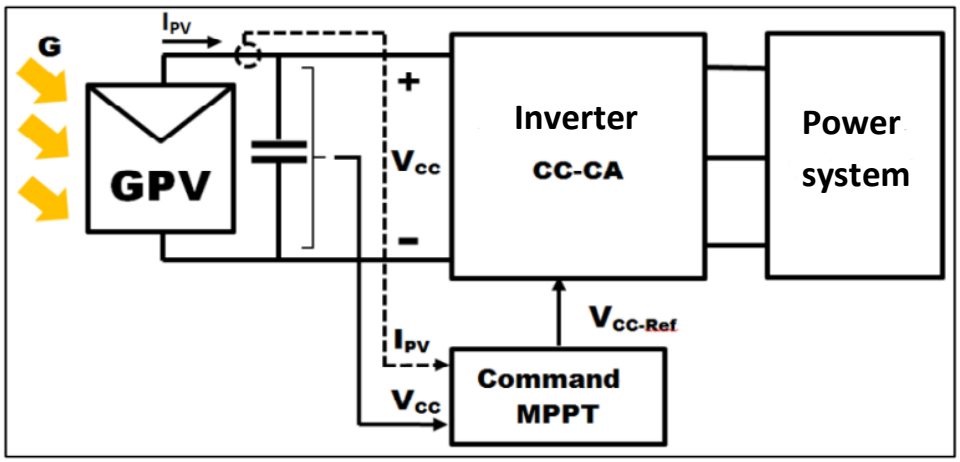

Figure III. 11. Photovoltaic conversion chain with a DC/AC converter controlled by an MPPT command on AC load (grid).

Several publications and various techniques on the MPPT control appear regularly in the literature since 1968, date of the first publication of a control law of this type, adapted to a photovoltaic renewable energy source [68]. Techniques frequently discussed in the literature are in [69].

III. 4. 1. 2. Optimization of power transfer

In a context of efficiency and energy restriction, given the high powers involved (photovoltaic power plant connection), the optimization of power transfer from the PV generator to the power system must be effective.

III. 4. 1. 3. Quality of the signal injected into the power system

The quality of the current at the output of the converter (harmonic distortion, waveform, etc.) is an important factor in the choice of a converter connected to the power system. The quality of the current can be evaluated by the Harmonic Distortion Rate (THDi), its value is generally fixed by the specifications. The load of the inverter being the network, the connection standards NF C 15-100 and IEEE 519 standard require a THDi < 5%.

III. 4. 2. Structure of converters

The classification proposed here is based on the use or not of an intermediate DC bus in the structure of the interface converter.

III. 4. 2. 1. Two-stage conversion structure

In this structure, the photovoltaic generator is first connected to a DC bus via a DC/DC converter then connected to the network through a DC/AC converter. The basic principle is to raise the voltage of the PV generator to the desired level through the DC/DC converter which also performs the MPPT function and then convert it to AC voltage through the DC/AC converter (inverter). Several architectures are proposed in the literature. As an example, the architecture using a converter of the "chopper-lifter" type is represented in Fig (III.12).

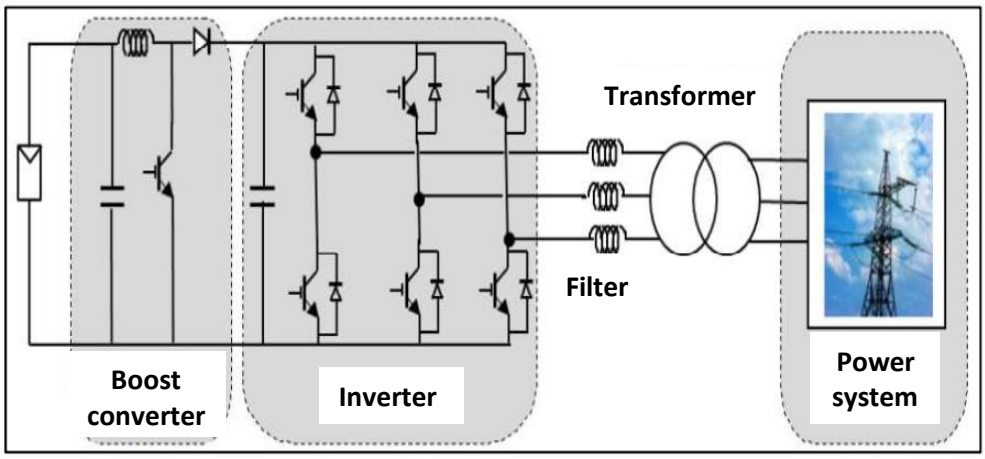

Figure III. 12. Power converter using a boost converter type DC bus.

III. 4. 2. 2. Structure using a single converter

The device shown in Fig (III. 13) is the simplest, because it comprises the fewest possible components. Several photovoltaic modules are connected in series to obtain a sufficiently high DC voltage. This solution is an alternative to using a DC/DC step-up converter. The DC voltage obtained directly feeds an inverter, which supplies the desired sinusoidal voltage. It could be advantageous to insert a transformer to isolate the photovoltaic system from the power system.

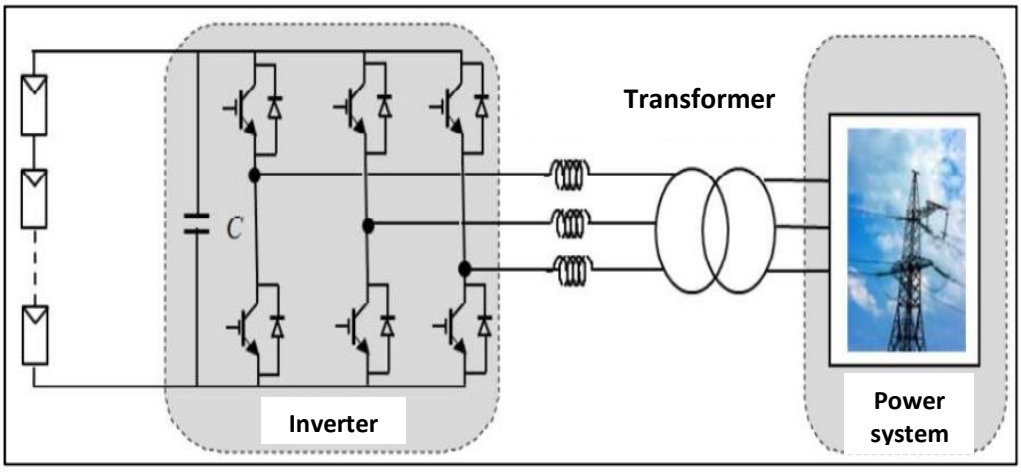

Figure III. 13. Direct connection power converter (without intermediate DC bus).

The major drawback of this device when using several modules in series is the total and immediate shutdown of energy production during a problem occurring upstream of the inverter. In addition, the control of the maximum power point is approximate because all the modules do not deliver the same current due to their differences in internal structure.

As we have seen previously, non-homogeneous lighting on a module or on a row of modules in series can have a negative impact on the energy production of the row in question. For example, if the installation consists of two rows in parallel, an imbalance on one row (by shading on a certain number of modules for example) will disturb the other row by the voltage drop caused by the weakest row. This disturbance is manifested by a drop in voltage and therefore forces the inverter to operate at a maximum power point slightly below that of the normal range.

III. 5. Interactions of a photovoltaic plant with the power system

III. 5. 1. Local interactions

III. 5. 1. 1. Modification of the power transit

One of the first impacts related to the connection of photovoltaic power plants to the power system that comes to mind concerns the modification of power transits [13]. In Fig (III. 14a), the representation of the active power transit is given for a distribution network without a photovoltaic plant. For this network, the total power consumed is equal to PB1a. This power comes from the HTB/MV transformer and is distributed over the various departures from the MV distribution network. When the CPV is introduced Fig (III. 14b), the power passing through the HTB/HTA substation decreases and becomes equal to PTB lb. PB2 (PB2b) can change direction (if the power of the CPV is greater than the sum of the powers of the loads connected to the JDB2 bus). In this case, the power passing through this branch no longer comes from the HTB/MV substation but from the CPV. Depending on the state of network load and the power delivered by the CPV, it may happen that the power passing through the source substation (PB2b = (P21 + P22) — Ppv) changes sign. A power transit can change when the CPV is connected to the grid and when the grid load status changes (period of strong sunlight and low consumption).

The modification of the power flow must be studied when the CPV is introduced in order to ensure that all the equipment present on the power system (metering devices, protections, etc.) will operate correctly. Changing the transit may require changing these materials, in particular the protection devices, which are very often unidirectional.

This modification of the operation is reflected in particular at the level of the protection devices by a loss of selectivity between the various protections of the power system. This loss of selectivity is due to the values modification of the fault

currents and the distribution of these currents. Depending on the point of the fault and the location of the CPVs.

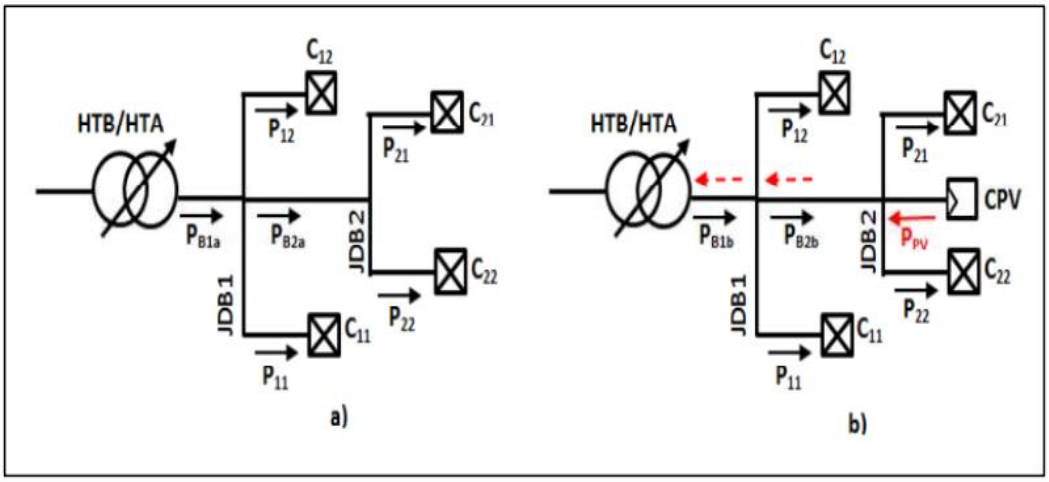

Figure III.14. Power transit: a) distribution network without CPV; b) Distribution network with CPV.

III. 5. 1. 2. Injection of current harmonics

The presence of electronic power interfaces can inject chopping harmonics into the power system if the inverters are not equipped with effective filters. Current inverters contribute all the same to the increase in current harmonics because they most often operate at reduced power (a device operating at reduced power cannot supply the same quality of current as at nominal power) [64]. It turns out that the old power converters with line-commutated thyristors produce higher levels of harmonic currents compared to the new inverters with IGBTs based on Pulse Width Modulation (PWM). The consequences of these harmonics can be instantaneous on certain electronic devices: functional disturbances (synchronization, switching), untimely tripping, measurement errors on energy meters, etc.

III. 5. 2. Global interactions

Apart from local interactions that have effects in the vicinity of the connection point, CPVs can have more global interactions at the scale of a region, especially if they are connected to the transmission power system. They are detailed below.

III. 5. 2. 1. Intermittency and predictability

An effect commonly associated with photovoltaic units is that of their variability. Indeed, CPVs of an intermittent nature bring variability and uncertainty in the management of power system. This inevitably leads to effects on the reliability of the network and its efficiency. In the context of conventional production, for which it is easy to predict the supply of electricity, producers are required to notify at least the day before their production plan.

In the case of photovoltaics, despite the weather forecasts, there remains significant uncertainty about the forecast of actual production. The electricity produced depends first on the sunshine, then on the cloud cover. As much as the first is simple to

determine, the second is difficult to predict. However, it seems that this is easier in the case of photovoltaics compared to other sources of renewable energy and especially for high installed power [66].

Variability and uncertainty relate to impacts related primarily to the achievement of the production-consumption balance at various time horizons. In addition to these concerns, there remain those related to the stability and security of the power system from a global point of view.

III. 5. 2. 2. Frequency balancing

Electrical energy cannot be stored in large quantities using conventional means, the balance between production and consumption must be respected at all times. It is this balance that guarantees the safe operation of the electricity power system at a constant frequency. To compensate for unforeseen fluctuations between the injection and withdrawal of electrical energy from the power system, the suppliers temporarily increase or decrease the power of the power stations. Network operators must continuously compensate for these deviations in their control area by means of control power [67].

As the photovoltaic plant is connected to the power system through an electronic interface (inverter) and this without mechanical inertia, the response to a rise or fall in demand is very fast. In addition, the solar radiation varies very slowly (except cloudy passage), the CPV can then be used to intervene in the supply/demand balancing of the power system, thus allowing a margin of adjustment or even a transitory control of the frequency.

III. 6. Conclusion

The operation of a photovoltaic system (generator + load) at its optimum efficiency requires the insertion of static converters between the PV generator and the load which is in this study the power system. The operation of these converters requires the application of control laws. To do this, a dynamic study of the overall system is necessary in order to identify the transient phenomena caused by this command and thus provide adequate solutions and configurations.

The analysis of the power system made it possible to characterize it as a system comprising a large number of elements which interact and are very complex to manage. The operation and planning of electrical systems pursue a number of contradictory objectives: the balance between production and consumption, the minimization of losses, investments, maintenance and operating costs, the improvement of quality power supply, etc.

The significant integration of CPVs in the power systems makes operation and planning even more difficult with power injections at all voltage levels. New technical challenges pose to power system managers, in particular because of the variability of production and also their low capacity to provide system services, even if the

evolution of technologies will surely overcome this last drawback. Furthermore, CPVs interact with electrical systems and can alter their performance locally or globally. The evaluation of these interactions and the risks involve prior studies to the connection of large photovoltaic power plants. Preliminary studies constitute a complex task with multiple objectives. The difficulties are related to the high number of variables, the uncertainty of the initial information and the dynamic nature of the problem.

Chapter IV

Applications and Results

IV. 1. Introduction

The main objective of this chapter is to display the optimal PSS regulator found by using the new improved version of CSA to ensure a satisfactory damping of the rotor oscillations and guarantee the stability of the system whatever the disturbance which appears on the system. As well as improving the power system stability with high penetration of photovoltaic generation. For that, the chapter will be organized as follow:

Firstly, we introduce our main contribution dynamic crow search algorithm based on adoptive parameters. Published article is presented as its original version.

Afterwards, we develop the optimal control design for power system stabilizer by using DCSA. Results are from under review article.

Finally, we present transit stability enhancement of power system with high solar energy integration.

IV. 2. Dynamic crow search algorithm based on adoptive parameters for large-scale global optimization

Abstract. Despite the good performance of Crow Search Algorithm (CSA) in dealing with global optimization problems, unfortunately it is not the case with respect to the convergence performance. Conventional CSA exploration and exploitation are strongly dependent on the proper setting of awareness probability (AP) and flight length (FL) parameters. In each optimization problem, AP and FL parameters are set in an ad hoc manner and their values do not change over the optimization process. To this date, there is no analytical approach to adjust their best values. This presents a major drawback to apply CSA in complex practical problems. Hence, the conventional CSA is used only for limited problems due to fact that CSA with fixed AP and FL is frequently trapped into local optimum. In this present paper, an enhanced version of CSA called dynamic crow search algorithm (DCSA) is proposed to overcome the drawbacks of the conventional CSA. In the proposed DCSA, two modifications of the basic algorithm are made. The first modification concerns the continuous adjustment of the CSA parameters leading to a DCSA, where AP will be adjusting linearly over optimization process and FL will be adjusting according to the generalized Pareto probability density function. This dynamic adjustment will provide more global search capability as well as more exploitation of the pre-final solutions. The second modification concerns the improvement of CSA's swarm diversity in the search process. This will lead to a high convergence accuracy, and fast convergence rate. The effectiveness of the proposed algorithm is validated using a set of experimental series using 13 complex benchmark functions. Experimental results highly proved the modified algorithm effectiveness compared to the basic algorithm in terms of convergence rate, global search capability and final solutions. In addition, a comparison with conventional and recent similar algorithms revealed that DCSA gives superior results in terms of performance and efficiency.

Keywords: dynamic crow search algorithm; large scale optimization; dynamic parameters adjustment; benchmark functions.

1 Introduction

Optimization problems have been widely existed in several engineering applications and science research [70]. The process of optimization is a selection of an optimal control vector in the objective function that can produce an optimal solution [71, 72]. Therefore, this solution will offer a better optimal physical process, as well as, lower cost, lower time consumption, and better performance. In the first time, several methods known as conventional optimization methods (COMs) have been proposed to solve these problems. Among these are Newton's method, gradient descent/ascend, scale conjugate gradient, and Nelder-Mead [73, 74]. COMs provide excellent performance, less time consuming, and can be easily implemented. Unfortunately, COMs have many limitations to cope with realistic and rather complicated empirical optimization problems. These limitations make COMs inefficient and often can be trapped in to local optimums, which is the major drawback of methods based on gradient [75, 76]. Hence, there is a need of developing new optimization techniques [71, 77]. Furthermore, the advance of artificial intelligence and computer science had an impact on stochastic algorithms and made them more reliable to be applied to complex real-world optimization tasks [72, 78]. These approaches initialize the optimization process with a set of random candidate solutions for a given problem and improve them over a pre–defined number of steps [74], and do not usually require the gradient information of problems, and they are not even sensitive for the selection of initial generation. Recently, more and more biologically-inspired approaches have been proposed and widely applied to practical problems [79].

Nature-inspired stochastic optimization (NISO) algorithms (Both as model and as metaphor) gain wide attention from the research community for decades. These algorithms either mimic individual or social behavior of a group of animal or natural phenomena, such as biological processes (e.g., reproduction, mutation, and interaction), or take advantages from species which have had adapted their physical attitude, structure, and learning to fit the environment over millions of years [72, 74, 80, 81].

The NISO algorithms start the optimization process by creating a set of random solutions that correspond to the number of problem variables. The metaheusteric algorithm is then applied to the initial solutions. Over a few iterations an improved set of solution is then generated. The fitness of all individuals (solutions) is evaluated at each iteration through the fitness function. In parallel, the resulting solutions are compared with those of previous iteration to select which solutions will be preserved to the next generation depending on algorithm strategy [79, 81]. For further information, the search process of meta-heuristic methods (MHM) is divided into two stages, exploration and exploitation [82, 83]. Firstly, exploration's aim is to lead individuals in the nearest region of the global solution, on other side, exploitation has to confine its search space into that region called promising area found previously to improve the solution. However, both of these stages are a trade-off and make the purpose of the MHM algorithms to balance between them to avoid getting trapped in local optima [73]. The MHM techniques have gained wide application in different field of science and engineering because their concept is simple, easy to implement, they proved to have quick convergence, great computational efficiency and are able to solve complicated global optimization problems.

Meta-heuristic algorithms are divided into three categories[84]. The first category is known as evolutionary algorithms. This category includes genetic algorithm (GA) [85], differential evolution (DE) [86], imperialist competitive algorithm (ICA) [87],cuckoo optimization algorithm (COA) [88]. The second category includes non-bio heuristic algorithms, such as: harmony search algorithm (HS) [89], gravitational search algorithm (GSA) [90], ions motion algorithm (IMO) [91], sine cosine algorithm (SCA) [92], exchange market algorithm (EMA) [93], teaching-learning-based optimization (TLBO) [94], mine blast algorithm (MBA) [95], soccer league competition algorithm (SLC) [96], multi-verse optimizer (MVO) [97].

The third category includes bio-inspired swarm intelligence algorithms such as: particle swarm optimization (PSO) [98], crow search algorithm (CSA) [99], butterfly optimization algorithm (BOA)[100], salp swarm algorithm (SSA)[101], grey wolf optimizer (GWO) [102], whale optimization algorithm (WOA) [103], ant lion optimizer (ALO) [104], ant colony optimization (ACO) [105], artificial bee colony (ABC) [106], bat algorithm (BA) [107], dragonfly algorithm (DA) [108], grasshopper optimization algorithm (GOA) [109], moth-flame optimization algorithm (MFO) [110], chicken swarm optimization (CSO) [111].

Askarzadeh has recently proposed a novel meta-heuristic optimizer, called crow search algorithm (CSA) [99]. CSA is a population-based optimization algorithm. CSA performs based on the idea that crows save their unneeded food in concealing places and retrieve it when it becomes in state of shortage. Therefore, crows turn into researcher in their environment for the best food source hidden by one of them, CSA algorithm has a simple mechanism controlled only by two parameters, that are: awareness probability (AP) and flight length (fl), a reason why it is easier to be implemented and makes it very suitable for solving complex optimization problems. In addition, CSA is able to provide optimal or near-optimal solutions for large scale optimization problems. Attracted by its simplicity and performance, researchers in many fields have applied CSA for solving complex engineering optimization problems such as: machine placement strategy in cloud data centers [112], optimal resonance-free third-order high-pass filters [113], image segmentation process[114], optimal selection conductor size in radial distribution network [115], optimal placement of STATCOM [116].

Based on “no free lunch” theorem [117], all optimization algorithms have shortcoming in solving some problems, clarifying the point that for a given algorithm, it could be well appropriate for solving a problem and provides good solutions and not for another. Therefore, there is no way to know the fittest algorithm for such problem that could be able to reach the global optimal solution in a competitive time. As other population-based optimization algorithms, CSA suffers of weak performance in some cases such as: premature convergence due to a weakness in its capacity to explore which leads to a local optimum and low convergence rate. On the other hand, conventional CSA exploration and exploitation are strongly dependent to the proper setting of AP and fl parameters. The values of these two parameters are fixed over the process of optimization, and there is not an analytical approach to adjust their best values. The missing approach to adjust the best parameters to each problem makes CSA search process limited and it could be frequently trapped into local optimum. The main motivation of this work is to propose a solution to overcome CSA weaknesses and combine them with its powerful aspects cited previously to extract an

algorithm capable of solving a wide range of complex engineering optimization problems.

In this present paper an enhanced version of CSA called dynamic crow search algorithm (DCSA) is proposed to overcome the drawbacks of the conventional CSA. In the proposed DCSA, two modifications of the conventional algorithm are made. The first modification concerns the continuous adjustment of the CSA parameters leading to a DCSA. This will provide more global search capability as well as more exploitation of the pre-final solutions. The second modification concerns the improvement of CSA's swarm diversity in the search process. This will lead to high convergence accuracy, and fast convergence rate. The effectiveness of the proposed algorithm is verified through a set of experimental series using 13 complex benchmark functions. The experimental results compared with those of other similar algorithms revealed that DCSA can give superior results in terms of performance and efficiency.

2 Background

2.1 Overview of Crow Search Algorithm

CSA is recent population-based optimization method, developed in 2016 by 'Alireza Askarzadeh', as its name indicates this algorithm inspiration came from an intelligent behavior of crows. Crows are considered among most intelligent animals in the world if aren't the smartest according to [118], that's owing to the fact that crow's brain to its body ration is almost or bit less than that of humans, and a lot of others genius behaviors like, they can memorize faces, they are self-aware in the mirror test, they are so skilled in using tools depending on situations and conditions, they can solve puzzles, they communicate in a sophisticated way and warn each other in case of danger, and they always score very highly on intelligence tests.

Additionally, the main inspiration of CSA is a cleverness behavior that kept the interest of 'Alireza Askarzadeh' to develop this algorithm, in a flock of crows, each crow hide its extra-food in a safety place depending on its own experience, and it come back to retrieve it when finding a new food source becomes a difficult task, and it can remember the place where the food is hidden after months. Moreover, having a relief food source don't prevent crows to search for another better food sources solicited by their greedy instinct, hence, crows follow each other in order to steal, when it comes that a crow visits its hidden place to put or retrieve food.

Stealing another's food promotes the experience of crows and protects them of being future victims, that's by taking additional precautions like moving their hidden places and predicting pilferer's behavior. From an optimization point of view, this behavior simulates an optimization process, where, crows are researchers, surrounding territory is search space, each position of the territory presents a possible solution, and quality of food source presents the objective function, as well as, the best food source is the global solution of the problem. Finally, fundamentals of CSA is relaying on those four points.

- Crows live in flock structure.
- Crows keep in mind their hidden places location.
- Crows follow each other to steal food.
- Crows get experience over time, so they protect their caches from others by probability.

2.1.1 Mathematical Modeling of CSA

It is assumed that the flock lives in a d-dimensional environment including a number of crows, the number of crows (population size) is mentioned by N, as well as, d corresponds to the decision variables of the problem, at each iteration crows change their positions looking for better food source, then, the position of crow i at time k (iteration) in the search space is specified by a vector, $x_{i,k} = \left[x_{i,k}^1, x_{i,k}^2, \dots, x_{i,k}^d\right]$ for i=1,2,…..,N and k=1,2,…..,kmax, where, kmax is the maximum number of iterations. Each crow has a memory in which the position of its hiding place is memorized. At iteration k, the position of the hiding place of crow i is defined by the vector, $m_{i,k} = \left[m_{i,k}^1, m_{i,k}^2, \dots, m_{i,k}^d\right]$, this is the best food position that crow i has obtained so far.

Assume that at iteration k, a crow j wants to check its hidden food, according to this visit we assume also that there is always another crow i following it in order to approach crow's j food, in this case, two possibilities may occur to update crow's i position.

Case 1: crow j doesn't note that crow i is following it, therefore, crow i can reach the position of crow's j hidden place. As a result, the position of crow i is updated asfollow:

$$x_{i,k+1} = x_{i,k} + r_i \times fl \times \left(m_{j,k} - x_{i,k}\right) \qquad (1)$$

Where: r_i is a random number with uniform distribution between 0 and 1, while fl indicates the flight length, pointing out here that fl has great effect on search procedure, choosing fl lower than 1 lead the search to local solution, where the next step will be near to the $x_{i,k}$ as shown in Fig. 1(a), otherwise, choosing fl greater than 1 lead the search to global solution because the next step will be far away than $x_{i,k}$ to promote further exploration of the search space Fig. 1(b).

Case 2: crow j is aware that crow i is following it, thus, crow j will dupe crow i and move randomly in the search space in order to protect its food.

Both cases can be gathered in one formula by introducing AP (awareness probability) parameter as follows:

$$x_{i,k+1} = \begin{cases} x_{i,k} + r_i \times fl \times (m_{j,k} - x_{i,k}) & rj \geq AP \\ a\ random\ position & otherwise \end{cases} \quad (2)$$

Where, r_j is a random number with uniform distribution between 0 and 1, AP parameter control the algorithm intensification and diversification. Small values of AP conduct to the local search, while large values of AP conduct to global search (randomization).

The crows update their memory as follow:

$$m_{i,k+1} = \begin{cases} x_{i,k+1} & if\ f(x_{i,k+1})\ is\ better\ than\ f(m_{i,k}) \\ m_{i,k} & otherwise \end{cases} \quad (3)$$

Where $f(.)$ symbolizes the fitness function value. Fig. 2, illustrates the pseudo code of CSA.

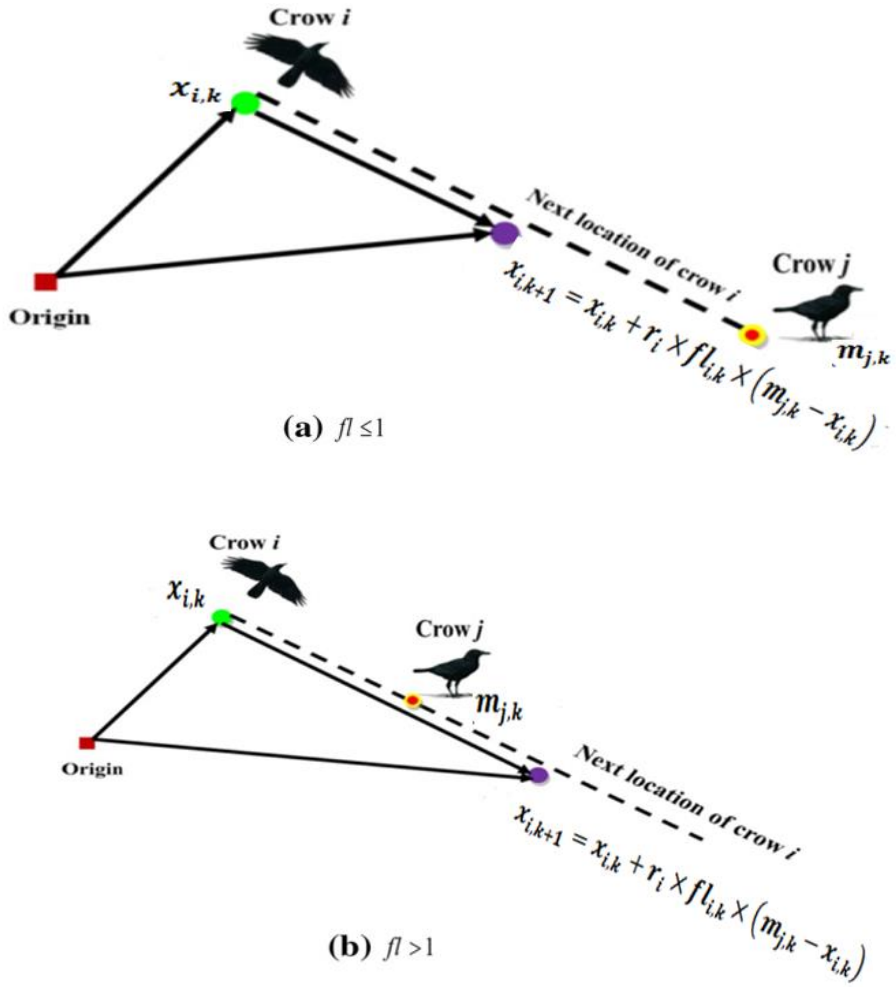

Fig. 1. fl effect on the position update.

CSA algorithm

Set the algorithm initial values: N, AP, fl, and kmax.
Set the problem dimension
Set equal and unequal constraint
Initialize the position of each crow randomly in the search space.
Set initial memory of each crow as its first position.
Evaluate the position of each crow by the fitness function.
Set k=1 (counter initialization).
While k ≤ kmax.
For i= 1:N.
Choose randomly one member of the flock to follow for example (j).
If AP ≤ r_j then.
$x_{i,k+1} = x_{i,k} + r_i \times fl \times (m_{j,k} - x_{i,k})$.
Else
$x_{i,k} = a\ random\ position\ in$ the search space.
End if.
End for.
Check the feasibility of new positions.
Update the position of each crow.
Evaluate the new positions by the fitness function.
Update the memory of each crow.
Set k= k+1.
End while.
Evaluate memory of each crow.
Extract the fittest objective function solution.
Extract the best solution.

Fig. 2. Basic CSA pseudo code.

2.2 Related Work

Since the proposition of crow search algorithm, many researchers have applied it in multiple optimization problems, and to boost its weak side as mentioned in introduction section some modifications were proposed on literature to improve the performance of CSA.

1- Modified crow search algorithm introduced in [119], proposes two modifications at the main CSA, first modification aim is to speed up the algorithm convergence, for that reason when a crow wants to generate a new position at given iteration, it must follow one of the (k) crows having best results where (k) is defined in Eq. 4, and not choosing randomly between N flock members, this selection objective is to ovoid bad solutions over iterations and can really improve the algorithm convergence and time

consumption, but it can also affect the algorithm exploration in high dimension problems.

$$K_{iter} = round\left(K_{max} - \frac{K_{max} - K_{min}}{itermax} \times iter\right) \qquad (4)$$

Second modification is about adjusting the flight length parameter according to a new concept that is the distance between the crow i and its target crow j, moreover, second modification aim is to improve the algorithm exploration by choosing fl bigger than a threshold if the distance between the crow i and crow j is small, because in this case crow i will not improve the solution, consequently, the crow i will explore another area than the region where they are located, this modification improve the exploration but it hardly weak the exploitation, owing to the fact that in the last iterations the distance between crows get closed, and the algorithm still setting high values of fl , doing so the algorithm will not been focused in the promoted region, thus, it will not provide good solutions.

2- Chaotic crow search algorithm introduced in [120], the main idea of the modification made by authors, is replacing the random variables of the algorithm, precisely in the formula that generate new positions, by chaotic variables came from ten different chaotic maps, subsequently, the algorithm will be formulated as follow.

$$x_{i,k+1} = \begin{cases} x_{i,k} + C_{i,k} \times fl \times \left(m_{j,k} - x_{i,k}\right) & C_{j,k} \geq AP \\ a\ random\ position & otherwise \end{cases} \qquad (5)$$

Where: $C_{i,k}\ and\ C_{j,k}$ are the chaotic values resulted from the chaotic map at k iteration.

This modification improve the convergence rate and the performance of the algorithm, on the other hand, the algorithm performance is only based on making a lot of tests to have better results, and setting proper values of chaotic maps can also affect the algorithm performance.

3- Rough crow search algorithm RCSA introduced in [121], authors in this article took benefits from rough set theory and integrated it with CSA to deepen the search in the promising region where the global solution is located. RCSA execution is done in two steps: firstly, CSA operates as global optimization solver to approach an approximate initial solution of a global optimization problem. Secondly, RSS (rough search scheme) is executed to ameliorate the solution quality through the roughness of the obtained optimal solution so far. Doing so, the roughness of the obtained optimal solution can be expressed as a pair of precise concepts based on the lower and upper approximations which are used to compose the interval of boundary region. Afterward, new solutions are randomly created inside this region to enhance the diversity of solutions and achieve an effective exploration to avoid premature convergence of the swarm.

3 Dynamic Crow Search Algorithm

This section is dedicated to the new concept of dynamic crow search algorithm DCSA, as mentioned previously that basic CSA suffers of premature convergence due to a weakness in its exploration capacity and low convergence rate, we could mention at this point over a deep analytic of basic CSA, that its main weakness performance came from fixed setting of its essential parameters AP and fl, moreover, fixed values of AP and fl cannot guarantee good exploration and exploitation in the same time or they can perform well at one stage of them and not another. To fix this problem two contributions are proposed in this article, the first one affects AP parameter while the second affects fl parameter to make them dynamic over iterations in favor of enhancing basic CSA performance, and extract all benefits of the search process two stages (exploration and exploitation) to have better results, detailed processes are as follow:

Firstly, awareness probability will be decreased linearly from AP_{max} to AP_{min} over iterations as it is shown in Fig. 3. Subjected to Eq. 6, the reason why this modification is introduced is that in the search process first stage, it is greatly recommended setting relatively high values of AP_{max} to stimulate further randomization in the algorithm search process making it exploring the global search space and steer the crows to a near region where the global optimal solution is located. Afterwards, AP will get lower values until AP_{min}, in this stage, AP low values promote CSA crows following process Eq. 1, and eliminate almost the randomization process, doing so, DCSA will be focused on exploitation phase to extract best results from the region approached previously, while proper setting of AP_{max} and AP_{min} has a crucial effect on DCSA performance.

$$AP_{iter} = \frac{AP_{min} - AP_{max}}{Iter_{max}} \times iter + AP_{max} \qquad (6)$$

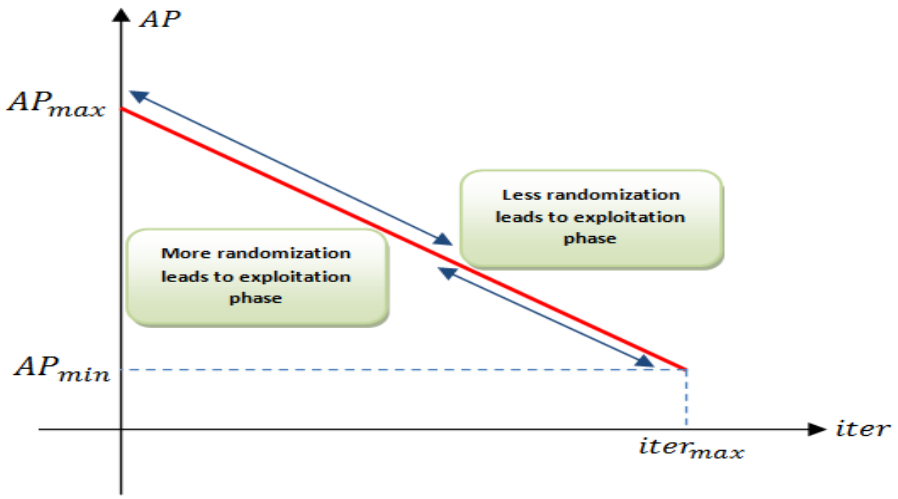

Fig. 3. AP variation and effect on optimization search process.

Secondly, based in CSA Eq. 1 it can easily noticed that fl parameter is multiplied by a random number with uniform distribution between 0 and 1, so that fl cannot be a control parameter of CSA, because it's hardly affected by the large random variation that's multiplied by over iterations. To make fl a real control parameter of CSA so that it can improve basic CSA performance the following modification is proposed where Eq. 2 will be as follow:

$$x_{i,k+1} = \begin{cases} x_{i,k} + fl_c \times (m_{j,k} - x_{i,k}) & rj \geq AP \\ a\ random\ position & otherwise \end{cases} \quad (7)$$

Where, fl_c is the flight length control parameter illustrated in Fig. 4, and is defined as:

$$fl_c = \begin{cases} fl * \left[F\left(\frac{y_{max}}{10}\right) - \left(F\left(\frac{y_{max}}{10}\right) - F(y_{min}) \right) \times rand \right] & if\ \ iter \leq \tau \times iter_{max} \quad (a) \\ fl * \left[F(y_{max}) - \left(F(y_{max}) - F(0.6 \times y_{max}) \right) \times rand \right] & else \quad (b) \end{cases} \quad (8)$$

Where,

fl: is the basic flight length.

τ: is time control report, bounded between 0 and 1.

F: is the generalized Pareto probability density function, while its characteristic parameters K, SIGMA, and THETA are set 1, 1, and 0, respectively.

y: is a discontinues regular variable between y_{min} and y_{max}, where $y_{min} = 0$ and $y_{max} = 10$, this interval is divided in 1000 uniform variables.

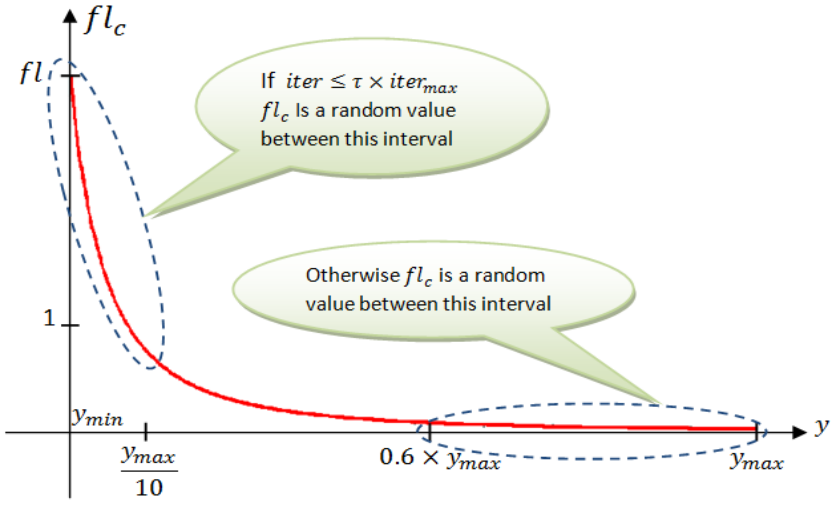

Fig. 4. The flight length control parameter curve.

As it is shown in Fig. 4, the search process exploration phase is taken from the beginning of iterations to $\tau \times iter_{max}$, to provide DCSA sufficient time amount to explore the overall search space without getting trapped in local optimum, while fl_c is set randomly from the region mentioned previously, this is for two reasons, firstly, to not delete the randomization process from the basic algorithm, secondly, setting fl_c with relatively high values from the generalized Pareto distribution function form can control more the range variation of it, moreover, based on this variation range, fl_c will be most of time between 1 and basic fl so this variation range promotes more exploration than exploitation as mentioned in the background section Fig. 1. As a result, DCSA centers its search on exploration phase to reach the optimum global solution region location.

While proper setting of τ is important to guarantee a good balance between exploration and exploitation depending on the problem complexity, afterwards, in the last iterations fl_c gets always lower values less than 1 from the region where Pareto distribution form takes almost steady variation from sixth-tenths y_{max} to y_{max}, because in last iterations, almost crows get gathered in the optimum global solution region so that fl_c low values boost more the exploitation on that region between the crows position that have better solutions, and don't waste main exploitation task by going to other regions where they will not improve the solution, eventually, DCSA offers the best global optimization solution, over following its own instructions showcased in Fig. 4, DCSA flowchart .

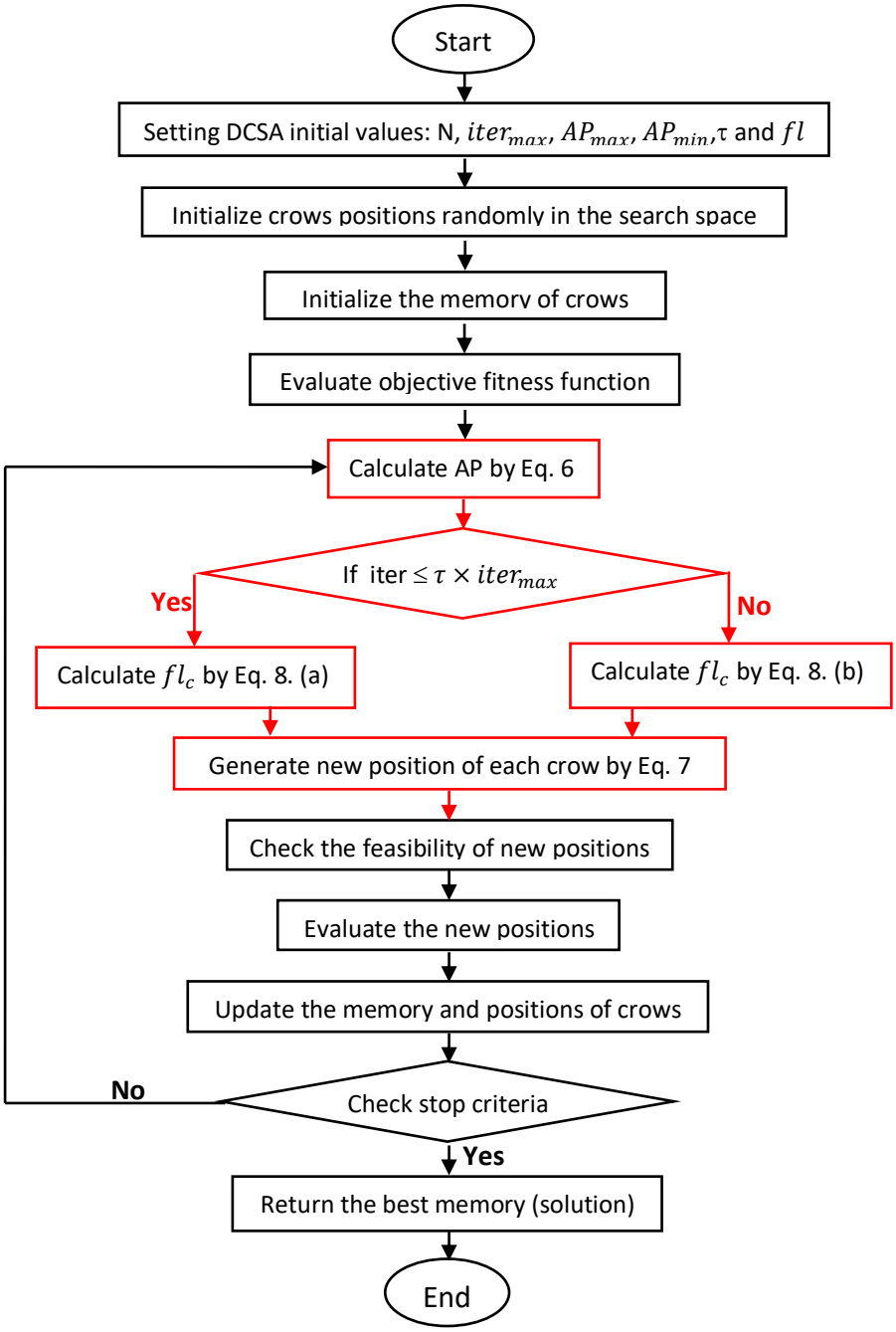

Fig. 5. Dynamic crow search algorithm flowchart.

4 Experimental results and discussion

To validate the proposed algorithm performance, DCSA is applied to thirteen selected classical benchmark functions to cover almost all perspectives that could face an optimization algorithm, while a short description of them is given below. Firstly, DCSA is compared with the basic CSA to prove its efficiency. To boost more DCSA performance some experiments are carried out to find the best parameters adjustment of it. Moreover, for the reason of abundance state of the art algorithms, DCSA is compared with four algorithms to establish its computational effectiveness over them,

and so GA and PSO are selected as conventional algorithms and two other recent algorithms SSA and BOA.

4.1 benchmark functions

Table 1 represents the benchmark functions used in this study and it also mentions boundaries (B), minimum value (Min), dimension (D), and type (T) of each function. Functions 1 to 7 are unimodal and they have only one optimum value, they are usually used to investigate the algorithm exploration capability and the solution convergence rate while final solution is not so important [74, 79, 122]. However, functions 8 to 13 are multimodal which are characterized by their local optimums number increasing exceptionally as the solution dimension, they are usually utilized to inspect the algorithm capability for escaping local optimums and approaching global solution, while last solution is important to make sure that the algorithm did not get trapped in one of them.

Table 1. Benchmark functions description.

Fun	Equation	B	Min	D	T
f_1	$f(x) = \sum_{i=1}^{n} x_i^2$	[-100, 100]	0	10	Unimodal
f_2	$f(x) = \sum_{i=1}^{n} \lvert x_i \rvert + \prod_{i=1}^{n} \lvert x_i \rvert$	[-10, 10]	0	10	Unimodal
f_3	$f(x) = \sum_{i=1}^{n} \left(\sum_{j-1}^{i} x_i \right)^2$	[-100, 100]	0	10	Unimodal
f_4	$f(x) = max_i \{ \lvert x_i \rvert, 1 \leq i \leq n \}$	[-100, 100]	0	10	Unimodal
f_5	$f(x) = \sum_{i=1}^{n-1} [100(x_{i+1} - x_i^2)^2 + (x_i - 1)^2]$	[-30, 30]	0	10	Unimodal
f_6	$f(x) = \sum_{i=1}^{n} ([x_i + 0.5])^2$	[-100, 100]	0	10	Unimodal
f_7	$f(x) = \sum_{i=1}^{n} i x_i^4 + random\ [0,1]$	[-1.28, 1.28]	0	10	Unimodal
f_8	$f(x) = \sum_{i=1}^{n} -x_i \sin\left(\sqrt{\lvert x_i \rvert}\right)$	[-500, 500]	418.9829 ×5	10	Multimodal
f_9	$f(x) = \sum_{i=1}^{n} [x_i^2 - 10\cos(2\pi x_i) + 10]$	[-5.12, 5.12]	0	10	Multimodal
f_{10}	$f(x) = -20exp\left(-0.2\sqrt{\frac{1}{n}\sum_{i=1}^{n} x_i^2}\right) - exp\left(\frac{1}{n}\sum_{i=1}^{n}\cos(2\pi x_i)\right) + 20 + e$	[-32, 32]	0	10	Multimodal
f_{11}	$f(x) = \frac{1}{4000}\sum_{i=1}^{n} x_i^2 - \prod_{i=1}^{n}\cos\left(\frac{x_i}{\sqrt{i}}\right) + 1$	[-600, 600]	0	10	Multimodal
f_{12}	$f(x) = \frac{\pi}{n}\left\{10\sin^2(\pi y_1) + \sum_{i=1}^{n-1}(y_i - 1)^2[1 + 10\sin^2(\pi y_{i+1})] + (y_n - 1)^2\right\} + \sum_{i=1}^{n} u(x_i, 10, 100, 4)$ $u(x_i, a, k, m) = \begin{cases} k(x_i - a)^m, & x_i > a \\ 0, & -a \leq x_i \leq a \\ k(-x_i - a)^m, & x_i < -a \end{cases}$	[-50, 50]	0	10	Multimodal
f_{13}	$f(x) = 0.1\left\{\sin^2(3\pi x_1) + \sum_{i=1}^{n}(x_i - 1)^2[1 + \sin^2(3\pi x_i + 1)] + (x_n - 1)^2[1 + \sin^2(2\pi x_n)]\right\} + \sum_{i=1}^{n} u(x_i, 5, 100, 4)$	[-50, 50]	0	10	Multimodal

4.2 Parameters settings

For all following experiments population size is set to 30, the maximum number of iteration is set to 1000, and for each function, algorithms are run 25 times independently. Performance metrics are as follow:

- Best value: is the best value that reached by an algorithm in different runs.

$$Best = Min_{1 \le i \le N_r} F_i^* \qquad (9)$$

Where: N_r is the number of different runs and F_i^* is the best value.

- Average value: is the mean of the best values acquired by an algorithm of different runs.

$$Mean = \frac{1}{N_r} \sum_{i=1}^{N_r} F_i^* \qquad (10)$$

- Standard deviation: is calculated to test if an algorithm can reach the same best value in different runs and test the repeatability of the results.

$$Std = \sqrt{\frac{1}{N_r - 1} \sum_{i=1}^{N_r} (F_i^* - Mean)^2} \qquad (11)$$

For the sake of comparison, algorithms are ranked from the best to the worst according to the average value, and if two algorithms get the same average, the best value will be the second index to rank them. Table 2 represents the most recommended parameters settings of all algorithms used on following experiments extracted from their original papers, except DCSA that will be detailed section by section.

Table 2. Parameter settings of each algorithm.

algorithm	CSA	GA	PSO	BOA	SSA
parameters	AP=0.1 $fl = 1.8$	Roulette is used for selection Crossover fraction=0.9 Mutation=0.005	C1=C2=2 $W_{max} = 0.9$ $W_{min} = 0.4$	p=0.3 a=0.2 c=0.02	Without parameters

4.3 Effectiveness of DCSA over CSA

To point out the overcoming contribution made by DCSA above CSA, following experiment runs them independently over former benchmark functions. DCSA parameters are set to $AP_{min} = 0.01, AP_{max} = 0.2$, and τ=0.9, experiment results are structured in table 3, while Fig. 6 illustrates algorithms convergence rate of some selected functions. Results from table 1, and Fig. 6 clearly showcase that DSCA outperforms basic CSA in all unimodal functions and all multimodal functions except f_7 in which DCSA does not make a real improvement, this superiority is for

convergence rate, quickness exploration capability, avoiding local optimums, and final solutions.

Table 3. Comparison results between DCSA and CSA.

Algorithm	Index	f_1	f_2	f_3	f_4	f_5	f_6	f_7
CSA	Best	1.03E-09	2.38E-03	1.06E-03	2.60E-03	3.16E+00	4.59E-09	2.52E+00
	Mean	1.50E-07	0.41E+00	0.02E+00	0.01E+00	3.93E+01	2.92E-06	3.28E+00
	Std	1.95E-08	0.27E+00	0.01E+00	0.01E+00	2.18E+01	6.62E-08	0.40E+00
	Rank	2	2	2	2	2	2	**1**
DCSA	Best	4.51E-13	1.47E-05	4.95E-07	3.09E-05	0.69E+00	6.08E-12	2.32E+00
	Mean	1.37E-11	0.01E+00	5.50E-04	7.70E-04	1.26E+01	8.34E-10	3.35E+00
	Std	1.83E-09	0.04E+00	9.46E-04	0.00E+00	2.26E+00	9.15E-10	0.49E+00
	Rank	**1**	**1**	**1**	**1**	**1**	**1**	2

Algorithm	Index	f_8	f_9	f_{10}	f_{11}	f_{12}	f_{13}
CSA	Best	-2.85E+03	5.98E+00	1.66E-04	0.06E+00	1.34E-06	2.33E-05
	Mean	-3.26E+03	1.31E+01	3.40E+00	0.28E+00	0.46E+00	0.12E+00
	Std	3.01E+02	3.96E+00	1.01E+00	0.09E+00	0.95E+00	0.21E+00
	Rank	2	2	2	2	2	2
DCSA	Best	-2.31E+03	0.97E+00	2.83E-06	0.04E+00	4.10E-08	2.72E-08
	Mean	-2.73E+03	1.05E+00	1.11E+00	0.13E+00	0.03E+00	0.01E+00
	Std	3.25E+02	3.14E+00	0.93E+00	0.08E+00	0.19E+00	0.02E+00
	Rank	**1**	**1**	**1**	**1**	**1**	**1**

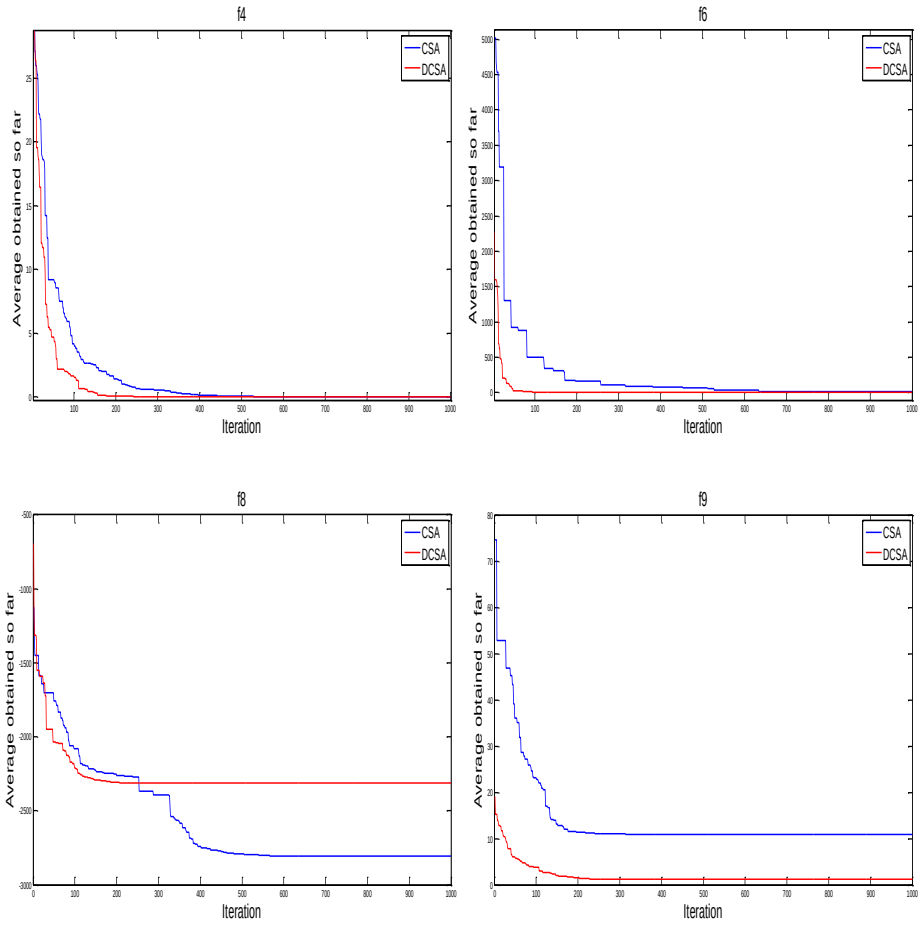

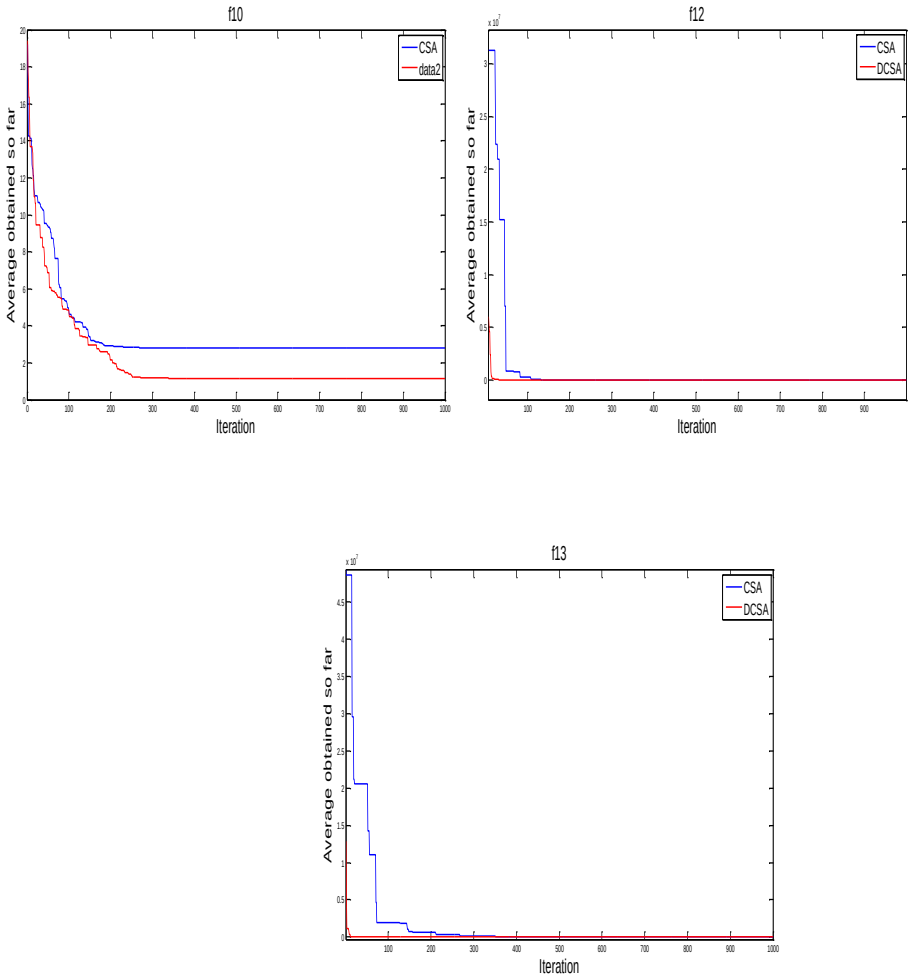

Fig. 6. Comparative convergence rates profiles.

4.4 Time control report and awareness probability decreasing influence

Proper setting of DCSA parameters can affect the algorithm solution process, in addition it is a tricky task to find out the best parameters adjustment for such a problem that could be different from a problem to another, this why following experiments will try to extract best parameters adjustment for each function problem. First of all, table 4 illustrates results of running different (AP_{max}, AP_{min}) couples to each function, while τ is fixed to 0.95, and AP_{min} is set always to 0.01 to guarantee a best exploitation in all cases, and AP_{max} is changed to handle the exploration phase. Table 5 illustrates results of multiple time control report parameters runs at each function problem, while AP_{min} and AP_{max} are set to 0.01 and 0.2 respectively.

Table 4 results display that various awareness probability bounds executed at each function provide different results from a couple to another this for ($f_1 \sim f_8$), and the best couple of previous functions is changed along them, moreover, results gap is important between different couples because some of them make a real improvement this is for f_1, f_3, f_4 and f_5. On the other hand, ($AP_{max} = 0.01, AP_{min} = 0.2$) is the

best couple for last multimodal functions due to high value of AP_{max} that promote the exploration phase on this complicated functions avoiding local optimums, so this couple is recommended for high dimensioned optimization problems. In the other hand, AP_{min} should always be set at lower values to guarantee best final solutions but avoid values very close to zero, as well as, AP_{max} should not exceed 0.3 value to not simulate further randomization into search process leading to worst exploration phase. Table 5 results make clear that good setting of τ can supply a real best solutions as $f_3, f_4, f_5 and\ f_8$, but it depends to the function problem where carrying out some trials could be useful to find the best τ adjustment to such a problem.

Table 4. Comparison results of different AP couples.

Function	Index	$AP_{min} = 0.01$ $AP_{max} = 0.2$	$AP_{min} = 0.01$ $AP_{max} = 0.15$	AP_{min} =0.01 $AP_{max} = 0.1$	AP_{min} =0.01 $AP_{max} = 0.05$
f_1	Best	2.18E-12	1.53E-12	2.11E-13	3.13E-13
	Mean	2.16E-10	6.62E-11	2.10E-11	2.07E-09
	Std	2.95E-10	9.96E-11	3.66E-11	3.88E-09
	Rank	3	2	**1**	4
f_2	Best	3.67E-05	4.73E-06	6.10E-05	7.03E-05
	Mean	0.01E+00	0.00E+00	0.01E+00	0.17E+00
	Std	0.04E+00	0.00E+00	0.02E+00	0.39E+00
	Rank	2	**1**	3	3
f_3	Best	1.65E-05	7.50E-07	6.83E-06	2.82E-04
	Mean	3.47Ee-04	5.65E-04	0.00E+00	0.02E+00
	Std	4.25E-04	9.59E-04	0.00E+00	0.05E+00
	Rank	**1**	2	3	4
f_4	Best	2.49E-05	4.25E-05	7.47E-05	6.16E-05
	Mean	0.00E+00	8.18E-04	0.00E+00	0.01E+00
	Std	0.00E+00	8.78E-04	0.00E+00	0.01E+00
	Rank	2	**1**	3	3
f_5	Best	2.01E+00	1.79E+00	1.99E+00	3.07E+00
	Mean	1.04E+01	2.43E+01	1.01E+01	2.60E+01
	Std	1.77E+01	7.55E+01	1.75E+01	8.17E+01
	Rank	2	3	**1**	4
f_6	Best	3.98E-12	1.49E-13	1.79E-12	3.32E-12
	Mean	2.93E-10	6.96E-11	1.55E-10	7.45E-10
	Std	3.67E-10	1.55E-10	2.72E-10	1.96E-09
	Rank	3	**1**	2	4
f_7	Best	2.41E+00	2.61E+00	1.77E+00	2.24E+00
	Mean	3.22 E+00	3.38E+00	3.21E+00	3.02 E+00
	Std	0.35E+00	0.34E+00	0.47E+00	0.49E+00
	Rank	3	4	2	**1**
f_8	Best	-2.35E+03	-2.23E+03	-2.38E+03	-2.10E+03
	Mean	-2.63E+03	-2.62E+03	-2.78E+03	-2.58E+03
	Std	2.97E+02	3.16E+02	4.37E+02	3.44E+02
	Rank	3	2	4	**1**
f_9	Best	2.98E+00	4.97E+00	2.98E+00	2.98E+00
	Mean	3.99E+00	8.11E+00	5.01E+00	6.11E+00
	Std	3.74E+00	4.27E+00	4.77E+00	4.57E+00
	Rank	**1**	4	2	3
f_{10}	Best	8.43E-07	6.93E-07	2.33E-06	5.67E-06
	Mean	1.46E+00	1.77E+00	1.97E+00	2.84E+00
	Std	1.00E+00	0.80E+00	0.88E+00	0.97E+00
	Rank	**1**	2	3	4
f_{11}	Best	0.02E+00	0.03E+00	0.03E+00	0.06E+00
	Mean	0.13E+00	0.14E+00	0.17E+00	0.24E+00
	Std	0.08E+00	0.08E+00	0.09E+00	0.17E+00
	Rank	**1**	2	3	4
f_{12}	Best	9.16E-09	2.73E-08	1.14E-08	6.07E-06
	Mean	0.08E+00	0.12E+00	0.30E+00	0.98E+00
	Std	0.13E+00	0.25E+00	0.43E+00	1.06E+00
	Rank	**1**	2	3	4
f_{13}	Best	2.61E-07	2.88E-07	2.73E-09	8.74E-05
	Mean	0.01E+00	0.01E+00	0.03E+00	0.13E+00
	Std	0.01E+00	0.01E+00	0.06E+00	0.18E+00
	Rank	**1**	2	3	4

Table 5. Comparison results of different time control report values.

Function	Index	τ=0.8	τ=0.85	τ=0.9	τ=0.95
f_1	Best	2.01E-09	7.12E-11	1.42E-11	9.47E-12
	Mean	1.25E-08	5.52E-09	9.07E-10	3.46E-10
	Std	1.28E-08	1.14E-08	1.45E-09	7.58E-10
	Rank	4	3	2	**1**
f_2	Best	1.16E-04	7.98E-06	1.90E-05	1.98E-05
	Mean	0.04E+00	0.02E+00	0.03E+00	0.13E+00
	Std	0.09E+00	0.09E+00	0.09E+00	0.35E+00
	Rank	3	**1**	2	4
f_3	Best	2.57E-05	2.24E-05	3.29E-07	2.60E-05
	Mean	0.00E+00	0.00E+00	3.30E-04	3.77E-04
	Std	0.00E+00	0.00E+00	4.43E-04	5.99E-04
	Rank	4	3	**1**	2
f_4	Best	1.69E-04	7.84E-05	5.07E-05	4.91E-05
	Mean	0.00E+00	0.00E+00	4.65E-04	8.77E-04
	Std	0.00E+00	0.00E+00	4.44E-04	0.00E+00
	Rank	4	3	**1**	2
f_5	Best	0.70E+00	3.00E+00	4.90E+00	1.36E+00
	Mean	1.84E+01	2.40E+01	1.32E+01	1.21E+01
	Std	5.31E+01	5.36E+01	4.69E+01	3.19E+01
	Rank	3	4	2	**1**
f_6	Best	3.10E-10	8.64E-11	5.26E-11	8.44E-12
	Mean	1.87E-08	3.32E-09	1.20E-09	1.83E-10
	Std	2.06E-08	3.85E-09	1.93E-09	2.66E-10
	Rank	4	3	2	**1**
f_7	Best	2.73E+00	1.85E+00	2.13E+00	2.16E+00
	Mean	3.42E+00	3.32E+00	3.25E+00	3.34E+00
	Std	0.36E+00	0.49E+00	0.42E+00	0.43E+00
	Rank	4	2	**1**	3
f_8	Best	-2.35E+03	-2.34E+03	-2.45E+03	-2.12E+03
	Mean	-2.71E+03	-2.70E+03	-2.75E+03	-2.69E+03
	Std	3.39E+02	2.95E+02	2.75E+02	3.12E+02
	Rank	3	2	4	**1**
f_9	Best	3.97E+00	3.97E+00	3.97E+00	1.98E+00
	Mean	1.03E+01	1.20E+00	1.11E+00	5.94E+00
	Std	4.54E+00	5.54E+00	5.00E+00	3.43E+00
	Rank	4	2	**1**	3
f_{10}	Best	1.07E-05	7.36E-06	4.15E-06	2.96E-06
	Mean	0.93E+00	1.05E+00	1.15E+00	1.22E+00
	Std	0.91E+00	0.98E+00	1.03E+00	0.92E+00
	Rank	**1**	2	3	4
f_{11}	Best	0.03E+00	0.02E+00	0.03E+00	0.03E+00
	Mean	0.15E+00	0.11E+00	0.12E+00	0.14E+00
	Std	0.06E+00	0.06E+00	0.08E+00	0.06E+00
	Rank	4	1	2	3
f_{12}	Best	2.04E-07	4.35E-08	1.00E-07	1.13E-07
	Mean	0.13E+00	0.18E+00	0.25E+00	0.21E+00
	Std	0.18E+00	0.32E+00	0.48E+00	0.49E+00
	Rank	**1**	2	4	3
f_{13}	Best	2.79E-06	1.16E-06	2.72E-08	1.32E-07
	Mean	0.01E+00	0.02E+00	0.01E+00	0.01E+00
	Std	0.01E+00	0.03E+00	0.01E+00	0.01E+00
	Rank	3	4	**1**	2

4.5 Comparison with state of the art algorithms

The proposed algorithm should be in a high range between the computational algorithms or this improvement does not make sense, for this reason DCSA is compared with four well known alogorithms GA, PSO, BOA and SSA executed in the same benchmark problems, while DCSA parameters are the same like in (4.3) section, results are giving in table 6 as well as the convergence rate of some selected functions in Fig. 7. Obtained results illustrate that DCSA outperforms all other algorithms in almost all functions problems, except two unimodal functions f_5 and f_7, and one multimodal function f_9. Superiority performance is manifested in fast and smooth

convergence rate, quickness exploration capability, avoiding local optimums, and best final solutions drawn from its exploitation capability.

Table 6. Comparison results between DCSA and some state of the art algorithms.

Function	Index	DCSA	GA	PSO	BOA	SSA
f_1	Best	4.51E-13	1.78E-09	1.74E-04	3.23E-04	2.48E-10
	Mean	1.37E-11	5.05E-08	0.09E+00	3.56E-04	7.20E-10
	Std	1.83E-09	2.51E-08	0.13E+00	1.91E-05	1.88E-10
	Rank	**1**	3	5	4	2
f_2	Best	1.47E-05	1.11E-03	0.02E+00	0.00E+00	1.11E-04
	Mean	0.10E-02	0.55E+00	1.34E+00	0.00E+00	0.00E+00
	Std	0.04E+00	0.69E+00	3.23E+00	1.95E-04	0.09E+00
	Rank	**1**	4	5	3	2
f_3	Best	4.95E-07	6.57E-06	0.00E+00	2.94E-04	2.94E-06
	Mean	5.50E-04	7.35E-03	3.19E+00	3.42E-03	8.42E-04
	Std	9.46E-04	0.00E+00	4.43E+00	1.96E-05	1.96E-04
	Rank	**1**	4	5	3	2
f_4	Best	3.09E-05	0.50E+00	0.09E+00	0.00E+00	4.05E-05
	Mean	7.70E-04	1.28E+00	0.74E+00	0.00E+00	6.80E-02
	Std	0.00E+00	0.43E+00	0.57E+00	1.77E-04	0.00E+00
	Rank	**1**	5	4	3	2
f_5	Best	0.69E+00	2.69E+00	0.48E+00	8.89E+00	2.92E+00
	Mean	1.26E+01	1.48E+01	1.44E+02	8.94E+00	1.18E+02
	Std	2.26E+00	7.01E+00	3.26E+02	0.02E+00	3.04E+02
	Rank	2	3	5	**1**	4
f_6	Best	6.08E-12	6.59E-10	3.03E-04	0.50E+00	4.02E-10
	Mean	8.34E-10	5.59E-08	0.09E+00	1.22E+00	6.35E-07
	Std	9.15E-10	3.06E-08	0.11E+00	0.33E+00	1.61E-07
	Rank	**1**	2	4	5	3
f_7	Best	2.32E+00	2.36E+00	2.39E+00	1.09E+00	1.54E+00
	Mean	3.35E+00	3.51E+00	3.38E+00	1.57E+00	2.15E+00
	Std	0.49E+00	0.48E+00	0.41E+00	0.20E+00	0.30E+00
	Rank	3	5	4	**1**	2
f_8	Best	-2.31E+03	-2.88E+03	-2.76E+03	-1.82E+03	-2.47E+03
	Mean	-2.73E+03	-3.25E+03	-3.22E+03	-1.26E+03	-2.84E+03
	Std	3.25E+02	3.21E+02	3.00E+02	2.93E+02	3.35E+02
	Rank	**1**	3	2	4	2
f_9	Best	0.97E+00	1.22E-06	2.01E+00	3.85E-02	5.96E+00
	Mean	1.05E+00	5.69E+00	1.46E+01	4.14E-02	2.34E+01
	Std	3.14E+00	4.65E+00	1.05E+01	1.56E-03	8.40E+00
	Rank	2	3	4	**1**	5
f_{10}	Best	2.83E-06	3.64E-05	0.00E+00	0.00E+00	8.46E-06
	Mean	1.11E+00	4.11E+00	2.64E+00	2.90E+00	3.36E+00
	Std	0.93E+00	0.96E+00	3.78E+00	1.41E-04	7.23E+00
	Rank	**1**	5	2	3	4
f_{11}	Best	7.76E-06	0.04E+00	0.04E+00	8.46E-04	0.07E+00
	Mean	0.00E+00	0.13E+00	0.23E+00	0.13E+00	0.24E+00
	Std	0.01E+00	0.08E+00	0.12E+00	0.15E+00	0.11E+00
	Rank	**1**	3	4	2	5
f_{12}	Best	4.10E-08	5.53E-09	3.85E-05	0.13E+00	6.27E-07
	Mean	0.00E+00	0.08E+00	0.19E+00	0.53E+00	0.15E+00
	Std	0.19E+00	0.20E+00	0.26E+00	0.31E+00	0.14E+00
	Rank	**1**	2	4	5	3
f_{13}	Best	2.72E-11	6.94E-09	9.50E-04	0.40E+00	3.45E-09
	Mean	0.01E+00	0.44E+00	0.47E+00	0.88E+00	0.75E+00
	Std	0.02E+00	0.14E+00	0.07E+00	0.20E+00	0.00E+00
	Rank	**1**	2	3	5	4

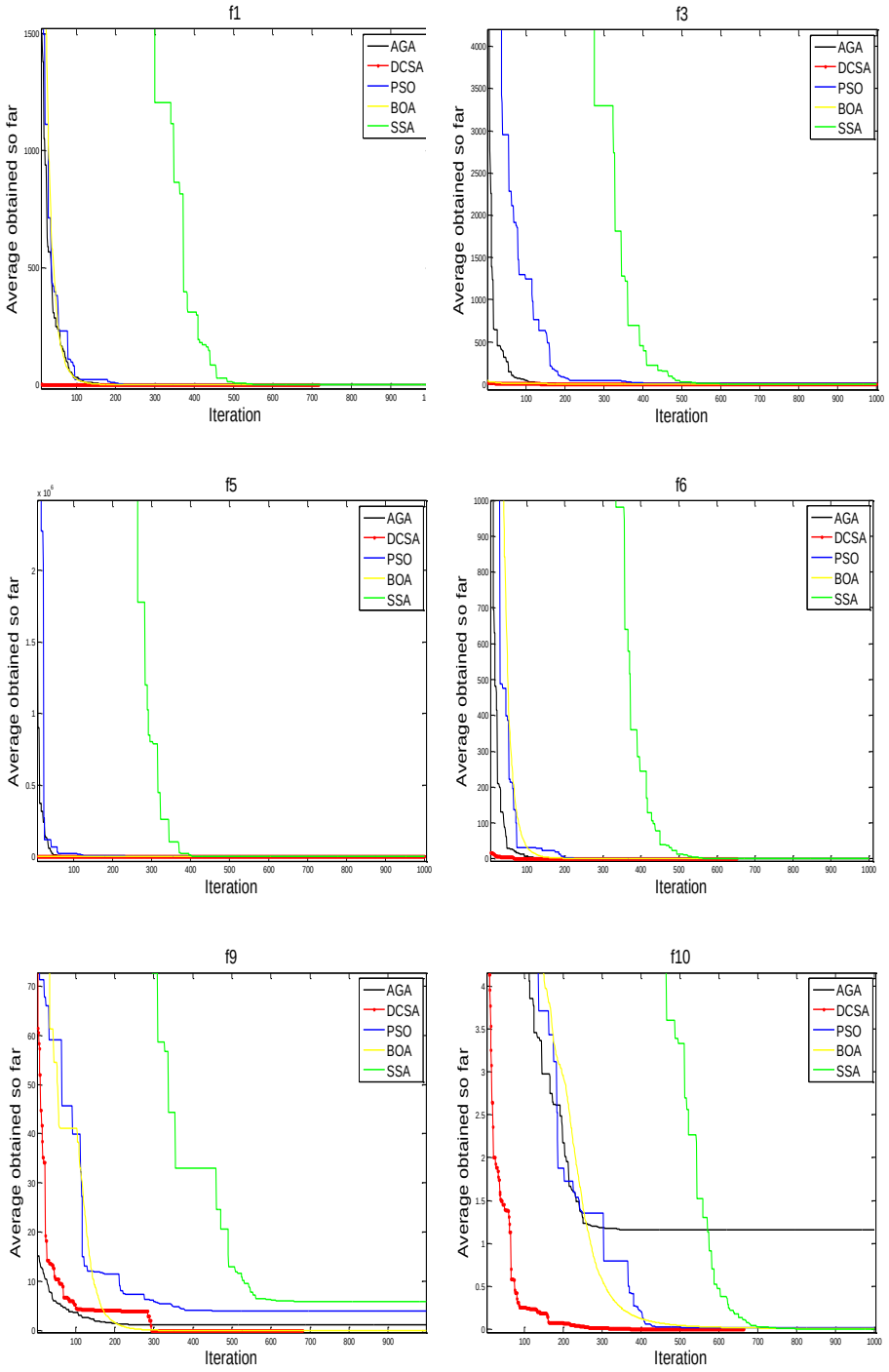

Fig. 7. Comparative convergence rates profiles.

5 Conclusion

In this paper, the original CSA is improved by introducing two modifications into the main algorithm. Hence, DCSA gain more advantages like the algorithm search process becomes dynamic and promising the exploration and exploitation phases independently by mean of adaptive parameters, DCSA convergence rate is faster toward the final solution, DCSA dynamic parameters are independent to each problem

and the final solution is most of time the best one. Multiple benchmark problems was used to assess the performance of the proposed algorithm, as well as, some experiments has been carried out to extract the best parameter adjustment of the new algorithm for each benchmark problem, finally, the proposed algorithm has been compared to those surfaced in the powerful and recent optimization field. Results obtained validate the effectiveness and superiority of the new algorithm that it can overtake the original algorithm weaknesses, promising its application to the practical and engineering problems for further research in which it can challenge high dimension and additional constraint problems that can effects its performance.

IV. 3. Optimal control design for power system stabilizer using a novel crow search algorithm dynamic approach

Abstract. This paper proposes the first application of a novel improved metaheuristic optimization technique, dynamic crow search algorithm (DCSA) to find the optimal design of the power system stabilizer (PSS). Using the novel DCSA adaptive approach provides a global search capability as well as fastness and effectiveness to get the PSS best parameters under the search space constraints and local optimums. Moreover, PSS parameters has a crucial effect on power system stability that is a major nowadays engineering concern, where its best parameters could make a difference by damping small-signal stability oscillations effectively and in the smallest amount of time if they are obtained through a robust algorithm. As a result, PSS will prevent large types of instabilities which could reach up to some generation stations shedding. The novel proposed algorithm is for first time used and tested under different power system instabilities scenarios by using single-machine infinity bus model over multiple operating conditions to damp out perturbation signals effectively by means of getting optimal PSS design parameters, where Integral absolute error (IAE) performance index is used as an objective function to be minimized. Additionally, results obtained by the proposed approach are compared with those obtained by other methods. It is observed that the proposed method has better convergence characteristics and robustness compared to the original version and other comparison methods. It is revealed that the proposed adaptive method is able to improve the power system stability dynamics and damp out perturbation oscillations successfully.

Keywords: Optimal control, small-signal stability, PSS controller, DCSA global adaptive optimization algorithm.

1. PSS control design formulation

1.1. Power System Modeling

In this paper, the power system under study is composed of a single machine connected to an infinite bus (SMIB) through a transmission line as shown in Fig. 1, whereas, Fig. 2 shows the well-known Phillips–Heffron block diagram of the linearized model of the SMIB power system simulation. Here, a fourth order model has modeled the synchronous machine, The interaction among its variables is expressed in terms of six constants K1-K6. These constants with the exception of K3, which is only a function of the ratio of impedance, are function of the operating active and reactive power load as well as the excitation levels in the machine. Hence, K1-K6 depend on operating point as well as PSS best parameters change according to them.A power system state equation can be formulated as follows:

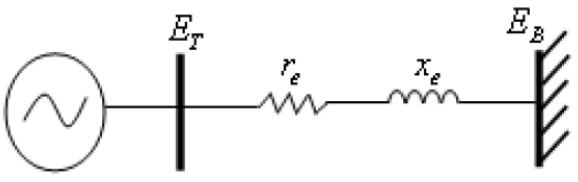

Fig. 1. Schematic line diagram for SMIB

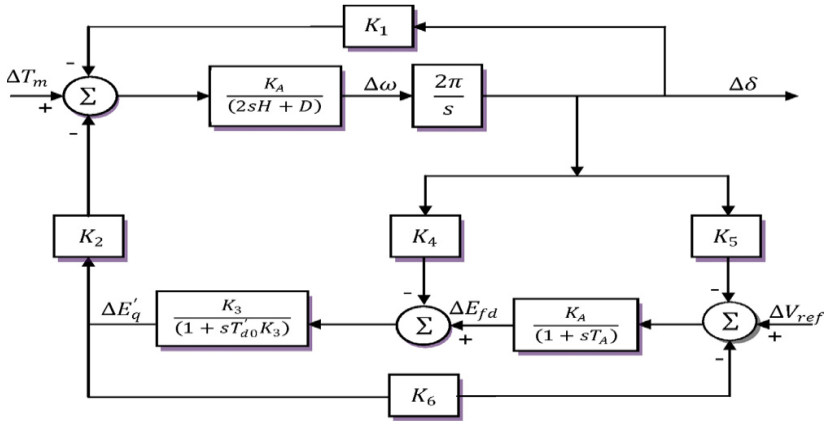

Fig. 2. The block diagram of the Phillips-Heffron model of SMIB

$$\dot{X} = f(X, U) \tag{1}$$

Where X is the vector of state variables and U is the vector of input variables. State vector consists of $[\Delta\delta, \Delta\dot{W}, \Delta\dot{E}'_q, \Delta\dot{E}_{fd}]^T$. Where, $\Delta\dot{\delta}$, $\Delta\dot{W}$, $\Delta\dot{E}'_q$, and $\Delta\dot{E}_{fd}$ are the rotor angle, rotor speed, q-axis component of internal generator voltage and excitation voltage, respectively. U is the PSS output signal. This linearized model is commonly used for the analysis of parameter values tuning of PSS.

$$\Delta\dot{\delta} = W_0\, \Delta W \tag{2}$$

$$\Delta\dot{W} = \frac{1}{M}\left(-K_1\, \Delta\delta - D\, \Delta W - K_2\, \Delta E'_q\right) \tag{3}$$

$$\Delta\dot{E}'_q = \frac{1}{T'_{d0}}\left(-K_4\, \Delta\delta - \frac{\Delta\, E'_q}{K_3} + \Delta E_{fd}\right) \tag{4}$$

$$\Delta\dot{E}_{fd} = \frac{1}{T_a}\left(-K_a\, K_5\, \Delta\delta - K_a\, K_6\, \Delta E'_q - \Delta E_{fd} + K_a V_s\right) \tag{5}$$

State space form equation is as follow:

$$\begin{bmatrix} \Delta\dot{\delta} \\ \Delta\dot{w} \\ \Delta\dot{E}'_q \\ \Delta\dot{E}_{fd} \end{bmatrix} = \begin{bmatrix} 0 & 2\pi f & 0 & 0 \\ \frac{-K_1}{M} & \frac{-D}{M} & \frac{-K_2}{M} & 0 \\ \frac{-K_4}{T'_{d0}} & 0 & \frac{-1}{T'_{d0}K_3} & \frac{1}{T'_{d0}} \\ \frac{-K_A K_S}{T_A} & 0 & \frac{-K_A K_6}{T_A} & \frac{-1}{T_A} \end{bmatrix} \cdot \begin{bmatrix} \Delta\delta \\ \Delta w \\ \Delta E'_q \\ \Delta E_{fd} \end{bmatrix} = \begin{bmatrix} 0 \\ 0 \\ 0 \\ \frac{K_A}{T_A} \end{bmatrix} . V_x(t) \tag{6}$$

1.2. Power System Stabilizer

PSS is a generic name for controllers that stabilize a synchronous machine by adjusting the excitation voltage, there is various models of PSS. The difference between models lies in the number of inputs to the controller, the choice of the signal to be used as an input signal to the PSS, and the components of the controller. Choice of PSS design is crucial to have an optimal perturbations damping possible. In the present study a second order lag compensator, in series with a washout filter is used as shown in Fig. 3. Eq. 7, illustrates its transfer function, the input signal in this PSS model is usually the negative of the machine's speed deviation.

$$G(s) = K_p \left(\frac{T_w\, S}{T_w S + 1}\right)\left(\frac{T_1 S + 1}{T_2 S + 1}\right)\left(\frac{T_3 S + 1}{T_4 S + 1}\right) \tag{7}$$

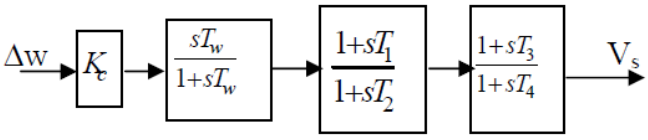

Fig.3 . Structure of power system stabilizer

2. PSS optimal damping control based DCSA

To enhance the PSS controller performance applied to a linearized model of a single machine infinite bus for the reason of having sufficient damping torque to damp out the synchronous machine electromagnetic oscillations after being subjected to a disturbance, and under wide range of operating conditions within smallest amount of time. DCSA is utilized to get the PSS best parameters design. Where, the objective function to be minimized is the integral absolute error (IAE) index of the speed angle deviation as given below.

$$\mathrm{IAE} = \int_0^t \left|\Delta \dot{W}(\mathrm{t})\right| \, \mathrm{dt} \tag{14}$$

Where, t is the simulation time.

To reduce the search space the washout filter's gain T_w is fixed to 5 s. While PSS controller gain and time constants are to be optimized and there are subjected to the following constraints.

$$0 \leq K_c \leq 50$$

$$0.01 \leq T_{i=1,..,4} \leq 5$$

2.1. Experimental Results

To showcase DCSA besed PSS superiority above its original version CSAPSS, GAPSS and conventional PSS, a small disturbance of 10% step increase is in mechanical torque is applied at three loading conditions at the same time t=0.5 s. Algorithms parameters in table 2 are the most recommended from their original papers. Otherwise, common parameters like population size and maximum number of iterations are set to 30 and 100 respectively. Fig. 4, represents the PSS based DCSA flowchart.

Table 1

Conventional algorithms parameters

algorithm	DCSAPSS	GAPSS	CSAPSS	CPSS[4]
parameters	AP=0.1 $fl = 1.8$ $AP_{min} = 0.01$ $AP_{max} = 0.2$ τ=0.9	Roulette is used for selection Crossover fraction=0.9 Mutation=0.005	AP=0.1 $fl = 1.8$	K_c =2.1783 $T_1 = 1.4557$ $T_2 = 0.6143$ $T_3 = 1.0083$ $T_4 = 0.005$

Simulation results in light and nominal load operating condition Fig. 5and Fig. 6. Illustrate that DCSAPSS is the best damping controller among CPSS, CSAPSS and GAPSS in terms of speed deviation and load angle deviation. Furthermore, oscillation damping is affected without overshoot and the system gain a new stable condition in small amount of time less than 1s. As well as, the DCSA gets the best PSS parameters in a competitive time at 20th iteration with smooth convergence curve which prove the DCSAPSS controller performance and exploration capability. In other hand, CSAPSS, GAPSS and CPSS present a multiple overshoots in their simulation responses and the system gets a new stable state in critical amount of time. As well as, GAPSS and CSAPSS convergence toward the PSS best parameters in a large amount of time. Heavy load operation condition is a critical operating condition despite that DCSAPSS still the best damping controller and outperforms other controllers in terms of overshoot and time response to get a stable new state as shown in Fig. 7.

Table 2

PSS optimal design parameters comparison in different operating conditions

Operating conditions	Algorithms	IAE	Kc	T1	T2	T3	T4
Light Load P=0.5 Q=0.169	**DCSA**	**0.61E-3**	**47.254**	**4.548**	**1.254**	**1.045**	**2.024**
	CSA	**0.002**	**29.746**	**1.485**	**3.004**	**1.784**	**0.148**
	GA	**0.05**	**25.248**	**2.078**	**0.278**	**1.485**	**1.789**
Nominal Load P=0.9 Q=0.2907	**DCSA**	**3.46E-5**	**40.078**	**4.338**	**2.838**	**1.756**	**3.128**
	CSA	**0.49**	**45.213**	**3.155**	**1.245**	**0.148**	**2.354**
	GA	**2.02E-1**	**25.142**	**2.178**	**2.145**	**4.789**	**1.245**
Heavy Load P=1.1 Q=0.35	**DCSA**	**2.46E-4**	**47.548**	**3.125**	**2.154**	**1.214**	**2.489**
	CSA	**1.64E-1**	**44.247**	**1.024**	**3.152**	**2.485**	**2.145**
	GA	**1.02E-1**	**43.215**	**0.125**	**3.125**	**2.145**	**1.025**

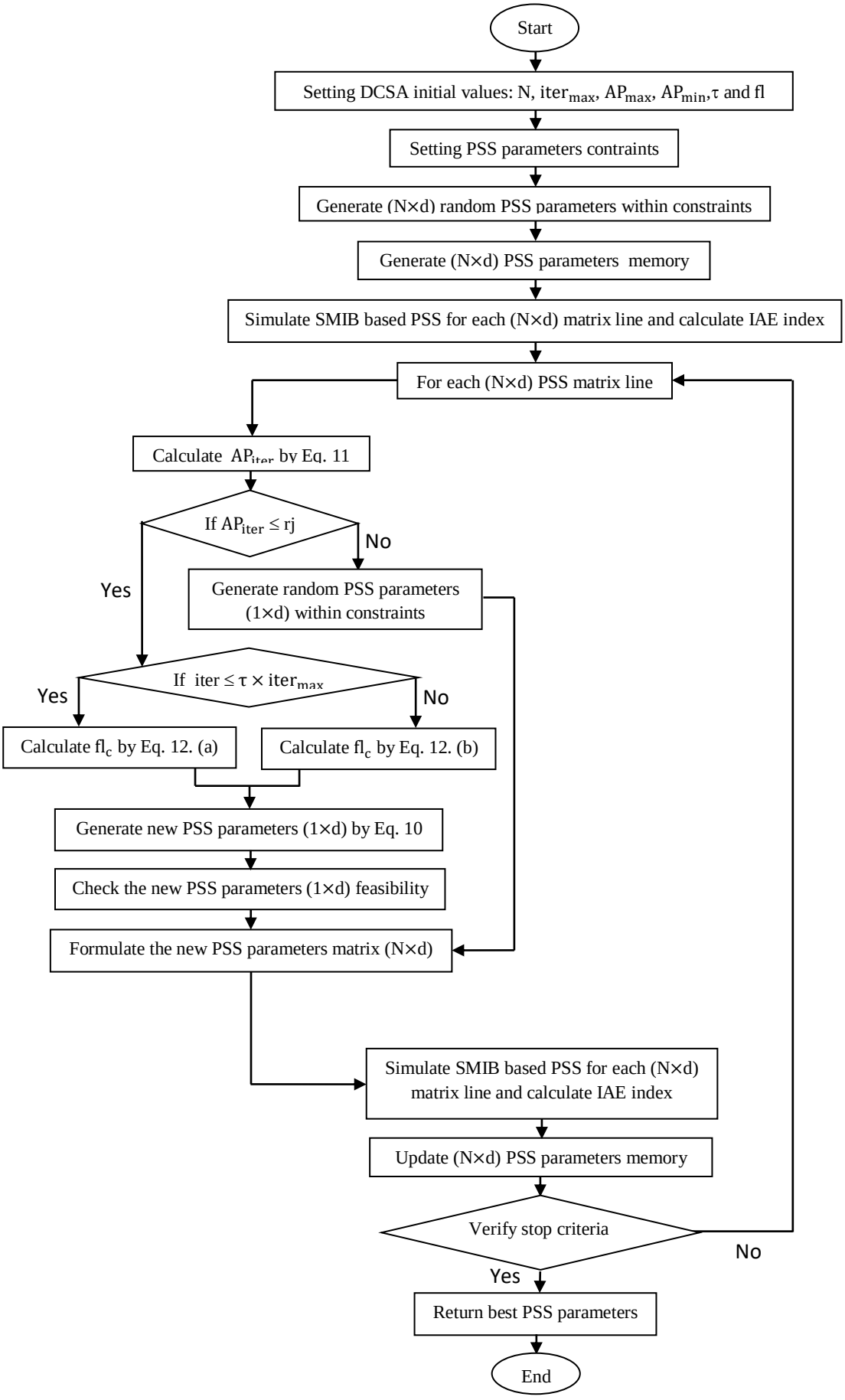

Fig.4 . PSS based DCSA optimal damping control.

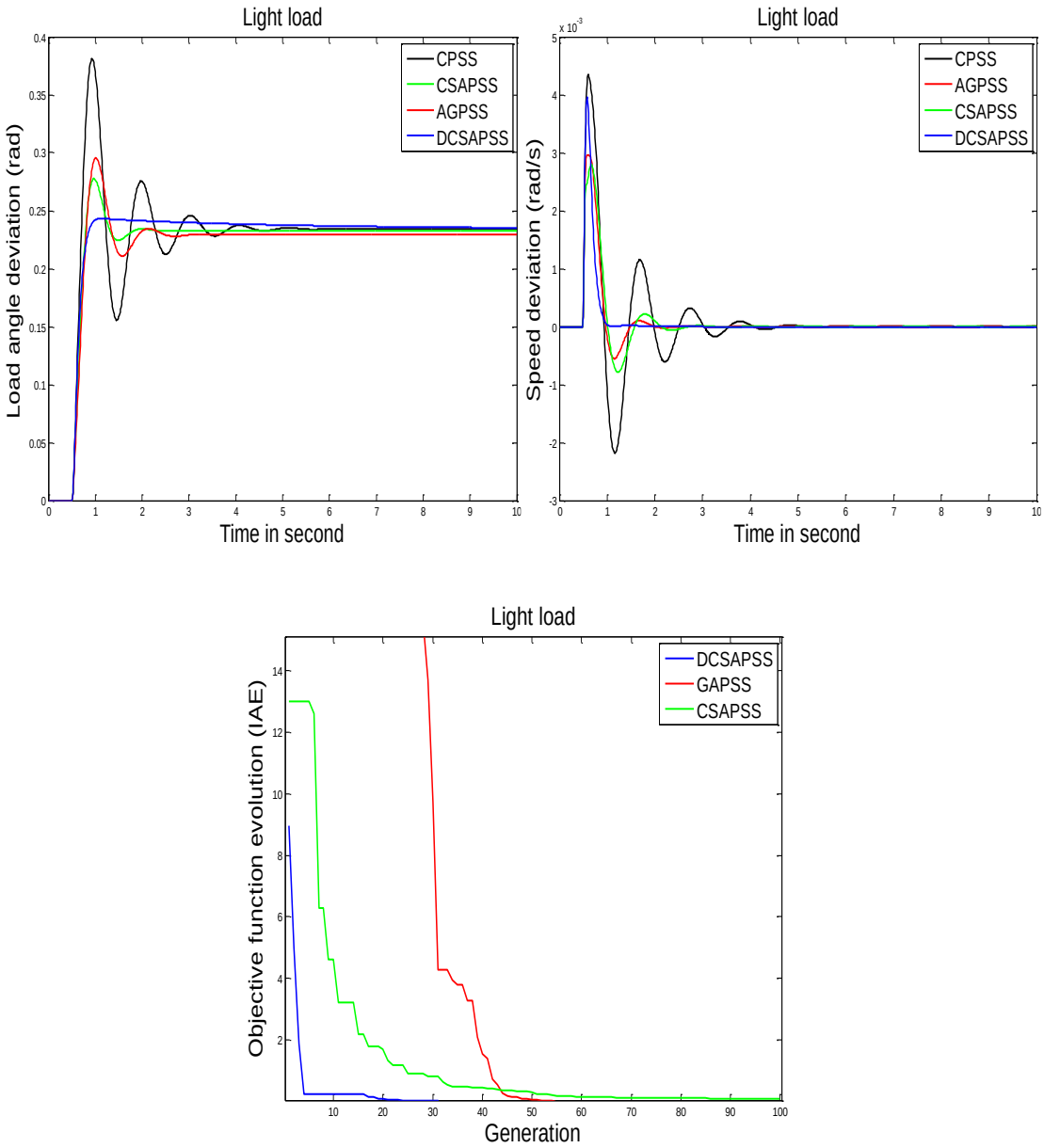

Fig.5 . Disturbanced system response comparison under different optimal PSS design based in DCSA, CSA and GA in light load.

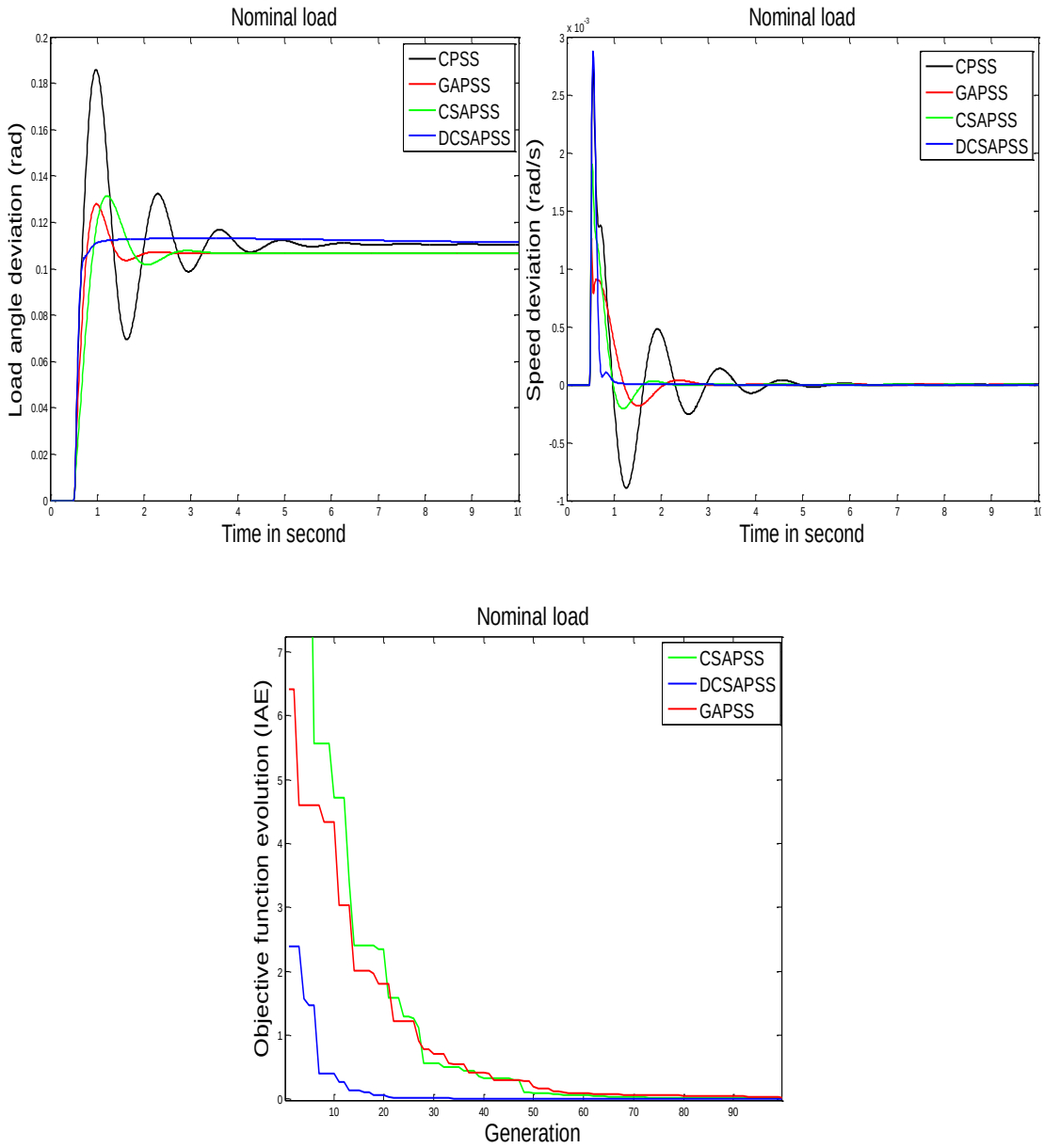

Fig.6 . Disturbanced system response comparison under different optimal PSS design based in DCSA, CSA and GA in nominal load.

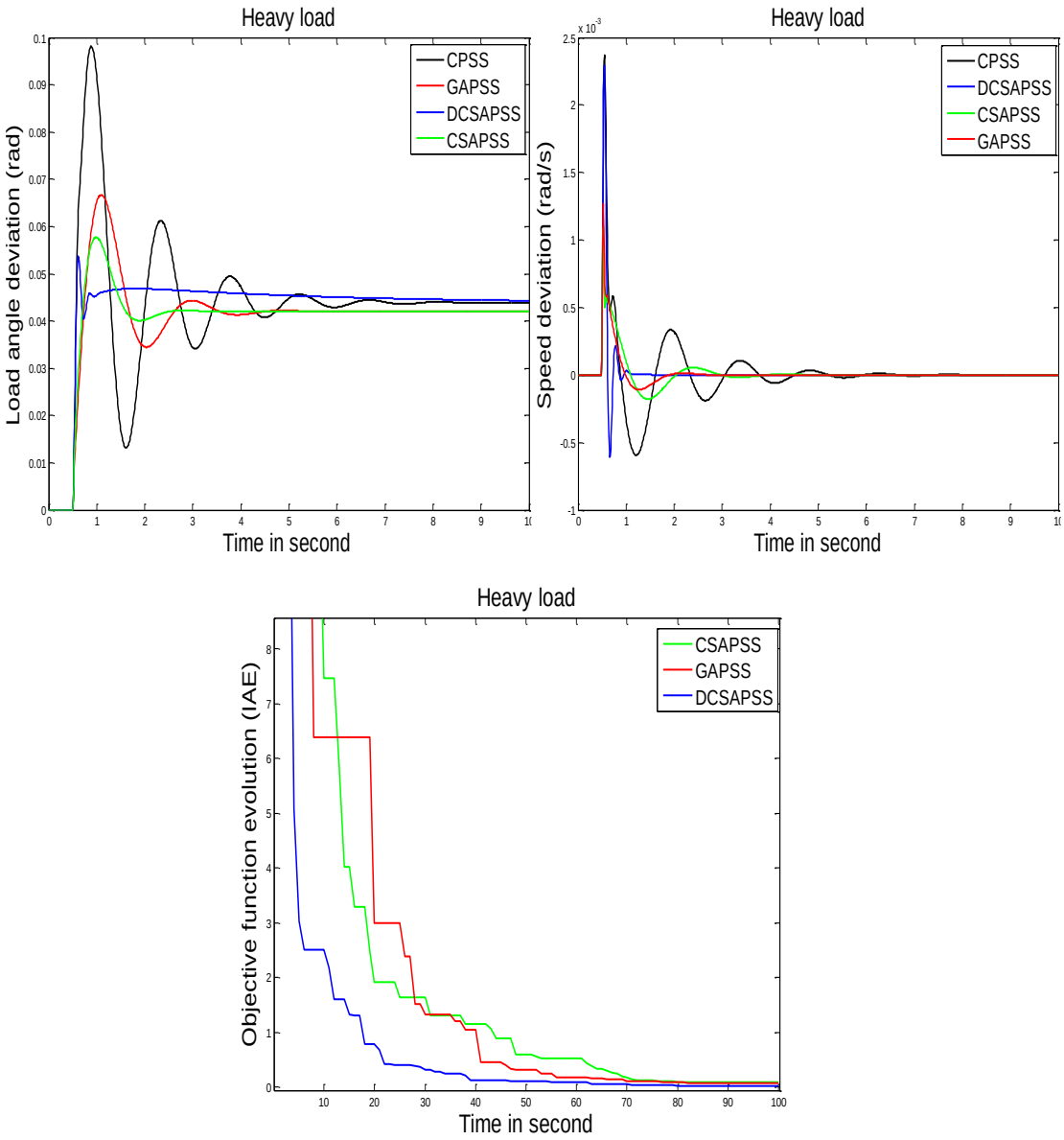

Fig.7 . Disturbanced system response comparison under different optimal PSS design based in DCSA, CSA and GA in heavy load.

3. Conclusion

In this paper, a new dynamic optimization approach called DCSA has been employed for the design of lead-lag controller based PSS to damp out the low frequency oscillations in a SMIB electric network. The PSS adjustment parameters is formulated as an optimization problem and the IAE stability index is considered as an objective function to be minimized which reflects the oscillation damping response of the system. Simulation results prove the robustness and superiority of the proposed controller DCSAPSS to achieve best damping characteristic to system oscillations over wide range of operating conditions. Additionally, results found by this dynamic approach prove its superiority against other conventional techniques. Eventually, good results found by this dynamic approach promote the application of DCSAPSS in large scale power system future works.

IV. 4. Transit stability enhancement of power system with high solar energy integration

IV. 4. 1. Introduction

Global primary energy demand has grown by an annual average of around 1.8% since 2011, although the pace of growth has slowed in recent years, with wide variations by country. Growth in primary energy demand has increased largely in developing countries, while in developed countries it has stagnated or even declined [123]. As of 2015, renewable energies provided around 19.3% of the world's final energy consumption, of which solar energy represented 1.6%. Consequently, in a rapidly changing global energy context marked by a reduction in conventional fossil fuels and greenhouse gas emissions, the development of renewable energies remains the most effective bulwark [123].

In the context of the development of large-scale photovoltaic power generation, solar PV power plants are relevant. They are growing all over the world. There are two main classes of photovoltaic installations [124]:

- So-called autonomous "off-grid" installations, where the energy produced by the sun must generally be stored in batteries if the use is not immediate.
- Installations connected to the network, capable of debiting the energy produced and which consists of a centralized system (direct injection into the power system) and decentralized (injection into the power system of the user's surplus energy).

Centralized systems connected to the grid, mainly composed of ground-based solar PV plants, occupied more than 60% of the share of PV installations at the end of 2015. While decentralized systems retreated over the years ahead of centralized systems and are of the order of 30% in 2015. Autonomous systems occupy the lowest share [123].

In a context of connected installations development to the power system, experiments on hybrid solutions are carried out and combine connection to the power system and large storage capacities in order to optimize the sale and purchase according to the dynamic evolution of kilowatt-hour prices and on the other hand to help maintain the power system frequency (at 50Hz)[125].

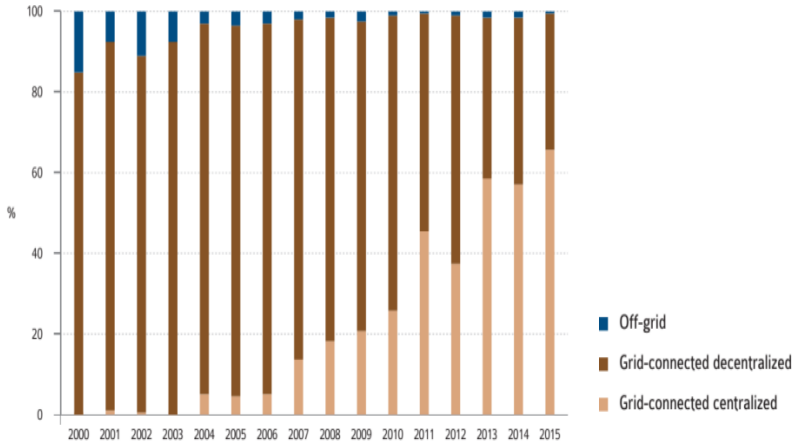

Figure VI. 1. Share of grid-connected and non-grid installations 2000-2015

The competitiveness of PV is defined by the fact that it can produce electricity at a lower cost than other sources of electricity at any given time. It is determined by the LCOE [124]. "Levelized Cost of Electricity". Therefore, the competitiveness of a photovoltaic system is linked to its location, the technology implemented and the cost of the photovoltaic system itself which strongly depends on the nature of the installation and its size [126]. However, it will also depend on the climatic conditions in which the system will operate.

This research focuses on the PV integration impact on the power system transient stability where the index of this stability is represented by the maximum time during which the grid can withstand the fault without losing its stability, this time is known as the critical clearing time (CCT). FACT system is used to improve the network performance in the presence of PV source, for the reason of the opportunity offered by power electronics to control reactive power balance of the power system and therefore improve buses voltage status. A three-phase short circuit is applied to a 30-bus IEEE test system to assess its stability. Simulations are performed under the Power System Analysis Toolbox software (PSAT).

IV. 4. 2. PV power plants analysis and modeling

PV generator consists of three key components, namely PV array, power electronics interface (converter) and the associated controllers. For power system stability studies, modeling of large-scale PV should consider steady state and dynamic models [123]. The physical difference between synchronous generators and PVs, i.e., inertial contribution of the rotating mass, utters that there will be significant variations of active power flows across the system for high PV penetrations. The power injection from zero inertia generators like PV, will affect the angular positions of all the synchronous machines. Hence, the electromagnetic capability of the whole system will be affected [127].

The power flow provides the initial condition for dynamic simulation. For power system dynamic studies, the solar farm is modeled as a single-generator equivalent as

shown in Figure (VI. 2) Acomplete model of solar farm with a large-number of PVs increasesthe computational burden. Moreover, this assumption is reasonable when power system under consideration is large, and themain purpose is to observe the effect of penetration on the externalnetwork rather than within the large-scale PV plant. The components that contribute to the dynamicbehavior of large-scale PV plants are included in the analysis andoutlined as follows [123, 126]:

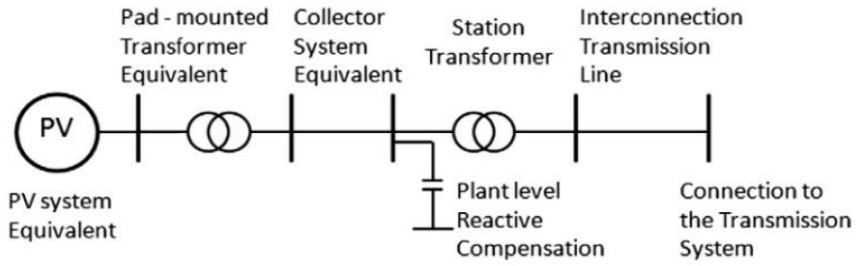

Figure VI. 2. Schematic diagram of single-generator equivalent PV plant.

- Non-linear characteristics of PV array.
- Power electronic converter-voltage source converter model.
- Converter control-two controllers are used to provide control ofreal power and voltage/reactive power.

Figure (VI. 3) shows the block diagram of PV converter model. There are different possibilities for converter transfer functions; however, first order function with steady state gain is highly adopted.

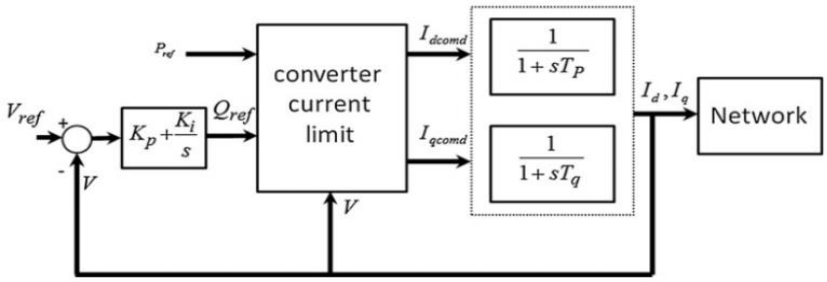

Figure VI. 3. Block diagram of PV generator converter.

The PV penetration level is defined as the ratio of total PV generation to totalsystem load, as expressed in the following equation:

$$PV\ penetration\ (\%) = \frac{Total\ PV\ generation\ (MW)}{Total\ power\ generation} \qquad \text{(IV. 1)}$$

IV. 4. 3. Transit stability

It relates to the power system ability to maintain synchronism after having undergone a severe transient disturbance such as a short circuit on a transmission line

or a loss of a significant part of the load or generation. The response of the system involves large variations in rotor angles [128].

For a system to be transiently stable during a disturbance, it is necessary for the rotor angle, to oscillate around an equilibrium point. If the rotor angle increases indefinitely, the machine is said to be transiently unstable as the machine continues to accelerate and does not reach a new state of equilibrium. So, to maintain this equilibrium, the power systemmust at any time keep one's balance between all torques applied on rotor of synchronous generators, as its behavior described by the swing equation as follow [129, 130].

$$\frac{2H}{W_{syn}} W_{pu} \left(\frac{d^2\delta}{dt^2}\right) = P_{mpu} - P_{epu} - \frac{D}{W_{syn}} \left(\frac{d\delta}{dt}\right) \quad \text{(IV. 1)}$$

Where:

t: is time in seconds,
P_{mpu}: is the mechanical power supplied by prime mover per unit.
P_{epu}: is the electrical power output of the generator, per unit.
W_{pu} , W_{syn} : are the per unit frequency and the synchronous radian frequency respectively
δ: is the rotor position with respect to synchronously rotating reference in rad.
D:is the damping torque at anytime the generator deviates from its synchronous speed.
H: is the normalized inertia constant.

In steady-state operation, all synchronous machines in the system rotate at the same electrical angular speed. The mechanical torque **Tm** has the same direction as the rotation of the generator axis. However, the electrical torque **Te** is in the opposite direction to that of rotation.

The critical clearing time *(CCT)*is the most decisive parameter in the analysis of the transient stability of an electrical grid, mathematically it is the solution of the second order non-linear differential equation known as the Swing equation, which physically represents the maximum time during which our power system can withstand a fault (short-circuit, over load, over current…) without losing its stability[131]. This is the stability assessment criterion adopted in this article.

IV. 4. 4. Flexible AC Transmission System (FACTS)

Flexible AC transmission system is an evolving technology to help electric utilities. Its first concept was introduced by N.G Hingorani, in 1988 .The solutions to improve the quality of supply in the electrical networks with go through the applications of the developments in semiconductor power devices, that is to say, the utilization of static power converters in electrical energy networks. The technological

advances in power semiconductors are permitting the development of devices that react more like an ideal switch, totally controllable, admitting high frequencies of commutation to major levels of tension and power [132, 133].

Recent development of power electronics introduces the use of FACTS controllers in power systems. FACTS controllers are capable of controlling the network condition in a very fast manner and this feature of FACTS can be exploited to improve the voltage stability, and steady state and transient stabilities of a complex power system [134]. This allows increased utilization of existing network closer to its thermal loading capacity, and thus avoiding the need to construct new transmission lines. The well known FACTS devices are namely SVC, STATCOM, TCSC, SSSC and UPFC. In this paper, we focus on shunt compensators (SVC, STATCOM).

A. Static Var Compensator (SVC)

SVC is a static Var compensator which is connected in parallel to transmission line. SVC acts as a generator/load, whose output is adjusted to exchange capacitive or inductive current so as to maintain or control specific power system variables. Static Var systems are applied by utilities in transmission applications for several purposes. The primary purpose is usually for rapid control of voltage at weak points in a network. Installations may be at the midpoint of transmission interconnections or at the line ends. SVC is similar to a synchronous condenser but without rotating part in that it is used to supply or absorb reactive power. The basic structure of SVC is shown in Figure (VI. 4). The SVC is connected to a coupling transformer that is connected directly to the ac bus whose voltage is to be regulated. From Figure (VI. 4), SVC is composed of a controllable shunt reactor and shunt capacitor(s). Total susceptance of SVC can be controlled by controlling the firing angle of thyristors. However, the SVC acts like fixed capacitor or fixed inductor at the maximum and minimum limits.

B. STATCOM

The STATCOM resembles in many respects a synchronous compensator, but without the inertia. The basic electronic block of a STATCOM is the voltage source converter (VSC), which in general converts an input dc voltage into a three-phase output voltage at fundamental frequency, with rapidly controllable amplitude and phase angle. In addition to this, the controller has a coupling transformer and a dc capacitor. The control system can be designed to maintain the magnitude of the bus voltage constant by controlling the magnitude and/or phase shift of the VSC output voltage.

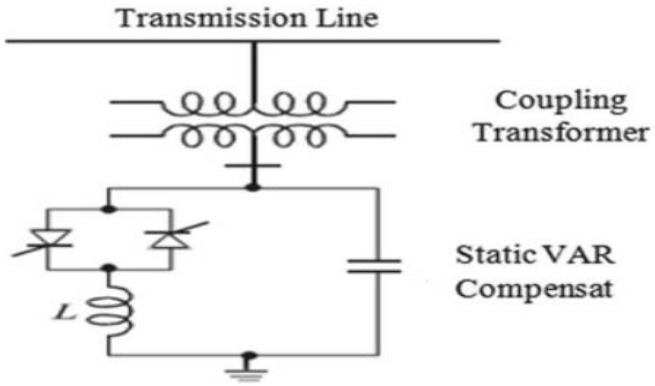

Figure VI. 4. SVC connected to a transmission line.

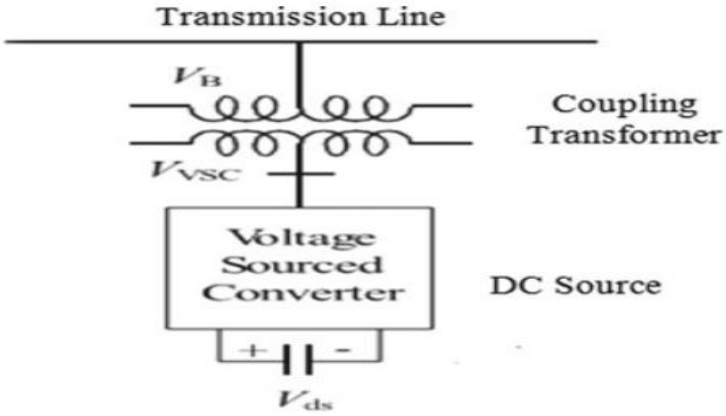

Figure VI. 5. STATCOM connected to a transmission line.

IV. 4. 5. Results and discussion

Simulation analysis was established on the famous 30 bus IEEE test system Fig. 6 by PSAT/MATLAB, which gives an access to an extensive library of the power system components.

TABLE IV. I. IEEE-30BUS TECHNICAL DATA

Number of Bus	Number of Charges	Number of Generators	Number of Transformers	Number of line of Transmissions
30	21	6	7	33

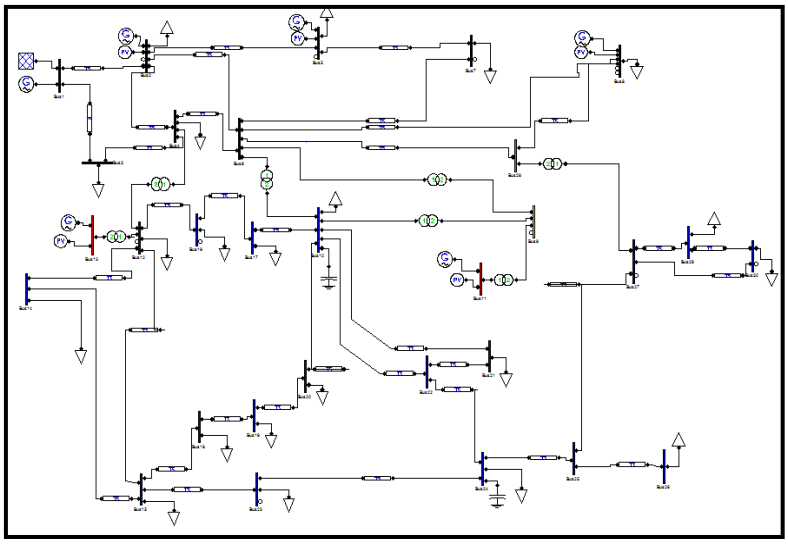

Figure VI. 6. IEEE 30 bus model with PSAT.

Three-phase short-circuit is the type fault chosen as a result of its most dangerous consequences against power system to assess its transit stability

Firstly a steady state analysis (before creating the default) is presented were essentially the voltage profile at all busses of the system are in their acceptable limits (0.90–1.1 p.u) Figure (VI. 7).

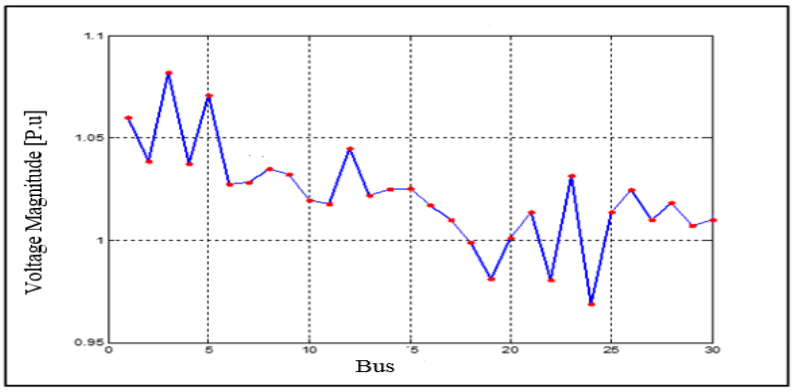

Figure VI. 7. Voltage profile.

A comparative study has been carried out dependent on the values of the critical clearing time calculated by singular value method. By creating a short circuit in different locations bus"i"in order to identify the most sensitive bus in the presence of the fault. According to Table II, it's clear that the critical time varies from one bus to another, this is due to the ability of each bus to support the fault.

TABLE IV. II. CRITICAL CLEARING TIME FOR DIFFERENT FAULT LOCATION

Bus	Bus 2	Bus 4	Bus 5	Bus 8	Bus 12	Bus 17	Bus 18	Bus 27
CCT(ms)	15	19	20	40	20	28	30	20

To show the importance of determining CCT and take in consideration for power system protection planning, a short circuit is simulated at bus 8 with time prolongation of 1ms further than its based CCT Figure (VI. 8). According to Figure (VI. 9, 10), we can see that the change of just 1 (ms) of CCT can cause the instability of the system or even a collapse.

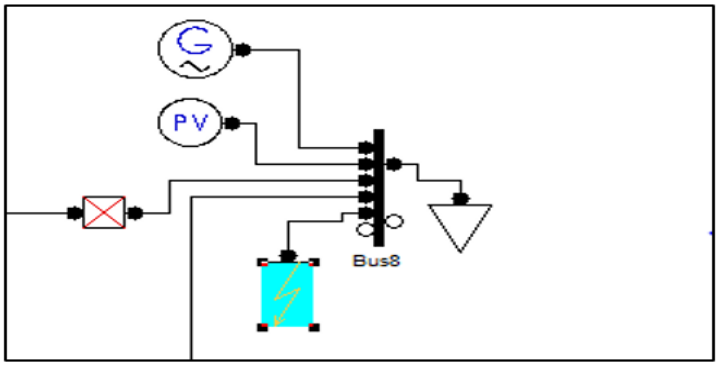

Figure VI. 8. Fault location at bus 8.

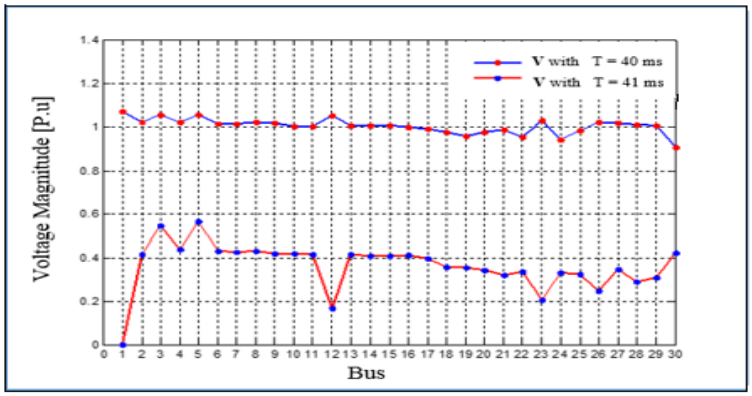

Figure VI. 9. Voltage profile at the presence of a fault at bus 8.

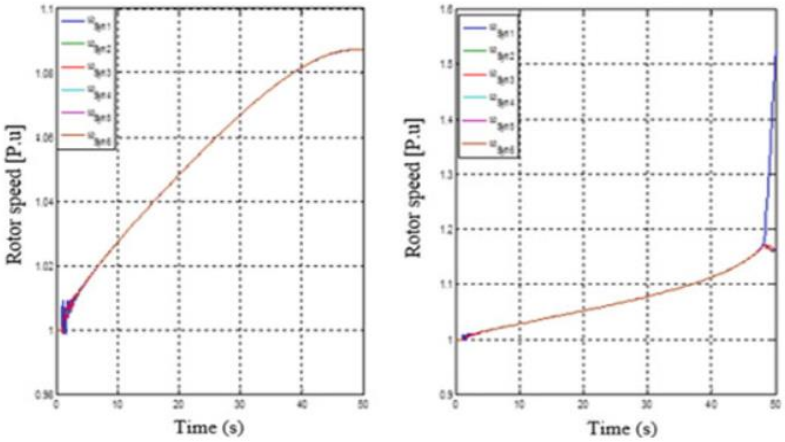

Figure VI. 10. Generators rotor speeds.

To evaluate the power system stability in terms of receiving power from PV plants, a fault has been considered at bus 18 with integration of a solar PV plant. The power injected by solar PV plant into the power grid is around 50 MW. Figure (VI. 11) shows the Penetration of a solar PV with presence of the fault at bus 18. Furthermore,

a comparison between the power system with and without PV integration is made in Figure (VI. 12) considering different fault locations.

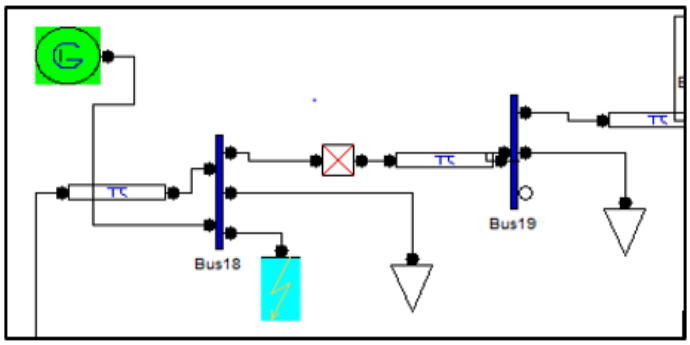

Figure VI. 11. Penetration of a solar PV with presence of the fault at bus 18.

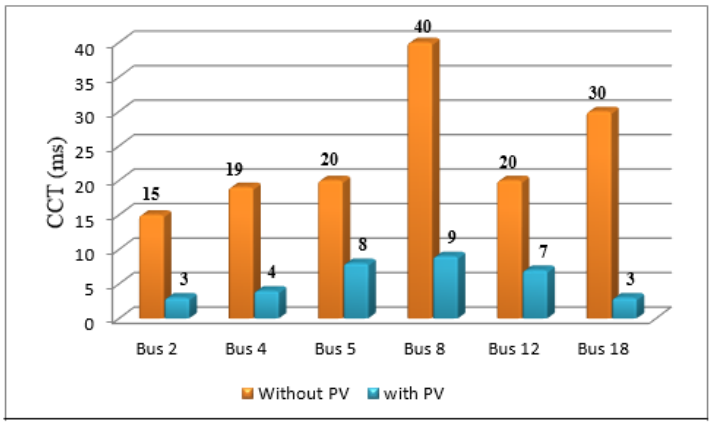

Figure VI. 12. CCT comparison histogram with and without PV integration.

According to Figure (VI. 12), it is clear that the penetration of solar PV has enormously reduced the CCT and consequently the ability of the power system to maintain its stability during the fault in all the cases studied. This is due to the inability of the PV to participate in the voltage setting plan in the absence of reactive power in such sources. Additionally, PV penetration rate is inversely proportional to the corresponding critical time values.

To improve power system transit stability multiple FACTS are used and a comparison of their performance is made. The use of the FACTS system is justified to improve the network's ability to withstand faults for longer periods of time. In this section, an SVC, STATCOM and UPFC have been introduced Figure (VI. 13, 14 and 15) in order to check their influence on solar power penetration. After several simulations important results are achieved:

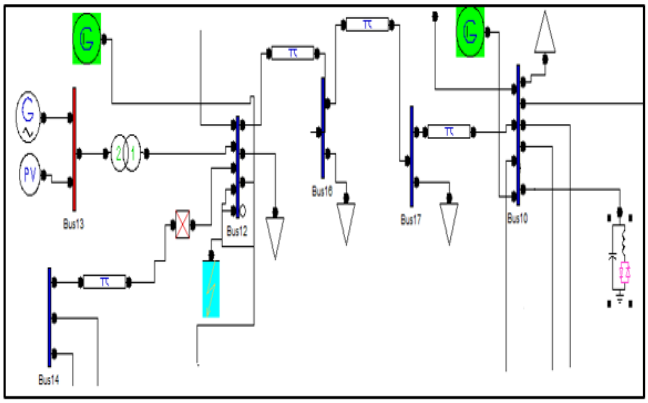

Figure VI. 13. Localization of SVC.

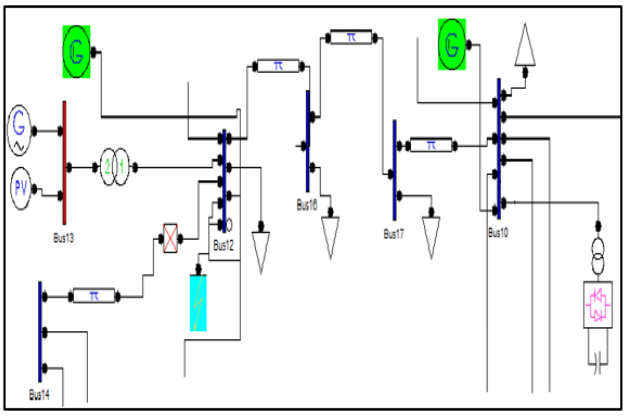

Fig VI. 14. Localization of STATCOM.

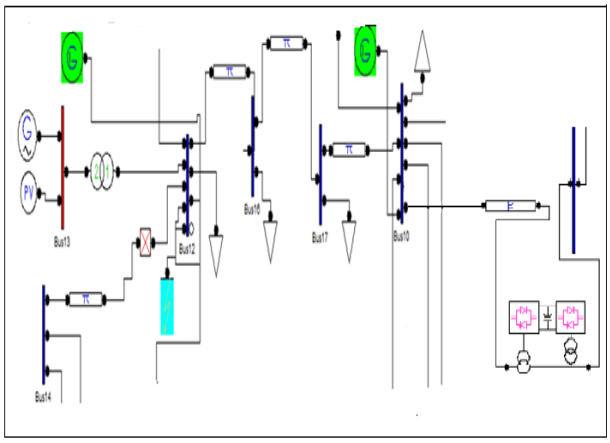

Figure VI. 15. Localization of UPFC.

After the integration of FACTS (UPFC, SVC and STATCOM) it can be seen that a considerable improvement in the CCT has been noticed, which will provide a great opportunity to integrate more energy from PV sources. UPFC as shown in the histogram in Figure (VI. 16) shows a modest superiority over STATCOM and SVC.

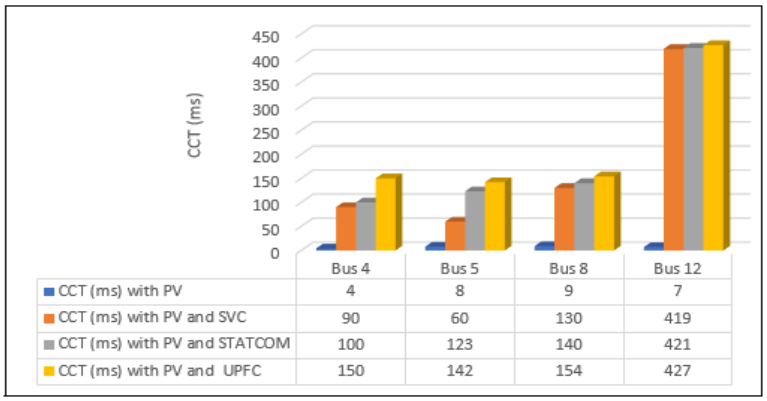

Figure VI. 16. CCT histogram comparison.

IV. 4. 6. Conclusion

Last work has mainly focused on the assessment of power system transient stability in the presence of PV sources and compensation systems FACTS. Critical clearing time (CCT) is the adopted assessment criterion for several cases by observing the simulation behavior of test systems during grid faults using a Power System Analysis Toolbox (PSAT).

According to previous simulations, it's found that:

- Penetration of solar PV has reduced the CCT and thus the ability of the power system to maintain its stability during the faults.
- Location of faults and PV integration has a great effect on transit stability (CCT).
- A considerable improvement on CCT has been noticed after the integration of FACTS (UPFC, SVC, STATCOM).

Simulation results clearly illustrate that there is an opportunity to integrate more energy from PV sources into the power system through FACTS.

General conclusion

The study presented in this thesis focuses on the application of optimization algorithms, in particular the developed algorithm DCSA in the synthesis and optimization of the parameters of the power system stabilizer. The role of the latter is to provide the necessary damping to the electromechanical oscillations of the generators, when the system undergoes disturbances around its operating point. As well as the effect of integrating a photovoltaic PV generator on the stability of the electrical system is studied.

In order to achieve this goal, we went through several steps:

First, as in any study of real dynamic systems, a modeling of the electrical system is developed in order to study its stability, two models are presented a nonlinear model to study its stability with respect to large disturbances such as a short circuit and a linear model to study its stability with respect to small disturbances. In this part of the work, we carried out a linearization of the equations of the system around an operating point in order to obtain the state representation of the system. The stability analysis method is based on the distribution of the system eigenvalues in the complex plane.

We have shown the action of the PSS, whose parameters were not optimized, on a single machine SMIB. The latter is a typical example of generators electromechanical oscillations of problem. We found that the results show a certain improvement in the dynamic stability compared to the case of the system without PSS, which however remains poorly damped.

In a second step, we approached the synthesis of the PSS parameters using the developed algorithm DCSA. The main objective in the optimization procedure is to obtain a PSS sufficiently robust with respect to possible changes in the operating conditions of the electrical system. The proposed algorithm makes it possible to consider different operating points or topologies, in order to ensure, at all times, a satisfactory stability of the whole system.

The last step consists in comparing the algorithm proposed by other recognized and recent algorithms for the PSS parameters optimization, with the same objective function and under the same operating conditions described for the DCSA. The obtained results show that the DCSA presents good dynamic performances with a better damping observed by surpassing the other comparison algorithms.

Finally, a study on the transient stability of the electrical system was carried out using several types of FACTS (Flexible AC Transmission System) such as SVC, STATCOM and UPFC, in particular when integrating a large amount of electrical energy produced by renewable sources, specifically by photovoltaic solar sources. This study is applied on the famous IEEE 30 bus test system, under the Power System Analysis Toolbox (PSAT) simulation software. Based on the critical clearing time

(CCT) as the stability index, the simulation results clearly showed the improved network stability with superiority in favor of UPFC over STATCOM and SVC.

Perspectives

This study allowed us to design a procedure for optimizing the PSS parameters, based on the developed DCSA algorithm. We were able to achieve the objectives set by obtaining a high-performance and robust PSS. There are still many avenues to explore, but it seems to us a priority to pursue a more in-depth study on the following themes:

- Apply this optimization technique in a multi-machine system.
- Apply this technique for simultaneous multi-objective optimization of PSSs and their locations by considering criteria such as response time minimization.
- Apply this technique to increase the rate of solar energy integration on the power system, by optimizing the location and the amount of use of the FACTS system.

Annexe

Annex A

Park transformation

In order to establish the equations describing the total system behavior, it is necessary to bring back the quantities (described in a local coordinate system (d-q)) of each generator to a single common coordinate system for all generators, it is about the reference (D-Q), as shown in Fig (A. 1).

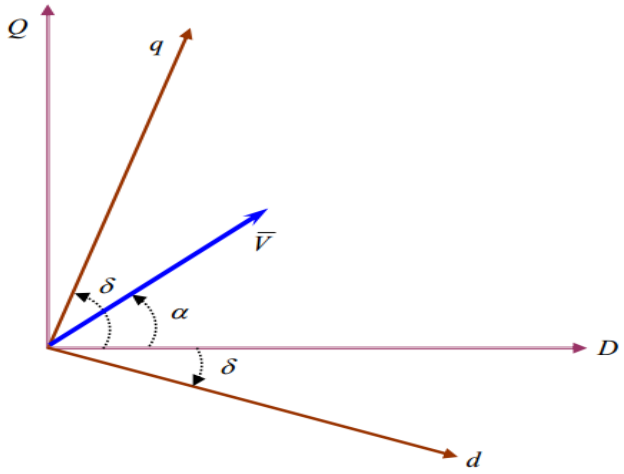

Figure A.1. Change reference from the local coordinate system (d-q) to the common coordinate system (D-Q).

From Fig (A. 1), let $\bar{V}$ be a vector in space.

In the reference (D-Q), it is written:

$$\bar{V}_{(DQ)} = Ve^{j\alpha} \quad \text{(A. 1)}$$

While in the reference (d-q), it is written:

$$\bar{V}_{(dq)} = Ve^{j(\alpha-\gamma)} \quad \text{(A. 2)}$$

Knowing that γ = δ - 90 °, Eq (A. 2) becomes:

$$\bar{V}_{(dq)} = Ve^{j\alpha}e^{-j(\delta-90°)}$$

Thus, the shift from one benchmark to another is carried out by a simple rotation as expressed by the following equation:

$$\bar{V}_{(dq)} = \bar{V}_{(DQ)} e^{j(90° - \delta)}$$

By breaking down into real and imaginary parts and grouping together in matrix form, we obtain the equations describing the passage from one reference to another:

$$\begin{pmatrix} V_d \\ V_q \end{pmatrix} = \begin{pmatrix} \sin\delta & -\cos\delta \\ \cos\delta & \sin\delta \end{pmatrix} \cdot \begin{pmatrix} V_D \\ V_Q \end{pmatrix}$$

$$\begin{pmatrix} V_D \\ V_Q \end{pmatrix} = \begin{pmatrix} \sin\delta & \cos\delta \\ -\cos\delta & \sin\delta \end{pmatrix} \cdot \begin{pmatrix} V_d \\ V_q \end{pmatrix}$$

References

[1] T. Hammons, Y. Kucherov, L. Kapolyi, Z. Bicki, M. Klawe, S. Goethe, A. Tombor, Z. Reguly, N. Voropai, and V. Djangirov, "European plicy on electricity infrastructure, interconnections, and electricity exchanges," *IEEE Power Engineering Review*, vol. 18, pp. 8-21, 1998.

[2] R. Billinton, L. Salvaderi, J. McCalley, H. Chao, T. Seitz, R. Allan, J. Odom, and C. Fallon, "Reliability issues in today's electric power utility environment," *IEEE transactions on Power Systems*, vol. 12, pp. 1708-1714, 1997.

[3] G. Andersson, P. Donalek, R. Farmer, N. Hatziargyriou, I. Kamwa, P. Kundur, N. Martins, J. Paserba, P. Pourbeik, and J. Sanchez-Gasca, "Causes of the 2003 major grid blackouts in North America and Europe, and recommended means to improve system dynamic performance," *IEEE transactions on Power Systems*, vol. 20, pp. 1922-1928, 2005.

[4] R. C. Eberhart and Y. Shi, *Computational intelligence: concepts to implementations*: Elsevier, 2011.

[5] L. L. Grigsby, *Power system stability and control*: CRC press, 2007.

[6] L. Cai and I. Erlich, "Coordination between transient and damping controller for series Facts devices using ANFIS technology," *IFAC Proceedings Volumes*, vol. 36, pp. 293-298, 2003.

[7] Y. Mansour, A. Chang, J. Tamby, E. Vaahedi, B. Corns, and M. El-Sharkawi, "Large scale dynamic security screening and ranking using neural networks," *IEEE transactions on Power Systems*, vol. 12, pp. 954-960, 1997.

[8] J. J. Sanchez-Gasca and J. H. Chow, "Performance comparison of three identification methods for the analysis of electromechanical oscillations," *IEEE transactions on Power Systems*, vol. 14, pp. 995-1002, 1999.

[9] P. Kundur, J. Paserba, V. Ajjarapu, G. Andersson, A. Bose, C. Canizares, N. Hatziargyriou, D. Hill, A. Stankovic, and C. Taylor, "Definition and classification of power system stability IEEE/CIGRE joint task force on stability terms and definitions," *IEEE transactions on Power Systems*, vol. 19, pp. 1387-1401, 2004.

[10] P. Kundur, "Power system stability," *Power system stability and control*, pp. 7-1, 2007.

[11] M. Pavella, D. Ernst, and D. Ruiz-Vega, *Transient stability of power systems: a unified approach to assessment and control* vol. 581: Springer Science & Business Media, 2000.

[12] M. Begovic, "Inter-area oscillations in power systems: A nonlinear and nonstationary perspective (messina, ar)[book reviews]," *IEEE Power and Energy Magazine*, vol. 9, pp. 76-77, 2011.

[13] L. A. Wehenkel, *Automatic learning techniques in power systems*: Springer Science & Business Media, 1998.

[14] I. C. Report, "Excitation system models for power system stability studies," *IEEE Transactions on power apparatus and systems*, pp. 494-509, 1981.

[15] H. Alkhatib and J. Duveau, "Dynamic genetic algorithms for robust design of multimachine power system stabilizers," *International Journal of Electrical Power & Energy Systems*, vol. 45, pp. 242-251, 2013.

[16] G. M. Huang, L. Zhao, and X. Song, "A new bifurcation analysis for power system dynamic voltage stability studies," in *2002 IEEE Power Engineering Society Winter Meeting. Conference Proceedings (Cat. No. 02CH37309)*, 2002, pp. 882-887.

[17] M. A. Pai, *Energy function analysis for power system stability*: Springer Science & Business Media, 2012.

[18] A.-A. Fouad and V. Vittal, *Power system transient stability analysis using the transient energy function method*: Pearson Education, 1991.

[19] J. A. Momoh and M. E. El-Hawary, *Electric systems, dynamics, and stability with artificial intelligence applications*: CRC Press, 2018.

[20] I. Erlich, "Analysis and simulation of the dynamic behavior of electrical power systems," *Postdoctoral lecture qualification, Department of Electrical Engineering, Dresden University, Germany*, 1995.

[21] G. K. Befekadu, "Robust Decentralized control of power systems: A Matrix Inequalities approach," Duisburg, Essen, Univ., Diss., 2006, 2006.

[22] A. Hoballah and I. Erlich, "Generation coordination for transient stability enhancement using particle swarm optimization," in *2008 12th International Middle-East Power System Conference*, 2008, pp. 29-33.

[23] J. L. Rueda, D. G. Colome, and I. Erlich, "Assessment and enhancement of small signal stability considering uncertainties," *IEEE transactions on Power Systems,* vol. 24, pp. 198-207, 2009.
[24] G. Rogers, *Power system oscillations*: Springer Science & Business Media, 2012.
[25] T. J. Browne, V. Vittal, G. T. Heydt, and A. R. Messina, "A comparative assessment of two techniques for modal identification from power system measurements," *IEEE transactions on Power Systems,* vol. 23, pp. 1408-1415, 2008.
[26] J. Hauer, "Application of Prony analysis to the determination of modal content and equivalent models for measured power system response," *IEEE transactions on Power Systems,* vol. 6, pp. 1062-1068, 1991.
[27] J. F. Hauer, C. Demeure, and L. Scharf, "Initial results in Prony analysis of power system response signals," *IEEE transactions on Power Systems,* vol. 5, pp. 80-89, 1990.
[28] S. P. Teeuwsen, I. Erlich, and M. A. El-Sharkawi, "Neural network based classification method for small-signal stability assessment," in *2003 IEEE Bologna Power Tech Conference Proceedings*, 2003, p. 6 pp. Vol. 3.
[29] L. Chaib, A. Choucha, and S. Arif, "Optimal design and tuning of novel fractional order PID power system stabilizer using a new metaheuristic Bat algorithm," *Ain Shams Engineering Journal,* vol. 8, pp. 113-125, 2017.
[30] Z. A. Obaid, L. Cipcigan, and M. T. Muhssin, "Power system oscillations and control: Classifications and PSSs' design methods: A review," *Renewable and Sustainable Energy Reviews,* vol. 79, pp. 839-849, 2017.
[31] R. C. Eberhart and Y. Shi, "Comparing inertia weights and constriction factors in particle swarm optimization," in *Proceedings of the 2000 congress on evolutionary computation. CEC00 (Cat. No. 00TH8512)*, 2000, pp. 84-88.
[32] J. Zhu, *Optimization of power system operation*: John Wiley & Sons, 2015.
[33] Y. Abdel-Magid and M. Abido, "Optimal multiobjective design of robust power system stabilizers using genetic algorithms," IEEE transactions on Power Systems, vol. 18, pp. 1125-1132, 2003.
[34] Y. Abdel-Magid, M. Abido, S. Al-Baiyat, and A. Mantawy, "Simultaneous stabilization of multimachine power systems via genetic algorithms," IEEE transactions on Power Systems, vol. 14, pp. 1428-1439, 1999.
[35] S. Abe and A. Doi, "A new power system stabilizer synthesis in multimachine power systems," IEEE Transactions on power apparatus and systems, pp. 3910-3918, 1983.
[36] M. E. Aboul-Ela, A. Sallam, J. D. McCalley, and A. Fouad, "Damping controller design for power system oscillations using global signals," IEEE transactions on Power Systems, vol. 11, pp. 767-773, 1996.
[37] G. Andersson, "Modelling and analysis of electric power systems," ETH Zurich, pp. 5-6, 2008.
[38] G. Andersson, "Dynamics and control of electric power systems," Lecture notes, pp. 227-0528, 2012.
[39] J. R. Arredondo, "Results of a study on location and tuning of power system stabilizers," International Journal of Electrical Power & Energy Systems, vol. 19, pp. 563-567, 1997.
[40] M. J. Basler and R. C. Schaefer, "Understanding power system stability," in 58th Annual Conference for Protective Relay Engineers, 2005., 2005, pp. 46-67.
[41] M. J. Basler, R. C. Schaefer, K. Kim, and R. Glenn, "Voltage regulator with dual PID controllers enhances power system stability," in Hydrovision, 2002.
[42] P. Bornard, M. Pavard, G. Testud, and d. I. Réseaux, "de Transport: Réglages et Stabilité," Techniques de l'Ingénieur, Traité Génie Electrique, D4-092, 2005.
[43] L. Cai, "Robust coordinated control of FACTS devices in large power systems," Duisburg, Essen, Univ., Diss., 2004, 2004.
[44] E. Lerch, D. Povh, and L. Xu, "Advanced SVC control for damping power system oscillations," IEEE transactions on Power Systems, vol. 6, pp. 524-535, 1991.
[45] N. Rizoug, "Modélisation électrique et énergétique des supercondensateurs et méthodes de caractérisation: Application au cyclage d'un module de supercondensateurs basse tension en grande puissance," Université des Sciences et Technologie de Lille-Lille I, 2006.
[46] P. L. Dandeno, A. N. Karas, K. R. McClymont, and W. Watson, "Effect of high-speed rectifier excitation systems on generator stability limits," IEEE Transactions on power apparatus and systems, pp. 190-201, 1968.

[47] F. De Mello, L. Hannett, and J. Undrill, "Practical approaches to supplementary stabilizing from accelerating power," IEEE Transactions on power apparatus and systems, pp. 1515-1522, 1978.
[48] F. P. Demello and C. Concordia, "Concepts of synchronous machine stability as affected by excitation control," IEEE Transactions on power apparatus and systems, vol. 88, pp. 316-329, 1969.
[49] A. L. Do Bomfim, G. N. Taranto, and D. M. Falcao, "Simultaneous tuning of power system damping controllers using genetic algorithms," IEEE transactions on Power Systems, vol. 15, pp. 163-169, 2000.
[50] A. Feliachi, "Optimal siting of power system stabilisers," in IEE Proceedings C (Generation, Transmission and Distribution), 1990, pp. 101-106.
[51] R. Fleming, M. Mohan, and K. Parvatisam, "Selection of parameters of stabilizers in multimachine power systems," IEEE Transactions on power apparatus and systems, pp. 2329-2333, 1981.
[52] E. G. Shahraki, "Apport de l'UPFC à l'amélioration de la stabilité transitoire des réseaux électriques," Université Henri Poincaré-Nancy 1, 2003.
[53] K. Hongesombut and Y. Mitani, "Implementation of advanced genetic algorithm to modern power system stabilization control," in IEEE PES Power Systems Conference and Exposition, 2004., 2004, pp. 1050-1055.
[54] P. Kundur, "Power system stability," Power system stability and control, pp. 7-1, 2007.
[55] N. P. Schmidt, "Comparison between IEEE and CIGRE ampacity standards," IEEE Transactions on Power Delivery, vol. 14, pp. 1555-1559, 1999.
[56] B. Sørensen and G. Watt, "Trends in Photovoltaic Applications, Survey report of selected IEA countries between 1992 and 2005: Report IEA-PVPS T1-15: 2006," 2006.
[57] A. Labouret and M. Villoz, Energie solaire photovoltaïque vol. 3: Dunod Malakoff, France, 2006.
[58] K. Emery, Y. Hishikawa, and W. D. Warta, "Solar cell efficiency tables (Version 39)," Progress in Photovoltaics: Research and Applications, vol. 20, 2012.
[59] T. Hammons, Y. Kucherov, L. Kapolyi, Z. Bicki, M. Klawe, S. Goethe, A. Tombor, Z. Reguly, N. Voropai, and V. Djangirov, "European plicy on electricity infrastructure, interconnections, and electricity exchanges," IEEE Power Engineering Review, vol. 18, pp. 8-21, 1998.
[60] S. Petibon, "Nouvelles architectures distribuées de gestion et conversion de l'énergie pour les applications photovoltaïques," Université Paul Sabatier-Toulouse III, 2009.
[61] L. M. Fraas, "History of solar cell development," in Low-cost solar electric power, ed: Springer, 2014, pp. 1-12.
[62] C. Bendel and A. Wagner, "Photovoltaic measurement relevant to the energy yield," in 3rd World Conference onPhotovoltaic Energy Conversion, 2003. Proceedings of, 2003, pp. 2227-2230.
[63] D. King, B. Hansen, J. Kratochvil, and M. Quintana, "Dark current-voltage measurements on photovoltaic modules as a diagnostic or manufacturing tool," in Conference Record of the Twenty Sixth IEEE Photovoltaic Specialists Conference-1997, 1997, pp. 1125-1128.
[64] A. C. Pastor, "Conception et réalisation de modules photovoltaïques électroniques," INSA de Toulouse, 2006.
[65] S. Vighetti, "Systèmes photovoltaïques raccordés au réseau: Choix et dimensionnement des étages de conversion," Institut National Polytechnique de Grenoble-INPG, 2010.
[66] S. Lyden, M. Haque, A. Gargoom, and M. Negnevitsky, "Modelling photovoltaic cell: Issues and operational constraints," in 2012 IEEE International Conference on Power System Technology (POWERCON), 2012, pp. 1-6.
[67] M. Abdulkadir, A. Samosir, and A. Yatim, "Modeling and simulation of a solar photovoltaic system, its dynamics and transient characteristics in LABVIEW," International Journal of Power Electronics and Drive Systems, vol. 3, p. 185, 2013.
[68] P. de Assis Sobreira, M. G. Villalva, P. G. Barbosa, H. A. C. Braga, J. R. Gazoli, E. Ruppert, and A. A. Ferreira, "Comparative analysis of current and voltage-controlled photovoltaic maximum power point tracking," in XI Brazilian Power Electronics Conference, 2011, pp. 858-863.
[69] M. A. De Brito, L. P. Sampaio, G. Luigi, G. A. e Melo, and C. A. Canesin, "Comparative analysis of MPPT techniques for PV applications," in 2011 International Conference on Clean Electrical Power (ICCEP), 2011, pp. 99-104.

[70] I. B. Mansour, I. Alaya, and M. Tagina, "A gradual weight-based ant colony approach for solving the multiobjective multidimensional knapsack problem," Evolutionary Intelligence, vol. 12, pp. 253-272, 2019.
[71] L. Wang, J. Pei, Y. Wen, J. Pi, M. Fei, and P. M. Pardalos, "An improved adaptive human learning algorithm for engineering optimization," Applied Soft Computing, vol. 71, pp. 894-904, 2018.
[72] K. Chen, F. Zhou, Y. Wang, and L. Yin, "An ameliorated particle swarm optimizer for solving numerical optimization problems," Applied Soft Computing, vol. 73, pp. 482-496, 2018.
[73] P. R. Singh, M. A. Elaziz, and S. Xiong, "Modified Spider Monkey Optimization based on Nelder–Mead method for global optimization," Expert Systems with Applications, vol. 110, pp. 264-289, 2018.
[74] A. A. Ewees, M. Abd Elaziz, and E. H. Houssein, "Improved grasshopper optimization algorithm using opposition-based learning," Expert Systems with Applications, vol. 112, pp. 156-172, 2018.
[75] I. B. Mansour and I. Alaya, "Indicator based ant colony optimization for multi-objective knapsack problem," Procedia Computer Science, vol. 60, pp. 448-457, 2015.
[76] I. B. Mansour, M. Basseur, and F. Saubion, "A multi-population algorithm for multi-objective knapsack problem," Applied Soft Computing, vol. 70, pp. 814-825, 2018.
[77] H. Shi, S. Liu, H. Wu, R. Li, S. Liu, N. Kwok, and Y. Peng, "Oscillatory Particle Swarm Optimizer," Applied Soft Computing, vol. 73, pp. 316-327, 2018.
[78] M. G. H. Omran, S. Alsharhan, and M. Clerc, "A modified Intellects-Masses Optimizer for solving real-world optimization problems," Swarm and Evolutionary Computation, vol. 41, pp. 159-166, 2018.
[79] Y. Sun, X. Wang, Y. Chen, and Z. Liu, "A modified whale optimization algorithm for large-scale global optimization problems," Expert Systems with Applications, vol. 114, pp. 563-577, 2018.
[80] B. Shaw, V. Mukherjee, and S. P. Ghoshal, "A novel opposition-based gravitational search algorithm for combined economic and emission dispatch problems of power systems," International Journal of Electrical Power & Energy Systems, vol. 35, pp. 21-33, 2012.
[81] H. Nenavath, D. R. Kumar Jatoth, and D. S. Das, "A synergy of the sine-cosine algorithm and particle swarm optimizer for improved global optimization and object tracking," Swarm and Evolutionary Computation, vol. 43, pp. 1-30, 2018.
[82] I. B. Mansour, I. Alaya, and M. Tagina, "Chebyshev-based iterated local search for multi-objective optimization," in 2017 13th IEEE International Conference on Intelligent Computer Communication and Processing (ICCP), 2017, pp. 163-170.
[83] I. Ben Mansour, I. Alaya, and M. Tagina, "A min-max Tchebycheff based local search approach for MOMKP," in Proceedings of the 12th International Conference on Software Technologies, ICSOFT, INSTICC, pp. 140-150.
[84] S. Torabi and F. Safi-Esfahani, "Improved Raven Roosting Optimization algorithm (IRRO)," Swarm and Evolutionary Computation, vol. 40, pp. 144-154, 2018.
[85] J. H. Holland, Adaptation in natural and artificial systems: an introductory analysis with applications to biology, control, and artificial intelligence: MIT press, 1992.
[86] R. Storn and K. Price, "Differential evolution–a simple and efficient heuristic for global optimization over continuous spaces," Journal of Global Optimization, vol. 11, pp. 341-359, 1997.
[87] E. Atashpaz-Gargari and C. Lucas, "Imperialist competitive algorithm: an algorithm for optimization inspired by imperialistic competition," in Evolutionary computation, 2007. CEC 2007. IEEE Congress on, 2007, pp. 4661-4667.
[88] R. Rajabioun, "Cuckoo Optimization Algorithm," Applied Soft Computing, vol. 11, pp. 5508-5518, 2011.
[89] Z. W. Geem, J. H. Kim, and G. V. Loganathan, "A new heuristic optimization algorithm: harmony search," simulation, vol. 76, pp. 60-68, 2001.
[90] E. Rashedi, H. Nezamabadi-pour, and S. Saryazdi, "GSA: A Gravitational Search Algorithm," Information Sciences, vol. 179, pp. 2232-2248, 2009.
[91] B. Javidy, A. Hatamlou, and S. Mirjalili, "Ions motion algorithm for solving optimization problems," Applied Soft Computing, vol. 32, pp. 72-79, 2015.
[92] S. Mirjalili, "SCA: A Sine Cosine Algorithm for solving optimization problems," Knowledge-Based Systems, vol. 96, pp. 120-133, 2016.
[93] N. Ghorbani and E. Babaei, "Exchange market algorithm," Applied Soft Computing, vol. 19, pp. 177-187, 2014.

[94] R. V. Rao, V. J. Savsani, and D. P. Vakharia, "Teaching–learning-based optimization: A novel method for constrained mechanical design optimization problems," Computer-Aided Design, vol. 43, pp. 303-315, 2011.
[95] A. Sadollah, A. Bahreininejad, H. Eskandar, and M. Hamdi, "Mine blast algorithm: A new population based algorithm for solving constrained engineering optimization problems," Applied Soft Computing, vol. 13, pp. 2592-2612, 2013.
[96] N. Moosavian and B. K. Roodsari, "Soccer league competition algorithm: A novel meta-heuristic algorithm for optimal design of water distribution networks," Swarm and Evolutionary Computation, vol. 17, pp. 14-24, 2014.
[97] S. Mirjalili, S. M. Mirjalili, and A. Hatamlou, "Multi-Verse Optimizer: a nature-inspired algorithm for global optimization," Neural Computing and Applications, vol. 27, pp. 495-513, 2015.
[98] R. Eberhart and J. Kennedy, "A new optimizer using particle swarm theory," in Micro Machine and Human Science, 1995. MHS'95., Proceedings of the Sixth International Symposium on, 1995, pp. 39-43.
[99] A. Askarzadeh, "A novel metaheuristic method for solving constrained engineering optimization problems: Crow search algorithm," Computers & Structures, vol. 169, pp. 1-12, 2016.
[100] S. Arora and S. Singh, "Butterfly optimization algorithm: a novel approach for global optimization," Soft Computing, vol. 23, pp. 715-734, 2019.
[101] S. Mirjalili, A. H. Gandomi, S. Z. Mirjalili, S. Saremi, H. Faris, and S. M. Mirjalili, "Salp Swarm Algorithm: A bio-inspired optimizer for engineering design problems," Advances in Engineering Software, vol. 114, pp. 163-191, 2017.
[102] S. Mirjalili, S. M. Mirjalili, and A. Lewis, "Grey Wolf Optimizer," Advances in Engineering Software, vol. 69, pp. 46-61, 2014.
[103] S. Mirjalili and A. Lewis, "The Whale Optimization Algorithm," Advances in Engineering Software, vol. 95, pp. 51-67, 2016.
[104] S. Mirjalili, "The Ant Lion Optimizer," Advances in Engineering Software, vol. 83, pp. 80-98, 2015.
[105] M. Dorigo and G. Di Caro, "Ant colony optimization: a new meta-heuristic," in Proceedings of the 1999 congress on evolutionary computation-CEC99 (Cat. No. 99TH8406), 1999, pp. 1470-1477.
[106] D. Karaboga and B. Basturk, "A powerful and efficient algorithm for numerical function optimization: artificial bee colony (ABC) algorithm," Journal of Global Optimization, vol. 39, pp. 459-471, 2007.
[107] X.-S. Yang, "A new metaheuristic bat-inspired algorithm," in Nature inspired cooperative strategies for optimization (NICSO 2010), ed: Springer, 2010, pp. 65-74.
[108] S. Mirjalili, "Dragonfly algorithm: a new meta-heuristic optimization technique for solving single-objective, discrete, and multi-objective problems," Neural Computing and Applications, vol. 27, pp. 1053-1073, 2015.
[109] S. Saremi, S. Mirjalili, and A. Lewis, "Grasshopper Optimisation Algorithm: Theory and application," Advances in Engineering Software, vol. 105, pp. 30-47, 2017.
[110] S. Mirjalili, "Moth-flame optimization algorithm: A novel nature-inspired heuristic paradigm," Knowledge-Based Systems, vol. 89, pp. 228-249, 2015.
[111] X. Meng, Y. Liu, X. Gao, and H. Zhang, "A new bio-inspired algorithm: chicken swarm optimization," in International conference in swarm intelligence, 2014, pp. 86-94.
[112] A. Satpathy, S. K. Addya, A. K. Turuk, B. Majhi, and G. Sahoo, "Crow search based virtual machine placement strategy in cloud data centers with live migration," Computers & Electrical Engineering, vol. 69, pp. 334-350, 2018.
[113] S. H. A. Aleem, A. F. Zobaa, and M. E. Balci, "Optimal resonance-free third-order high-pass filters based on minimization of the total cost of the filters using Crow Search Algorithm," Electric Power Systems Research, vol. 151, pp. 381-394, 2017.
[114] D. Oliva, S. Hinojosa, E. Cuevas, G. Pajares, O. Avalos, and J. Gálvez, "Cross entropy based thresholding for magnetic resonance brain images using Crow Search Algorithm," Expert Systems with Applications, vol. 79, pp. 164-180, 2017.
[115] A. Y. Abdelaziz and A. Fathy, "A novel approach based on crow search algorithm for optimal selection of conductor size in radial distribution networks," Engineering Science and Technology, an International Journal, vol. 20, pp. 391-402, 2017.

[116] G. Choudhary, N. Singhal, and K. Sajan, "Optimal placement of STATCOM for improving voltage profile and reducing losses using crow search algorithm," in Control, Computing, Communication and Materials (ICCCCM), 2016 International Conference on, 2016, pp. 1-6.
[117] D. H. Wolpert and W. G. Macready, "No free lunch theorems for optimization," IEEE transactions on evolutionary computation, vol. 1, pp. 67-82, 1997.
[118] D. Gupta, J. J. Rodrigues, S. Sundaram, A. Khanna, V. Korotaev, and V. H. C. de Albuquerque, "Usability feature extraction using modified crow search algorithm: a novel approach," Neural Computing and Applications, pp. 1-11, 2018.
[119] F. Mohammadi and H. Abdi, "A modified crow search algorithm (MCSA) for solving economic load dispatch problem," Applied Soft Computing, vol. 71, pp. 51-65, 2018.
[120] G. I. Sayed, A. E. Hassanien, and A. T. Azar, "Feature selection via a novel chaotic crow search algorithm," Neural Computing and Applications, vol. 31, pp. 171-188, 2019.
[121] A. E. Hassanien, R. M. Rizk-Allah, and M. Elhoseny, "A hybrid crow search algorithm based on rough searching scheme for solving engineering optimization problems," Journal of Ambient Intelligence and Humanized Computing, pp. 1-25, 2018.
[122] J. Luo and B. Shi, "A hybrid whale optimization algorithm based on modified differential evolution for global optimization problems," Applied Intelligence, vol. 49, pp. 1982-2000, 2019.
[123] R. Shah, N. Mithulananthan, R. Bansal, and V. Ramachandaramurthy, "A review of key power system stability challenges for large-scale PV integration," Renewable and Sustainable Energy Reviews, vol. 41, pp. 1423-1436, 2015.
[124] P. Denholm and R. M. Margolis, "Evaluating the limits of solar photovoltaics (PV) in traditional electric power systems," Energy policy, vol. 35, pp. 2852-2861, 2007.
[125] N. K. Roy, "Stability assessment of power systems integrated with large-scale solar PV units," in Advances in Solar Photovoltaic Power Plants, ed: Springer, 2016, pp. 215-230.
[126] R. Shah, N. Mithulananthan, and R. Bansal, "Oscillatory stability analysis with high penetrations of large-scale photovoltaic generation," Energy Conversion and Management, vol. 65, pp. 420-429, 2013.
[127] Y. Hashemi, H. Shayeghi, M. Moradzadeh, and A. Safari, "Design of hybrid damping controller based on multi-target gravitational search optimization algorithm in a multi-machine power system with high penetration of PV park," Journal of Central South University, vol. 23, pp. 1163-1175, 2016.
[128] P. Kundur, "Power system stability," Power system stability and control, pp. 7-1, 2007.
[129] R. Krishan, A. Verma, and S. Mishra, "An efficient multi objective optimization approach for robust tuning of power system stabilizers," in 2016 National Power Systems Conference (NPSC), 2016, pp. 1-6.
[130] K. Sebaa and M. Boudour, "Optimal locations and tuning of robust power system stabilizer using genetic algorithms," Electric Power Systems Research, vol. 79, pp. 406-416, 2009.
[131] G. S. Ghfarokhi, M. Arezoomand, and H. Mahmoodian, "Analysis and simulation of the single-machine infinite-bus with power system stabilizer and parameters variation effects," in 2007 International Conference on Intelligent and Advanced Systems, 2007, pp. 167-171.
[132] V. G. Mathad, B. F. Ronad, and S. H. Jangamshetti, "Review on comparison of FACTS controllers for power system stability enhancement," International Journal of Scientific and Research Publications, vol. 3, pp. 2250-315, 2013.
[133] E. Barrios-Martínez and C. Ángeles-Camacho, "Technical comparison of FACTS controllers in parallel connection," Journal of applied research and technology, vol. 15, pp. 36-44, 2017.
[134] N. K. Sharma, A. Ghosh, and R. K. Varma, "A novel placement strategy for FACTS controllers," IEEE Transactions on Power Delivery, vol. 18, pp. 982-987, 2003.